1974

The determination of molecular structures by vapor phase electron diffraction.

Frank J. Mustoe
University of Windsor

THE DETERMINATION OF MOLECULAR STRUCTURES BY VAPOR PHASE ELECTRON DIFFRACTION

I APPARATUS AND METHOD

II THE STRUCTURES OF $(CH_3)_2GeH_2$, $(CH_3)_4Ge$, CH_3GeBr_3 AND CH_3GeF_3

III THE CONFORMATION OF RACEMIC 4,6-DIMETHYL TRIMETHYLENE SULFITE

By

Frank J. Mustoe

A Dissertation

Submitted to the Faculty of Graduate Studies through the Department of Chemistry in Partial Fulfillment of the Requirements for the Degree of Doctor of Philosophy at the University of Windsor

Windsor, Ontario

1973

This work is dedicated to my Mother and Father

ABSTRACT

An electron diffraction apparatus has been constructed which allows the molecular structure of vapor phase molecules to be determined with an accuracy of a few thousandths of an angstrom in favorable cases. This instrument has been used to determine the molecular structures of $(CH_3)_2GeH_2$, $(CH_3)_4Ge$, CH_3GeF_3 and CH_3GeBr_3. The following bond distances (r_g values) were determined: in dimethylgermane, Ge-C = 1.953 $\pm$ 0.003, Ge-H = 1.56 $\pm$ 0.04, C-H = 1.074 $\pm$ 0.016Å; in tetramethylgermane, Ge-C = 1.955 $\pm$ 0.005, C-H = 1.08 $\pm$ 0.03Å. On correction to an r_e value the Ge-C bond length is in excellent agreement with microwave results for dimethyl germane and the other methyl germanes. This observation parallels the results for the Si-C bond length in the methyl silanes, although in contrast d orbital involvement of germanium is not necessary to explain the Ge-C bond length.

Progressive halogen substitution is found to decrease the Ge-X and Ge-C bond lengths in germanium compounds. The molecular structures of trifluoro(methyl)germane and tribromo(methyl)germane were determined with the following parameters: in CH_3GeF_3, Ge-C = 1.921 $\pm$ 0.012, Ge-F = 1.708 $\pm$ 0.003, C-H = 1.14 $\pm$ 0.08 Å $\angle$CGeF = 114 $\pm$ 0.1 $\angle$FGeF = 104.6 $\pm$ 0.9°; in CH_3GeBr_3, Ge-C = 1.87 $\pm$ 0.04, Ge-Br = 2.284 $\pm$ 0.002Å, $\angle$CGeBr = 111.2 $\pm$ 0.3, $\angle$BrGeBr = 107.7 $\pm$ 0.3°. The Ge-C and Ge-X bond lengths in these molecules have been interpreted

as evidence for a small or negligible amount of d-orbital involvement.

The molecular geometry of the racemic trans-4,6-dimethyl trimethylene sulfite has been studied in the gas phase by electron diffraction. Six trial conformations were examined by least squares fitting of the intensity data. A significance test applied to the fits obtained for each of the six static models tested indicate that the best single representation of the molecule has a chair conformation, although a mixture containing other conformations could not be definitely eliminated. It was not possible to conclusively discriminate between an axial or an equatorial S=O bond, although the axial position is favored. The following bond distances and angles were determined: C-H = 1.119 ± 0.020, C-C = 1.505 ± 0.014, C-O = 1.413 ± 0.003, S=O = 1.480 ± 0.022, S-O = 1.622 ± 0.009Å; <CCO = 111.1 ± 1.3, <OS=O = 116.7 ± 1.4, <COS = 114.1 ± 1.0, <OSO = 100.7 ± 2.0°. The following angles were assumed to be tetrahedral: <CCC, <HCH, <CCH.

All the parameters listed above are based on r_g values with uncertainties three times those calculated from the least squares analysis. The standard errors are believed to include systematic errors in the analysis.

ACKNOWLEDGEMENTS

Every piece of work, no matter how original, is but an extension of the efforts of others. The foundation for this thesis will be found in the references contained therein, but on a more immediate level special thanks are due to a relatively small number of individuals who freely gave of their time and expertise to encourage and direct this research. Dr. A. van Wijngaarden provided many valuable suggestions during construction of the diffraction camera. Compounds for analysis were provided by Drs. G. Wood and M. Miskow (racemic 4,6-dimethyl trimethylene sulfite) and J. Drake and R. Hemmings (the halo(methyl) germanes).

It has been a special privilege to work closely with my research supervisor, Dr. J. L. Hencher, as a colleague and a friend; this work would have been impossible without his understanding and dedication. The cooperation of Dr. S. H. Bauer and his co-workers at Cornell University was invaluable and readily given.

Finally, this work owes a considerable debt to the patience and understanding of my wife Judy.

TABLE OF CONTENTS

PART III

LIST OF FIGURES

PART III

LIST OF TABLES

Chapter 1

INTRODUCTION

The first gas electron diffraction pattern was recorded by Mark and Wierl (1) in 1930, and the following year Wierl (2) published the results of an investigation of the molecular structures of some twenty compounds in which electrons were diffracted by vapor phase molecules. These studies were accomplished by visually estimating optical densities directly from the photographic plates. This subjective procedure was further handicapped by the very rapid decrease in intensity of scattered electrons with increase in scattering angle, which is proportional to about the third power of the sine of the scattering angle. This problem is now overcome experimentally by rotating a sector immediately in front of the photographic plate. The sector reduces the intensity of electrons striking the plate at small angles relative to that at large angles, bringing the density across the whole of the plate within the useful dynamic range of the emulsion. The sector improvement was suggested by Finbak (3) and introduced by Debye (4) in 1939. Optical densities are now obtained from the photographic plates using a microdensitometer.

The diffracted electrons make an interference pattern which can be analysed to deduce information about the molecules causing the scattering. The total experimental intensity I_x which is recorded is a sum of contributions:

$$I_x(s) = \phi(s)[I_m(s) + I_a(s) + I_{ext}(s)] \qquad (I.1)$$

where $I_m(s)$ is the desired molecular component (5):

$$I_m(s) = P\Sigma\Sigma_{ij} \frac{|f_i(s)||f_j(s)|\cos(\eta_i - \eta_j)\exp(-\ell_{ij}^2 s^2/2)\sin(sr_{ij} - \ell_{ij}^2 s/r_{ij} - a\ell_{ij}^4 s^3/6)}{s^4 \, sr_{ij}} \qquad (I.2)$$

P is a scale factor which is the asymptotic atomic scattering at large angles: $P = \sum_i (Z_i^2 + Z_i)$ where Z_i is the atomic number.

f_i is the form factor for electrons which is related to the X-ray form factor F in the first Boron approximation:

$$\overline{|f_i(s)|} = Z_i - F_i(s)$$

η_i is a phase shift

r_{ij} and ℓ are the interatomic distances and mean square amplitudes of vibration respectively.

a is a parameter used to account for anharmonic molecular motions.

$I_a(s)$ is due to atomic and inelastic scattering:

$$I_a(s) = \frac{1}{\overline{s^4}} \sum_i (|f_i(s)|^2 + S_i(s)) \qquad (I.3)$$

where $S_i(s)$ denotes the inelastic scattering

$I_{ext}(s)$ represents extraneous scattering from parts of the diffraction apparatus where s is the scattering variable

$$s = 4\pi/\lambda \sin(\theta/2) \qquad (I.4)$$

λ is the wavelength of the electron beam and θ is the angle of diffraction.

These contributions are modified by the shape of the sector opening ϕ. The last two terms in (I.1) are independent of the molecular structure and may be regarded as experimental background B, which is a smooth curve cleaving the oscillations in I_x.

$$B(s) = I_a(s) + I_{ext}(s) \tag{I.5}$$

When the sector function is known, the experimental molecular scattering $M_{exp}(s)$ can be obtained by subtracting the background:

$$M_{exp}(s) = \frac{s^4 I_x(s)}{I_a(s)\phi(s)} - \frac{s^4 B(s)}{I_a(s)} \tag{I.6}$$

When the sector function is unknown, I_{ext} is assumed to be negligable; then, the experimental molecular component is determined by dividing by the background:

$$M_{exp}(s) = \frac{I_x(s)}{B(s)} - 1 \tag{I.7}$$

The theoretical expression for the molecular scattering corresponding to $M_{exp}(s)$ is

$$M_t(s) = \frac{I_m(s)}{I_a(s)} \tag{I.8}$$

M(s) is fit to $M_{exp}(s)$ by least squares refinements on the molecular

parameters r_g and ℓ.

A probability function of interatomic distances, known as the radial distribution $f(r)$, can be obtained as the Fourier transform of the nuclear molecular scattering $I'_m(s)$:

$$f(r) = \int_0^\infty I'_m(s) \sin s\, r\, ds \qquad (I.9)$$

The nuclear molecular scattering $I'_m(s)$ is obtained by subtracting the the component $\Delta I_m(s)$ due to the electrons from $I_m(s)$:

$$\Delta I_m(s) = I_m(s) - \frac{P}{B^4} \sum\sum Z_i Z_j \exp(-\ell_{ij}^2 s^2/2) \sin(Dr_{ij} - \ell_{ij}^2 s^2 / r_{ij} - a\ell_{ij}^4 s^3/6) \Big/ Dr_{ij} \qquad (I.10)$$

where $I_m(s)$ is given by equation (I.2).

Since the data do not cover the range $0 < s < \infty$, the integral is replaced by a summation over s_{min} to s_{max} with a damping constant b to minimise series termination

$$f(r) = \sum_{s_{min}}^{s_{max}} I'_m(s) \sin sr \exp(-bs^2) \Delta s \qquad (I.11)$$

where $\exp(-bs_{max}^2) = 0.1$

Since the first publications by Wierl the electron diffraction technique has become an increasingly useful method for structural analysis. In 1971 Bartell (6) estimated that more than 750 compounds have been studied by vapor phase electron diffraction; at the time of writing this figure must be close to a thousand. Some recent reviews have been written by Bauer (7), Bastiansen, et al (8), Hilderbrandt and Bonham (9), Bartell (6), Karle (10), Kuchitsa (11), Spiridonov (12) and by Hargittai and Lengyel (13).

Chapter II

THE DIFFRACTION RECORDING

An electron diffraction camera has been constructed that enables molecular structure determinations to be made with a precision of a few thousandths of an angstrom in favorable cases. A general view of the camera, high voltage control panel, and gas inlet system is provided in Fig. 1. The diffraction chamber area is shown in more detail in Fig. 2.

The high voltage power supply, gun and electron optics are those of an RCA EMU 3B electron microscope which was rebuilt for the diffraction apparatus. The accelerating voltage was fixed at about 58kV. The beam is defined by a platinum aperture 700 microns in diameter and two further clean up apertures constructed of aluminum, both 1/16 inch in diameter are provided. Flourescent plates were used to view the beam through a telescope of magnification X30, the diameter of the spot being about 20 microns. The beam current was in the range 10^{-8} to 5×10^{-7} ampere and was measured using a Keithley 414A picoammeter. Exposure times were controlled by a mechanical shutter.

A vacuum of about 1×10^{-5} torr was obtained using a six inch Edwards oil diffusion pump backed by an Edwards oil rotary pump (500 l/s). Scattering patterns were recorded at two camera positions allowing useful data to be obtained over the ranges $s = 2.24 - 15.71 A^{-1}$ (camera distance L = 296.2 mm) and $s = 11.00 - 47.12 A^{-1}$ (L = 95.5 mm)

Notations in Figure 1

A General View of the Diffraction Apparatus

C Diffraction Camera Chamber

E Electron gun and lens

H High voltage power supply and lens control panel

SCHEMATIC DIAGRAM

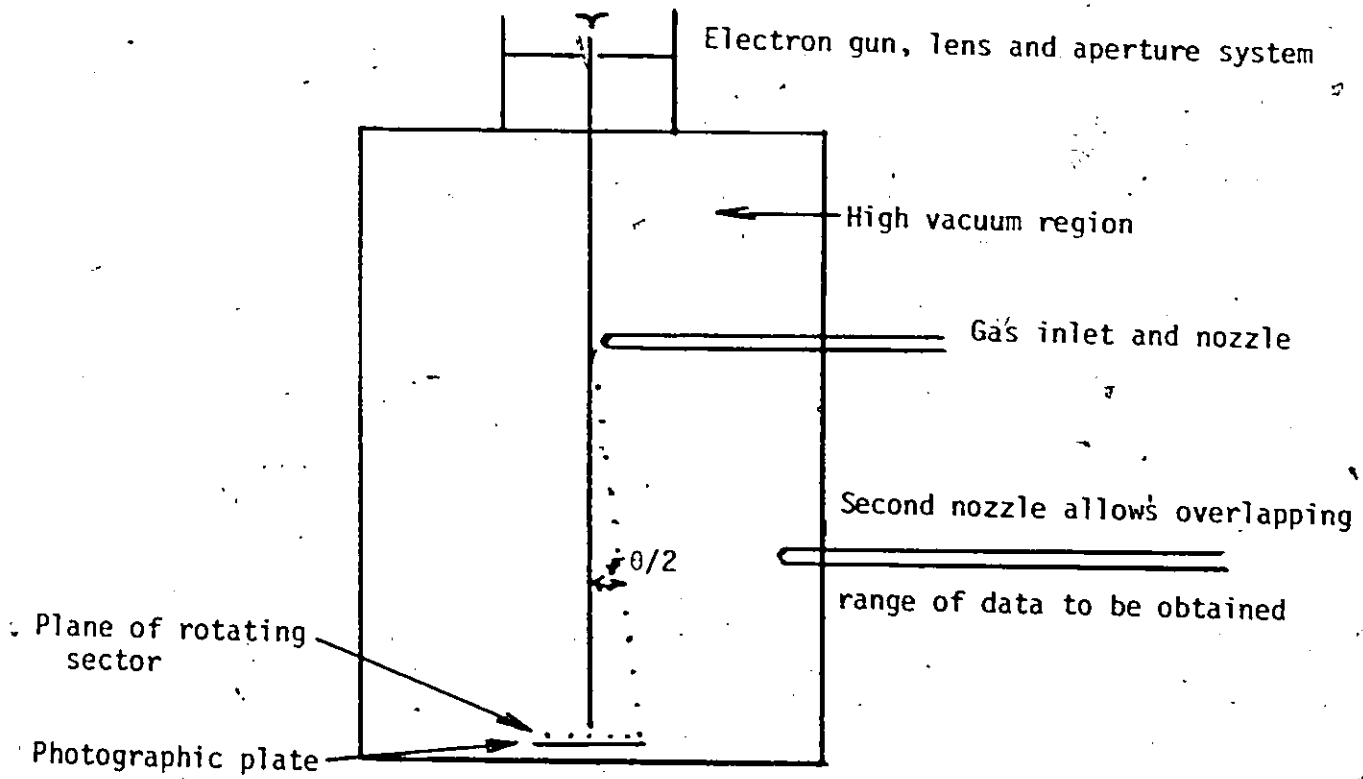

Figure 1

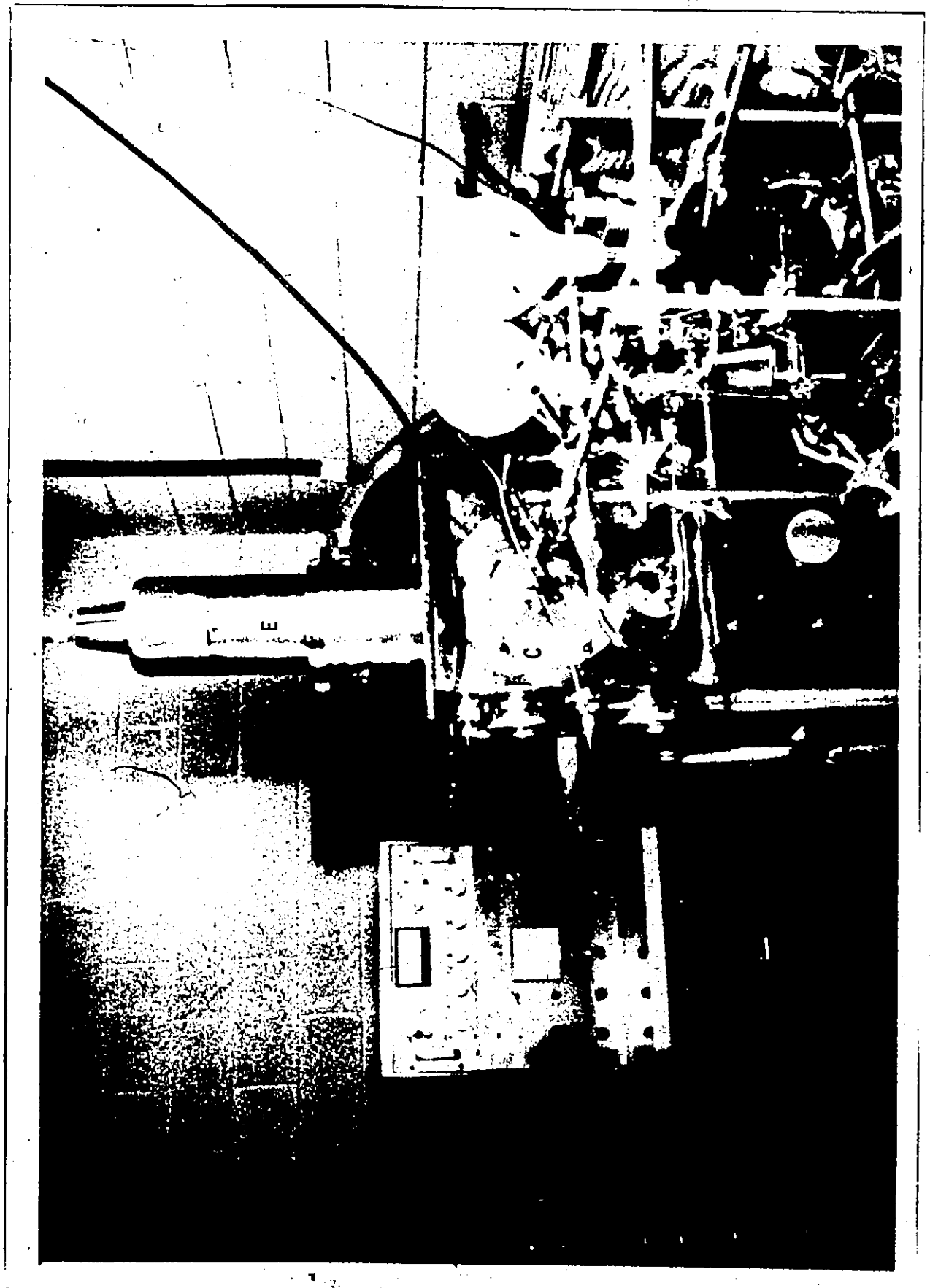

Notations in Figure 2

The Diffraction Chamber

F Coaxial feedthrough to the Faraday cup

N Nozzle inlet tubes

S Mechanical shutter

W Viewing windows

Figure 2

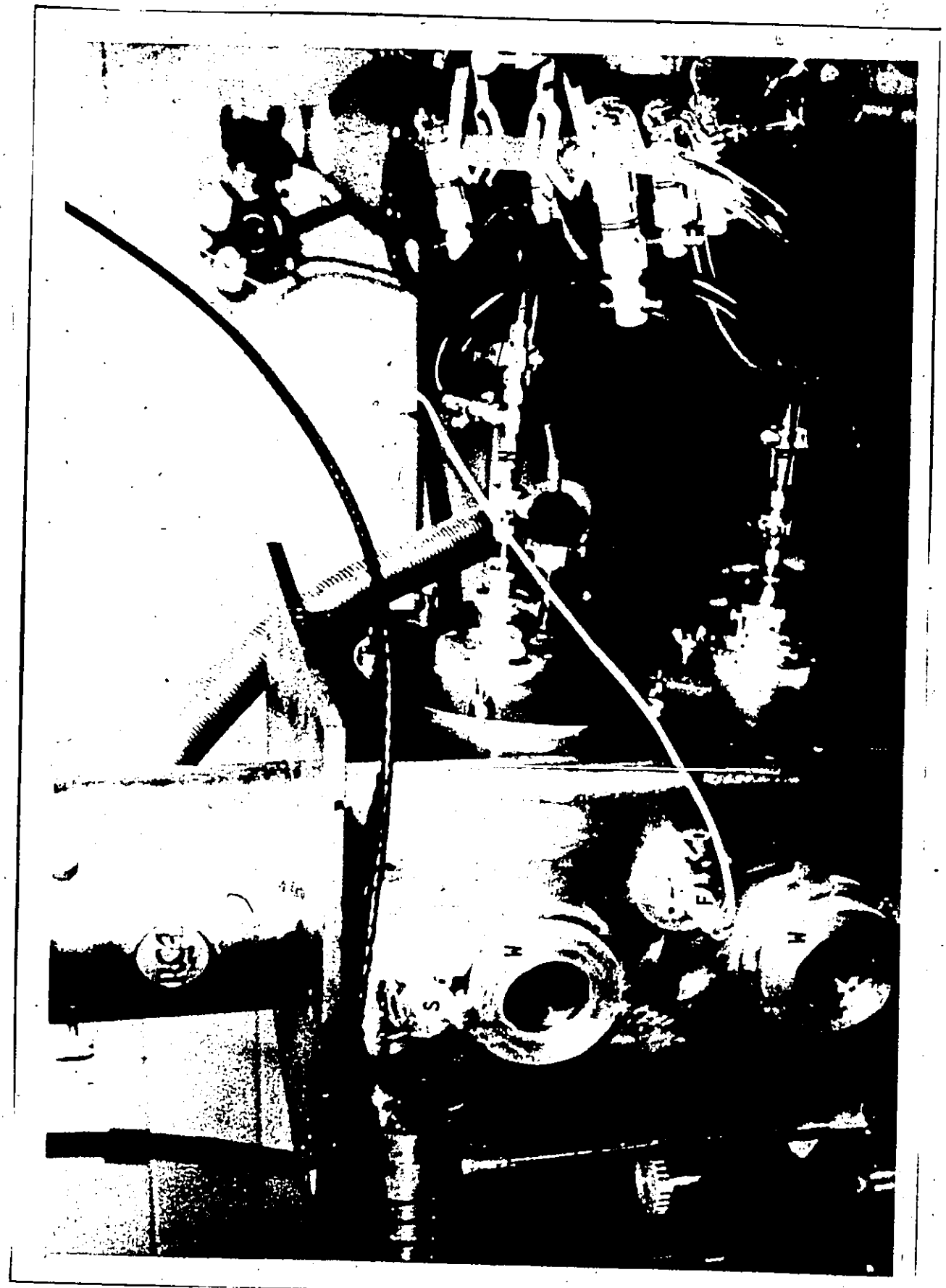

The nozzle to photographic plate distances L were measured with a cathetometer. The upper nozzle has an exit hole 0.5 mm in diameter, the lower being 0.25 mm diameter. Sample molecules were absorbed on a cryounit covered with activated charcoal and kept at liquid nitrogen temperatures, thus preventing sample delocalisation throughout the chamber. The inside of the chamber is coated with a colloidal suspension of graphite to minimise secondary scattering. The extraneous scattering was checked for each series of patterns by taking a blank exposure. Also included in each series for the purpose of calibrating the scale parameters (L, λ) were an exposure of solid magnesium oxide and another of a vapor sample of carbon disulfide. The MgO sample was offset 11.0 mm from the nozzle, at 90 degrees to the axis of the electron beam, so that it could be rotated into the path of the beam when required.

The Sector

The sector used in this work has an angular opening proportional to the radius cubed, with the function normalised to 175 degrees to allow attachment to the sector race. It is a heart shaped piece of aluminum 1/8 inch thick with a maximum radius of 5.1 cm. The sector race is 15.2 cm in diameter and constructed from 304 stainless steel with bronze ball bearings. The edge of the sector is milled to 45° so that in all cases a very sharp edge was presented to the beam. The sector, which was rotated at about 500 rpm, is shown in Fig. 3 in position 6.25 mm above the photographic plate. A beam stop which operates by centrifugal force is situated at the center

Notations in Figure 3

The Sector Area

B Beam stop

D Drive shaft for the sector race. A wheel normally fits over the shift with the outer edge in contact with the sector race.

G Gas inlet tube. The nozzle and its attachment have been unscrewed.

P Photographic plate

S Sector cut to an r^3 shape.

Figure 3

and consists of a small lead weight attached to a weak spring of phosphor-bronze wire.

A determination of the sector function ϕ is very important for the analysis of diffraction patterns, and was deduced from the experimental scattering by CS_2 using the known molecular structure (14). Starting with the experimental intensity

$$I_x(s) = \phi(s) \, (I_m(s) + I_a(s) + I_{ext}(s))$$

and dividing by the background $I_a(s) + I_{ext}(s)$, the experimental molecular component is obtained as

$$M_{exp}(s) = \frac{I_x(s)}{\phi(s) \, (I_a(s) + I_{ext}(s))} \qquad \text{(II.1)}$$

This was compared to the theoretical molecular component M_t using an index of resolution R to bring the experimental expression into quantitative agreement with the theoretical:

$$R \, M_{exp}(s) = \frac{M_t(s)}{1 + \frac{I_{ext}(s)}{I_a(s)}} \qquad \text{(II.2)}$$

The refined background was obtained as

$$I_{ext}(s) = \left[\frac{M_t(s)}{R.M_{exp}(s)} - 1\right] \cdot \frac{1}{I_a(s)} \qquad \text{(II.3)}$$

I_{ext} was fit to a polynomial to ensure a smooth function.

A correlation background B_{corr} can be defined which is the background which would bring the experimental curve into perfect agreement with the theoretical:

$$M_t(s) = R\left[\frac{I_x(s)}{B_{corr}(s)} - 1\right] \qquad \text{(II.4)}$$

$$B_{corr}(s) = \frac{I_x(s)}{[(M_t(s)/R) + 1]} \qquad \text{(II.5)}$$

Also, $$B_{corr}(s) = \phi(s)[I_a(s) + I_{ext}(s)] \qquad \text{(II.6)}$$

$$\therefore \quad \phi(s) = \frac{B_{corr}(s)}{I_a(s) + I_{ext}(s)} \qquad \text{(II.7)}$$

where I_{ext} is the smooth curve found in (II.3)

The sector function was determined for several CS_2 plates taken

at each distance. An average was determined for each distance to account for random errors in I_x. The individual determinations agree with the average to better than 2%. The long and short distance sector functions are given in Appendix A.

Digitized Data Collection

The diffraction patterns were recorded on Kodak electron image plates (15) of size 10.2 x 12.7 cm. A double beam Jarrell-Ash microdensitometer modified with a rotating stage and interfaced to a digital recorder (16) was used to obtain transmittances at 100 micron intervals across the pattern for the short camera position, and 150 microns for the long camera. The center of the diffraction pattern was located to within 0.001 mm by minimising the sum of the squares of the deviations between equivalent readings in each half of the scan. A correction for backlash in the drive screw was made to the displacements associated with the transmittance data. Typical values of the drift per reading are of the order of 0.0002 mm. Optical densities were calculated from the transmittance T by

$$O.D. = -\log T \qquad \text{(II.8)}$$

Chapter III

DATA ANALYSIS

Scale Calibration

Initial calculations for the scale parameters L,λ were based on the scattering patterns due to solid MgO. The diameters of the sharp rings were measured with a travelling microscope, each ring being independently measured across at least four different diameters.

Magnesium oxide forms a face centered cubic lattice with lattice constant $a_o = 4.2117 \pm 0.0005$ Å (17), and a temperature dependence

$$a_o' = a_o (0.999695 + 0.0000122T)$$

where T is in degrees absolute. The initial value for L was measured using a cathetometer. Each ring of radius r was assigned a set of Miller indeces (h,k,l) and the trial values for L,λ were varied to bring the experimental scattering variable s into agreement with the theoretical value:

$$s(\text{experimental}) = (4\pi/\lambda)\sin(0.5 \tan^{-1}(r/L)) \qquad \text{(III.1)}$$

$$s(\text{theoretical}) = 4\pi(h^2+k^2+l^2)^{1/2}/2a_o \qquad \text{(III.2)}$$

Typical calibration data for the long distance position are given in Appendix B. Final values for the scale parameters were determined by comparing the experimental scattering from CS_2 with that calculated from

the known structure (14). Optical densities from the two halves of the microdensitometer scan were then interpolated at integral values of the scattering variable q:

$$q = 40/\lambda \sin (0.5 \tan^{-1} (r/L)) = \frac{10.}{\pi} S \qquad \text{(III.3)}$$

where r is the distance of a point on the plate to the center of the pattern.

The relativistic corrected wavelength is related to the voltage V by

$$\lambda = [150/V (1 + 9.834 \times 10^{-7})]^{1/2} \qquad \text{(III.4)}$$

The mean voltage calculated from 13 calibration experiments taken over a period of three months was 57.88 kV with a standard deviation during that time of 0.13 kV. The MgO patterns showed no evidence of elliptical diffraction rings that might be caused by extraneous magnetic fields. The diffraction laboratory is situated in a ferro-concrete building and the effect of terrestial magnetism is expected to be negligible (18).

The Experimental Molecular Scattering Curve

A linear density-intensity relationship was assumed for densities less than about 0.8 (19) and a correction was applied for darker plates (20). The electrons are scattered in a cone but are recorded on a flat photographic plate. To correct the intensities for this effect the following expression was used:

$$I(q) = I_o(q)/\cos^3\theta \qquad \text{(III.5)}$$

where θ is the angle between the incident and scattered wave vectors, I_o is the intensity of electrons at the cone surface, and I is the intensity of electrons at the photographic plate. The relationship is shown in the following diagram.

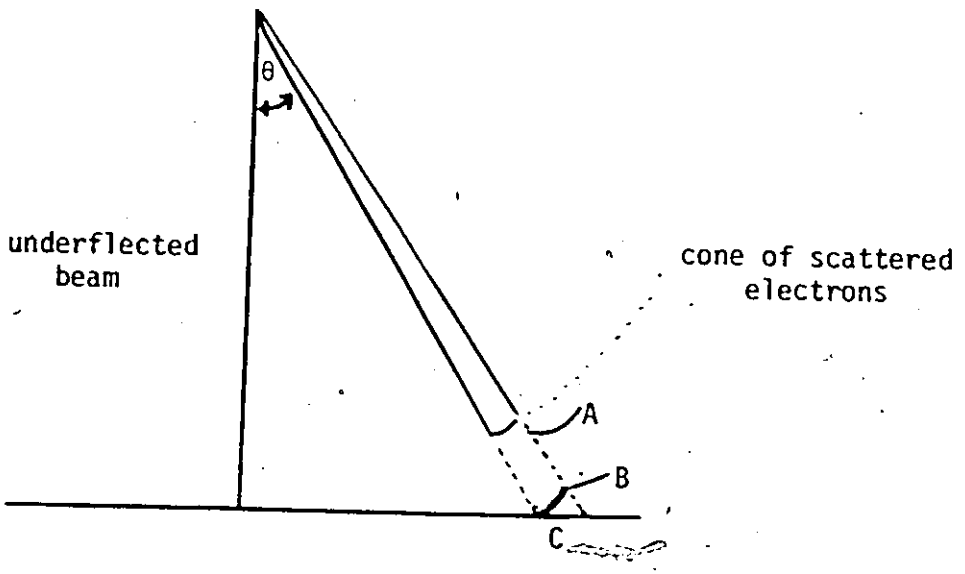

B is related to A as $B = A/\cos^2\theta$

$C = B/\cos\theta = A/\cos^3\theta$

$$A_i = \sum_q (\text{Unscaled Average}) / \sum_q (\text{Data set } i) \qquad \text{(III.6)}$$

The intensities of each data set were then multiplied by the corresponding scale factor and the resultant sets were numerically averaged to obtain a composite curve.

A smooth background was drawn through the oscillations in each composite curve to obtain the experimental molecular scattering component. Data from the two camera positions were spliced together (20) to form one continuous experimental curve from which the radial distribution function was calculated. Errors in the non-structural regions are due to a poorly drawn background and were useful for obtaining corrections to the trial background (21). The difference between the theoretical and experimental radial distribution function was then reinverted to obtain the correction to the molecular scattering:

$$(sM_{expt}(s)) = \int_0^{r_{max}} (f_{theor}(r) - f_{exp}(r))\sin(sr)dr \qquad \text{(III.7)}$$

The corrected scattering curve was then used to determine the refined background.

Least Squares Analysis

Initial structure refinements were made on the radial distribution curve because it can be readily interpreted in terms of molecular parameters, and also because of an economy in computing costs. However, since it is necessary to splice in theoretical data from s = 0 to s_{min}, the experimental radial distribution is to some extent dependent on the assumed structure. Final refinements were based on the experimental molecular scattering curve.

The least squares method was used in the manner proposed by Hedberg and Iwasaki (22). An algorithm was used which allows dependent internuclear distances to be calculated from a set of independent geometric parameters (23), usually bond lengths and angles. The transformation may be represented as

$$\mathbf{T}P = R \qquad \text{(III.8)}$$

where P is the vector of independent parameters and R is the NxN matrix of internuclear distances. In order to calculate elements of the Jacobian matrix A, a matrix D is defined for the kth parameter:

$$D^k_{ij} = (\partial R_{ij}/\partial P_k) \qquad \text{(III.9)}$$

The derivative of the intensity curve with respect to the internuclear distance is

$$H_{ij} = (\partial sM(s)/\partial R_{ij}) \qquad \text{(III.10)}$$

The elements of H are obtained by differentiation:

$$H_{ij} = \frac{2sf_if_j\cos(\eta_i-\eta_j)\exp(-1/2l_{ij}^2s^2)}{\sum_i (f_i^2 + S_i)}\left[\frac{\cos(X)}{sr_{ij}}\left\{1 + \left(\frac{l_{ij}}{r_{ij}}\right)^2\right\}\frac{\sin(X)}{s^2r_{ij}^2}\right] \qquad \text{(III.11)}$$

where $X = sr_{ij} - l_{ij}^2 - a_{ij}l_{ij}^4s^3/6$

The derivative of the intensity curve with respect to the mean square amplitudes is given by

$$H_{ij} = \frac{-2sf_if_j\cos(\eta_i-\eta_j)\exp(-1/2l_{ij}^2s^2}{\sum_i (f_i^2 + S_i)sr_{ij}}\left[\sin(X)sl_{ij} - \cos(X)\left(\frac{2l_{ij}}{r_{ij}} + \frac{a_{ij}l_{ij}^3s^2}{2}\right)\right] \qquad \text{(III.12)}$$

The matrix D is then defined using

$$D = (T[P + \Delta P] - TP)/\Delta P \qquad \text{(III.13)}$$

The Jacobian may then be defined as

$$A = \text{Trace } (HD) \tag{III.14}$$

The Weight Matrices

When only two sets of data were available a unit diagonal matrix with exponential weighting at the beginning and end of the data was used:

Weight	Data Region
$\exp(-a_1[s-s_1]^2)$	$s_{min} < s < s_1$
1	$s_1 < s < s_2$
$\exp(-a_2[s_1-s_2]^2)$	$s_2 < s < s_{max}$

(III.15)

When three or more sets of data were available the diagonal weight matrix was composed from estimates of the variances of the individual observations. The sample variance V is given by

$$V = \frac{1}{n-1} \sum_i (x_i - \bar{x})^2 \tag{III.16}$$

where n is the number of data sets

x_i is a scaled data set

$\bar{x}$ is the average curve.

An estimate for the best weight of each data point can be made from 1/V.

Correlations between the uncertainties of adjacent data points were taken into account by an off-diagonal weighting calculated in the manner proposed by Murata and Morino (24).

References

(1) H. Mark and R. Wierl. Naturwissenshaften 18, 205 (1930).

(2) R. Wierl. Ann. d. Physik 8, 521 (1931).

(3) C. Finbak. Avhandl. Norske Videnskaps-Akad. Oslo, I, Mat.

(4) P. Debye. Physik Z. 40, 404 (1939).

(5). K. Kuchitsu and L. S. Bartell. J. Chem. Phys. 35, 1945 (1961).

(6) L. S. Bartell in "Physical Methods in Chemistry," A. Weissberger and B. W. Rossiter, Ed., 4th ed., Interscience, New York, N.Y.,1972.

(7) S. H. Bauer in "Physical Chemistry, An Advanced Treatise," ed. by H. Eyring, et al, Academic Press, N.Y. 1970.

(8) O. Bastiansen, H. M. Seip, and J. E. Boggs. Perspect. Struct. Chem. 4, 60 (1971).

(9) R. L. Hilderbrandt and R. A. Bonham. Annu. Rev. Phys. Chem. 22, 279 (1971).

(10) J. Karle in "Determination of Molecular Structures by Physical Methods," E. A. Braude and F. C. Nachod, Ed., Academic Press, N.Y. 1972.

(11) K. Kuchitsu. M T P (Med. Tech. Publ. Co.) Int. Rev. Sci.: Phys. Chem., Ser. One. 203 (1972).

(12) V. P. Spiridonov. Kem. Kozlem. 37, 399 (1972).

(13) I. Hargittai and S. Lengyel. Kem. Kozlem. 37, 433 (1972).

(14) Y. Morino and T. Iijima. Bull. Chem. Soc. Japan. 35, 1661 (1962).

(15) Kodak Pamphlet No. P-116. Eastman Kodak Company, Rochester, New York 14650.

(16) S. H. Bauer and K. Kimura. J. Phys. Soc. Japan. 17, 300 (1962).
R. L. Hilderbrandt and S. H. Bauer. J. Mol. Struct. 3, 325 (1969).

(17) M. E. Swanson and E. Tage. J. C. Fel. Reports, NBS (1949).

(18) Y. Murata, K. Kuchitsu and M. Kimura. Jap. J. Appl. Phys. 9, 591 (1970).

(19) H. R. Foster. J. Appl. Phys. 41, 5344 (1970).

(20) J. L. Hencher and S. H. Bauer. J. Amer. Chem. Soc. 89, 5527 (1967).

(21) J. Karle and I. L. Karle. J. Chem. Phys. 18, 957 (1950).

(22) K. Hedberg and M. Iwasaki. Acta Cryst. 17, 529 (1964).

(23) R. L. Hilderbrandt. J. Chem. Phys. 51, 1654 (1969).

(24) Y. Murata and Y. Morino. Acta Cryst. 20, 605 (1966).

PART II

THE MOLECULAR STRUCTURES OF $(CH_3)_2GeH_2$, $(CH_3)_4Ge$, CH_3GeF_3 AND CH_3GeBr_3

PART II

CHAPTER I

INTRODUCTION

The induction of double-bond character by the partial ionic nature of another bond has been used by Pauling (1) to explain the observed shortening of the carbon-halogen bond with progressive substitution of fluorine atoms. Resonance hybrids are proposed as the major contribution Similar effects have been observed in silicon compounds and resonance hybrids have been proposed (2) using d-orbitals not available in the case of carbon. Ebsworth (3) gives a review of information regarding d-orbital participation in π bonding which has been extensively considered for second, but not third row elements.

The induced formation of partial double-bond character in the other group IV elements would be expected to occur with increasing difficulty, and there have been different interpretations drawn from a variety of techniques. The photoelectron spectra of the series $(MH_3)_2Y$ and MH_3SH (M = S, Si, Ge; Y = O, S, Se, Te) have been interpreted (4) on the basis of (p - d)π bonding with M = Si and Ge. Evidence for (p-d)π bonding between chlorine and silicon or germanium has also been drawn from the photoelectron spectra of the silyl and germyl halides (5). However, an ab initio molecular orbital calculation of the electronic structures of SiH_3F and GeH_3F (6) indicates that the spectra could be attributed to changes in the molecular structure on ionisation. Furthermore, the electric dipole moments of the series GeH_3X (S = Cl, Br, I) follow expected trends and do not support the postulation of (p-d)π bonding (7).

At present there is not a great deal of structural information known about germanium compounds, and it seems worthwhile to investigate the effect of halogen substitution in some simple molecules. A study of the germanium-carbon bond was undertaken for $(CH_3)_2GeH_2$ and $(CH_3)_4Ge$ by the vapor phase electron diffraction method to confirm the microwave structure of dimethylgermane (8) and to complete the methylgermane series. The molecular structures of CH_3GeF_3 and CH_3GeBr_3 have been examined to determine the effect of halogen substitution on the Ge-C and Ge-X bonds.

CHAPTER II

EXPERIMENTAL

The sample of tetramethylgermane was purchased from Alfa Inorganics Inc., while samples of $(CH_3)_2GeH_2$, CH_3GeF_3 and CH_3GeBr_3 were prepared and purified by Dr. R.T. Hemmings, to whome the author expresses his sincere thanks. Dimethylgermane was prepared (9) from $LiAlH_4$ reduction of dichloro(dimethyl)germane in $n\text{-}Bu_2O$. The purity was established from the vapor pressure (9), infra red and Raman bands (10) and from the reported ^1H n.m.r. spectrum (11). The purity of $(CH_3)_4Ge$ was verified by comparison with the reported vapor pressure (12), vibrational spectra (13) and ^1H n.m.r. spectrum (11). The sample of CH_3GeF_3 was prepared (14) from $Pb(II)F_2$ exchange with CH_3GeBr_3 and the purity established from the ^1H n.m.r. spectrum, infra red and Raman bands, sublimation pressure and melting point (15). The tribromide was prepared (16) by HBr exchange with CH_3GeCl_3 at room temperature and its purity was checked by ^1H n.m.r. (17), and infra red and Raman spectroscopy (18). The impurities in each sample were estimated to be less than 2%.

Sectored electron diffraction photographs were recorded on 4 x 5 in. Kodak Electron Image Plates using the instrument described in Part I. An accelerating voltage of about 58kV for nozzle to plate distances of 296.16 mm and 95.45 mm as measured with a cathetometer provided useful data covering the range $7 < q < 130$ $Å^{-1}$ where $q = (40/\lambda)\sin(\theta/2)$. Scale factors were obtained from CS_2 diffraction patterns taken concurrently with the gas patterns. The temperature at the nozzle was about 20^oC. Tracings of the diffraction patterns were obtained using a Jarrell Ash microphotometer modified with a rotating stage and digital output (19) The relative intensities interpolated at integral q for $(CH_3)_2GeH$, $(CH_3)_4Ge$, CH_3GeF_3 and CH_3GeBr_3 are reproduced in Appendices C - F respectively.

CHAPTER III

ANALYSIS

The relative intensities obtained from traces of different plates taken under the same conditions were scaled and averaged to reduce the effect of random fluctuations. The experimental molecular intensity was calculated from each composite curve according to

$$M_{exp}(s) = \frac{s^4}{I_a(s)} \cdot \frac{I_x(s) - B(s)}{\phi(s)}$$

where $I_x(s)$ is the experimental sectored intensity

$I_a(s)$ is the theoretical atomic scattering

$B(s)$ is the experimental background

$s = \pi q/10$

The curves were then spliced together (20). The experimental molecular intensity curve was fitted by a least squares procedure (19) which incorporated the Hartley modification (21). A diagonal weight matrix was based on the variance of each data point, and correlations of errors between data points was allowed for by means of a non-diagonal weight matrix (22).

The scattering factors used were obtained by a four-point interpolation to 58 kV from the values tabulated by Bonham, Schafer and Yates (23). Anharmonicity corrections were made for bonded atom

pairs (24,25). The structures were parametrized by means of a set of standard coordinate types (26). The calculated parameter values are based on r_g distances.

CHAPTER IV

RESULTS

In view of the microwave structure for dimethylgermane (8) and the tetrahedral geometry of tetramethylgermane, the choice for initial parameters in these molecules was routine. For the methyl trihalides, the input value for the Ge-C distance was that found in $(CH_3)_3GeCl$ (27), the Ge-F bond distance was taken from GeF_4 (28) and the Ge-Br bond distance from $GeBr_4$ (29). The final estimates for the bond distances and angles are presented in Table I. Estimates for the root mean square amplitudes of vibration are given in Table II. The errors are three times those calculated from the least squares analysis and are estimated to be at the 95% confidence level. Drawings of the structures of $(CH_3)_2GeH_2$, $(CH_3)_4Ge$, CH_3GeF_3 and CH_3GeBr_3 are presented in Figures 1 through 4 respectively.

The molecular scattering curve for dimethylgermane is reproduced in Figure 5. The radial distribution function which is shown in Figure 6 illustrates some of the problems encountered in the parameter refinements. The Ge-C bond distance is well resolved, but the contribution to the scattering curve from non bonded Ge..H distances is greater than that due to the bonded pairs C-H and Ge-H. Least squares refinements tend to fit the Ge..H contribution rather than the C-H and Ge-H parameters directly. When the CGeC angle was allowed to vary a value of 106 degrees was found, all other parameters remaining

Table I

The structural parameters[a] and standard deviations for $(CH_3)_2GeH_2$, $(CH_3)_4Ge$, CH_3GeF_3 and CH_3GeBr_3

Parameter	$(CH_3)_2GeH_2$	$(CH_3)_4Ge$	CH_3GeF_3	CH_3GeBr_3
Ge-C	1.953 ± 0.003	1.955 ± 0.005	1.921 ± 0.012	1.87 ± 0.04
Ge-X	1.56 ± 0.04	-	1.708 ± 0.003	2.284 ± 0.002
C-H	1.074 ± 0.016	1.08 ± 0.03	1.14 ± 0.08	1.08[b]
<CGeC	110.0[b]	109.47[b]	-	-
<CGeX	109.5[b]	-	114.0 ± 0.1	111.2 ± 0.3
<XGeX	108.9[b]	-	104.6 ± 0.9	107.7 ± 0.3

[a]Bond lengths are r_g values in A units, angles in degrees

[b]Parameter constrained during least squares.

Table II

Root mean square amplitudes of vibration[1] and standard deviations for $(CH_3)_2GeH_2$, $(CH_3)_4Ge$, CH_3GeF_3 and CH_3GeBr_3

Parameter	$(CH_3)_2GeH_2$	$(CH_3)_4Ge$	CH_3GeF_3	CH_3GeBr_3
Ge-C	0.046 ± 0.004	0.044 ± 0.007	0.045[2]	0.042 ± 0.06
Ge-X	0.08[2]	-	0.051 ± 0.003	0.047 ± 0.002
C-H	0.078[2]	0.078[2]	0.078[2]	0.078[2]
Ge..H	0.079 ± 0.015	0.085 ± 0.029	0.09[2]	0.1[2]
C..C	0.09[2]	0.086 ± 0.029	-	-
C..X	0.12[2]	-	0.089 ± 0.021	0.076 ± 0.036
X..X	0.13[2]	-	0.094 ± 0.016	0.105 ± 0.006

[1]Parameters are in A units

[2]Constrained during final least squares

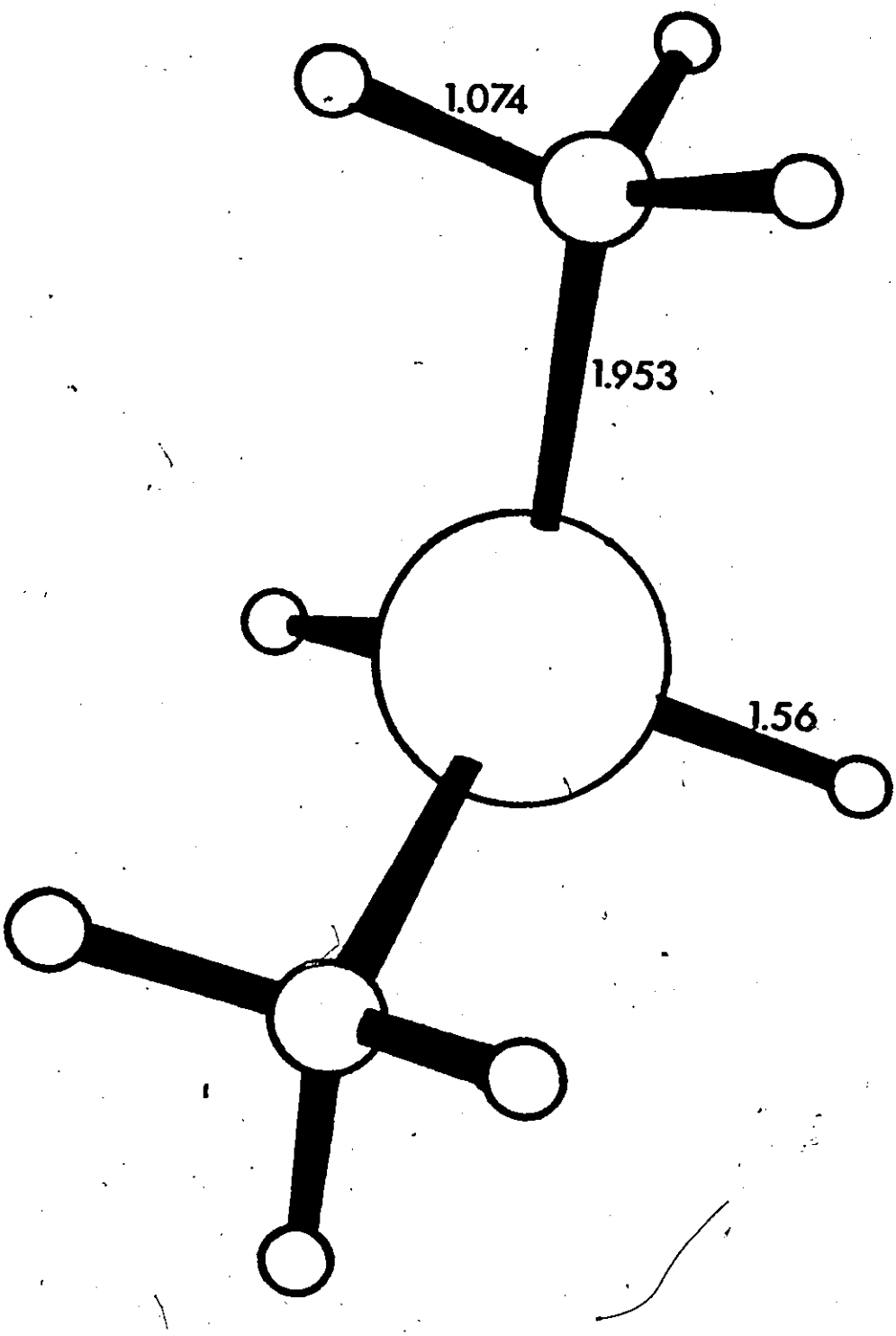

Figure 1. The Molecular Structure of Dimethylgermane

Figure 2

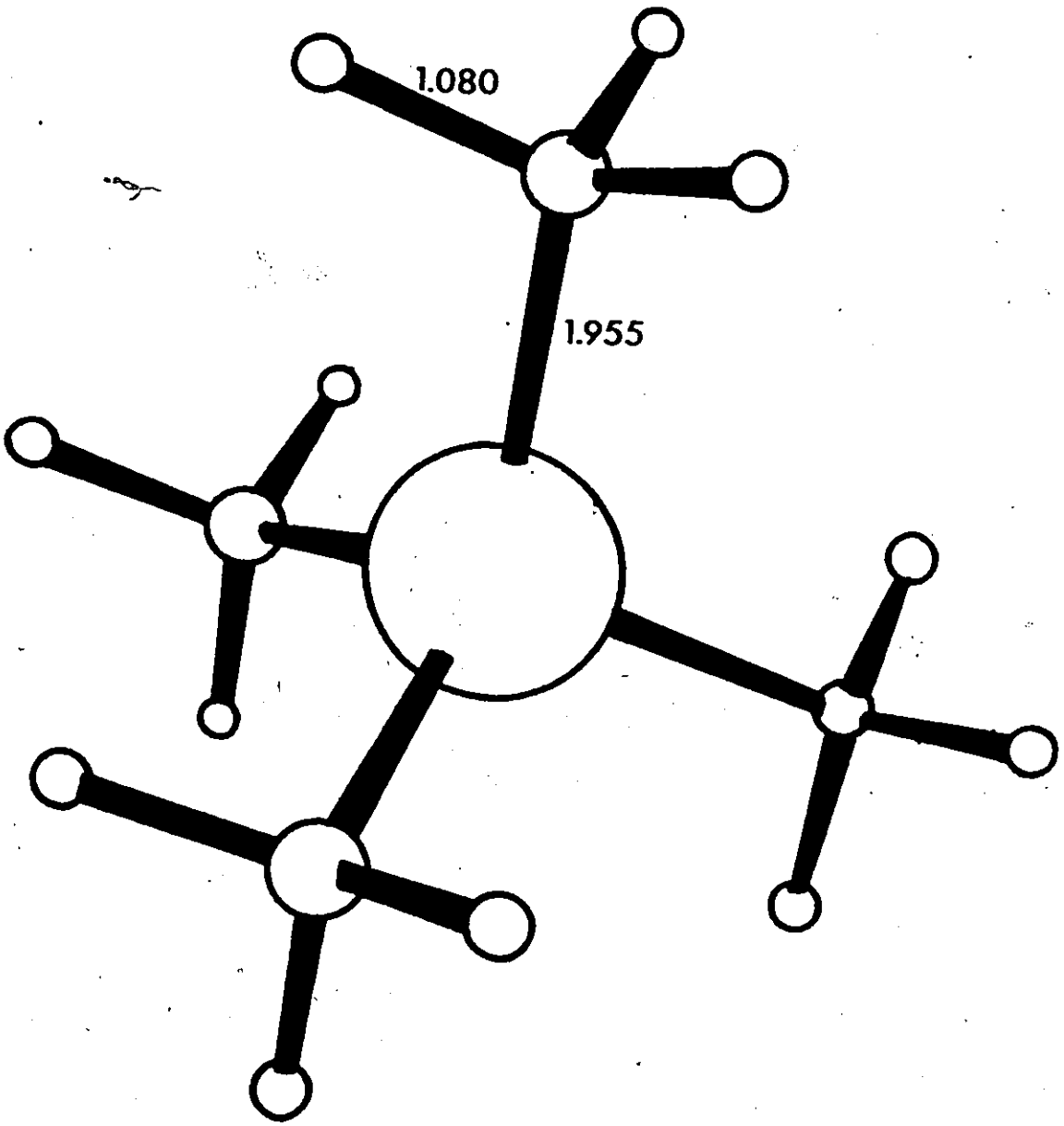

Figure 2. The Molecular Structure of Tetramethylgermane

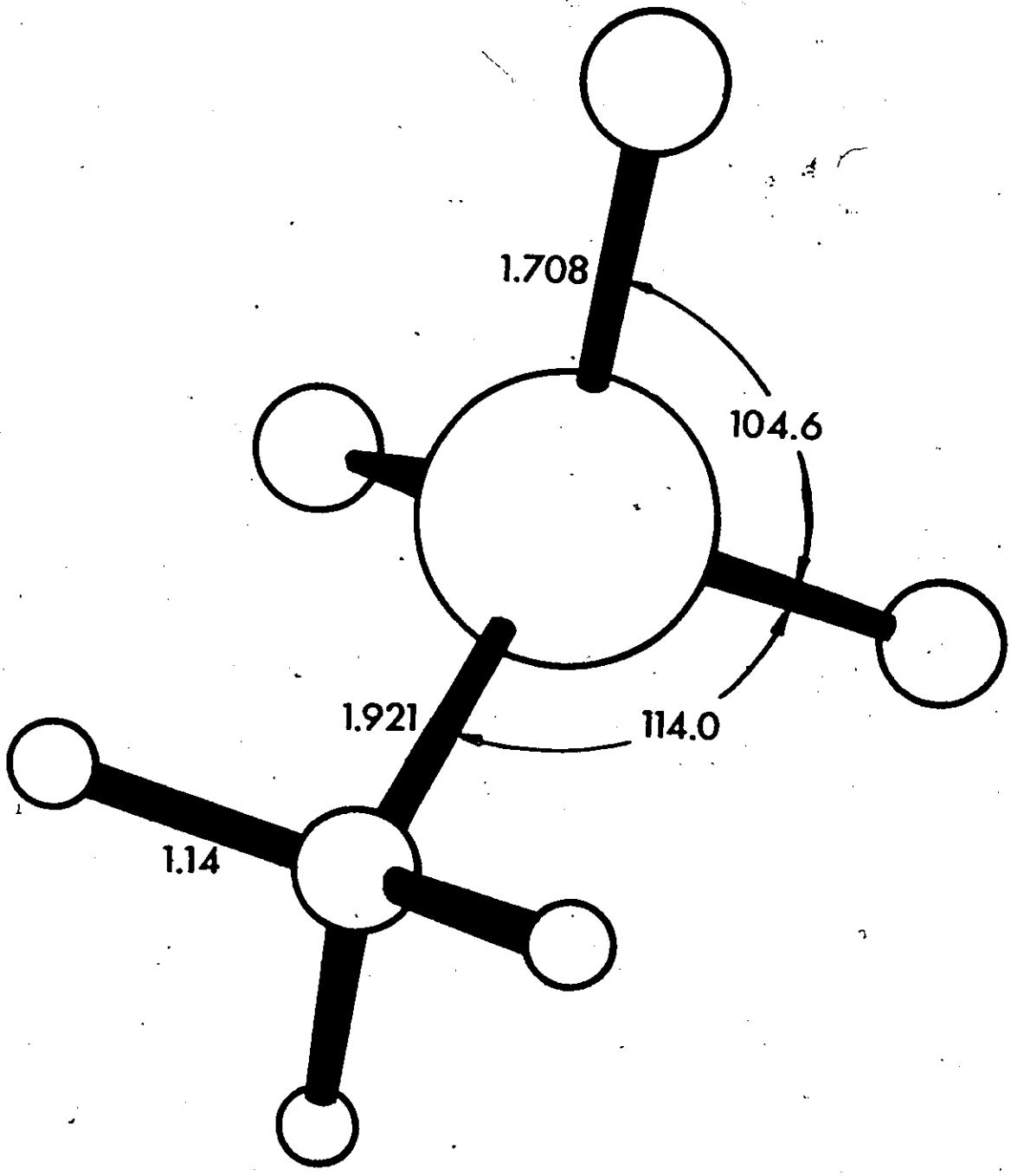

Figure 3. The Molecular Structure of Trifluoro(methyl)germane

Figure 4

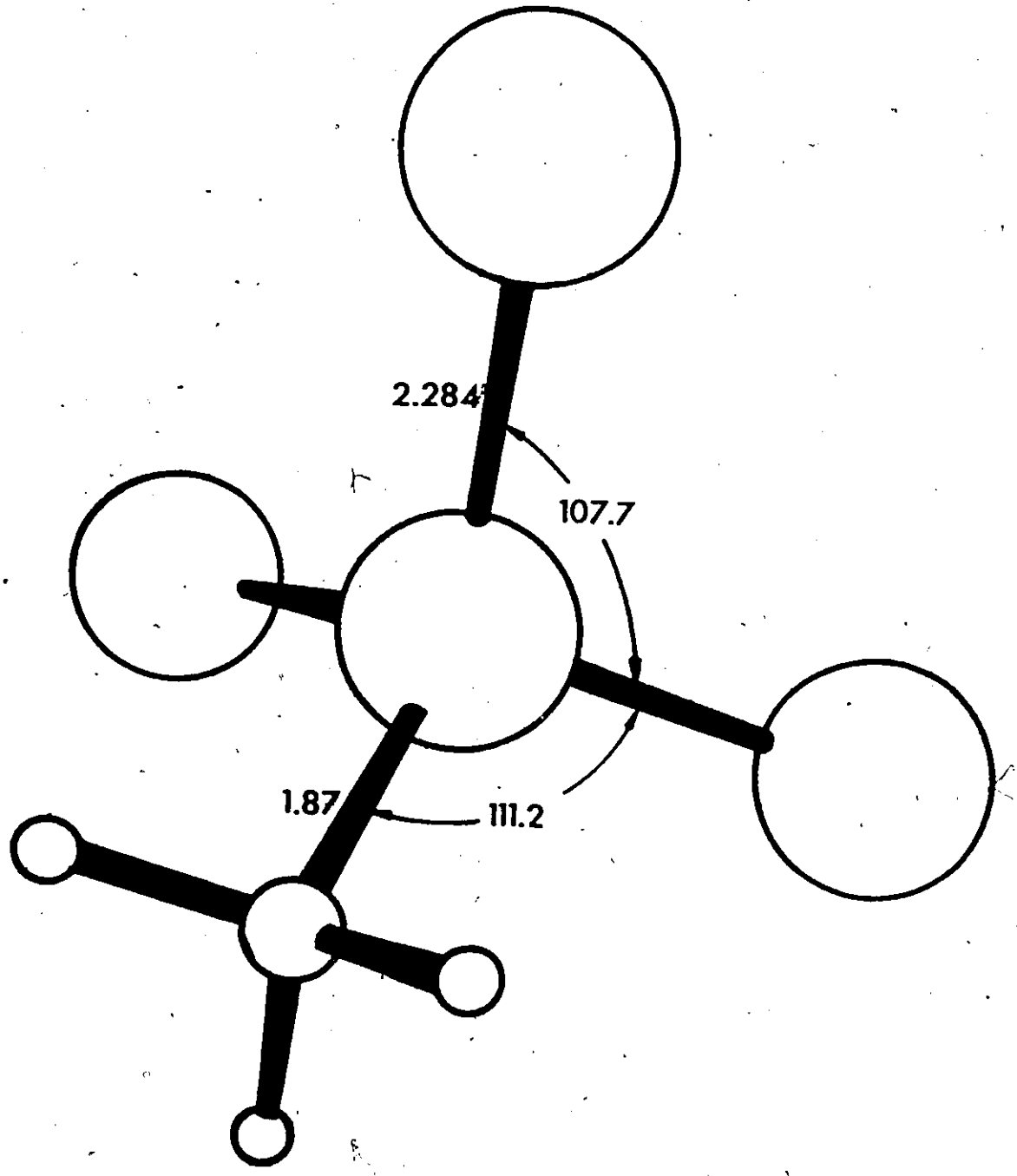

Figure 4. The Molecular Structure of Tribromo(methyl)germane

Figure 5

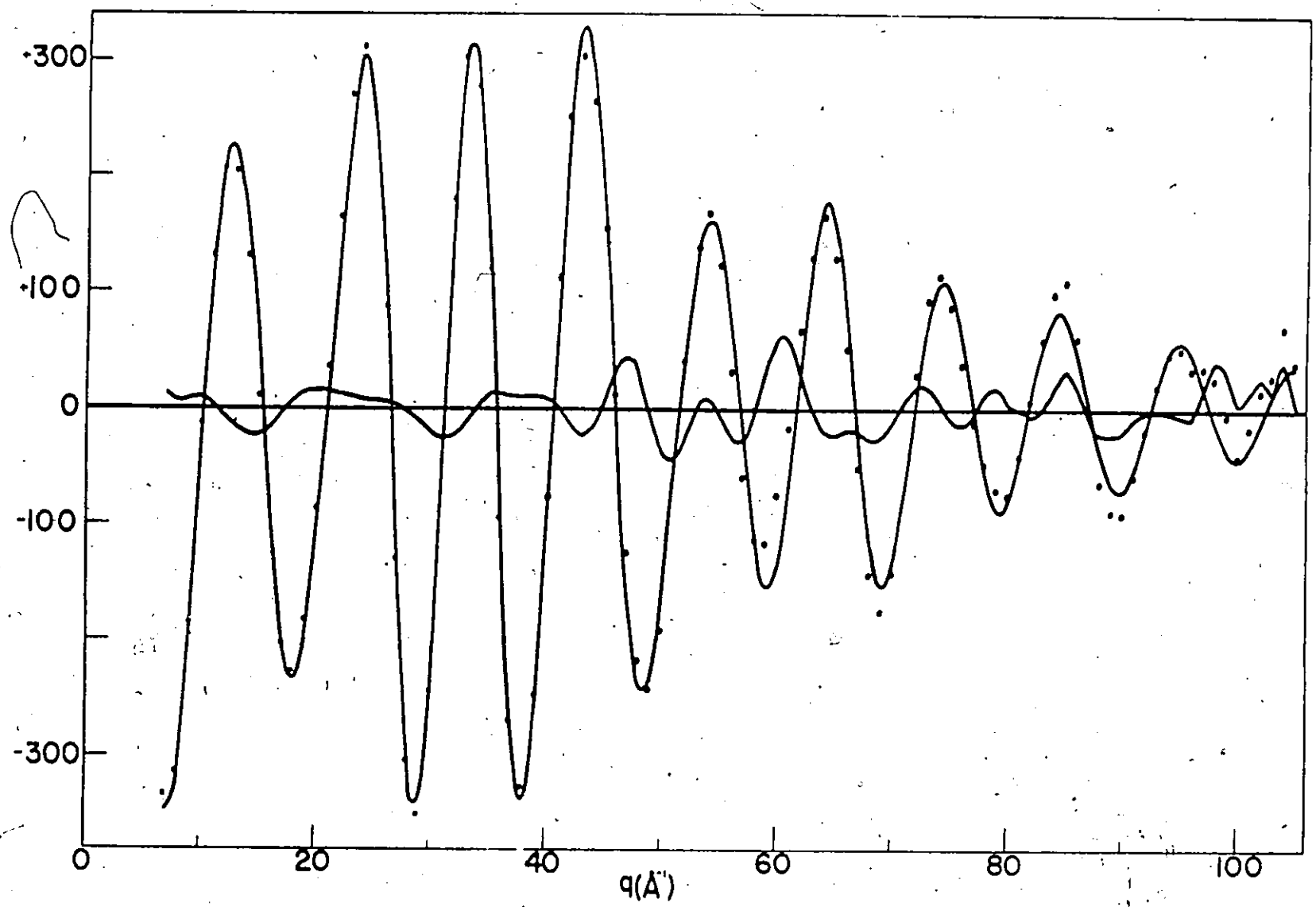

Figure 5. The Theoretical, Experimental (dots) and Difference Molecular Scattering Curve for Dimethylgermane.

Figure 6

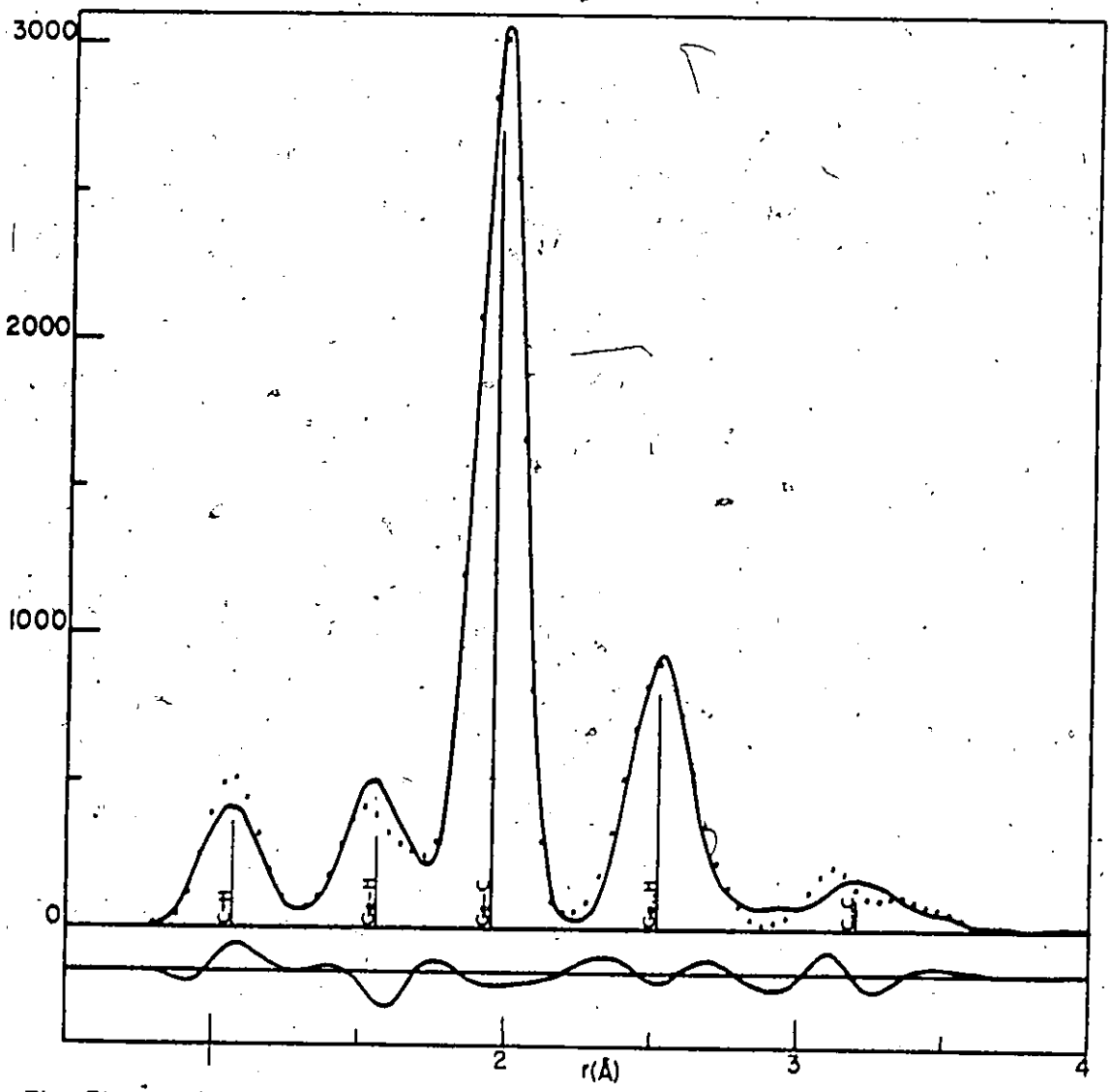

Figure 6. The Theoretical, Experimental (dots) and difference Radial Distribution Function for Dimethylgermane.

unchanged within the estimated errors. Accordingly, this angle was constrained to 110.0 degrees (8). There were no large correlations between the parameters.

The molecular scattering curve and radial distribution function for tetramethylgermane are shown in Figures 7 and 8 respectively. Once again, the radial distribution function illustrates that the non-bonded contributions of Ge..H and C..C are larger contributors to the molecular scattering than the C-H bond. Correlations between parameters presented no problems during parameter refinements.

The molecular scattering curve and radial distribution function for CH_3GeF_3 are reproduced in Figures 9 and 10 respectively. Although correlations between the parameters were small, the contribution due to the Ge-C bond at 1.92Å appears as a shoulder on the Ge-F bond. Attempts to simultaneously refine the Ge-C mean square amplitude resulted in an unrealisticly large value of 0.068Å, all other parameters remaining at those given in Tables I and II, within the quoted uncertainities . The Ge-C mean square amplitude was therefore constrained to 0.045Å in accordance with the value for this parameter in di- and tetra methyl germane.

The molecular scattering curve and radial distribution function for CH_3GeBr_3 are illustrated in Figures 11 and 12 respectively. The radial distribution function shows that the Ge-C contribution is relatively small and that the non-bonded C..Br distance appears as a shoulder on Br..Br. Although correlations between the parameters

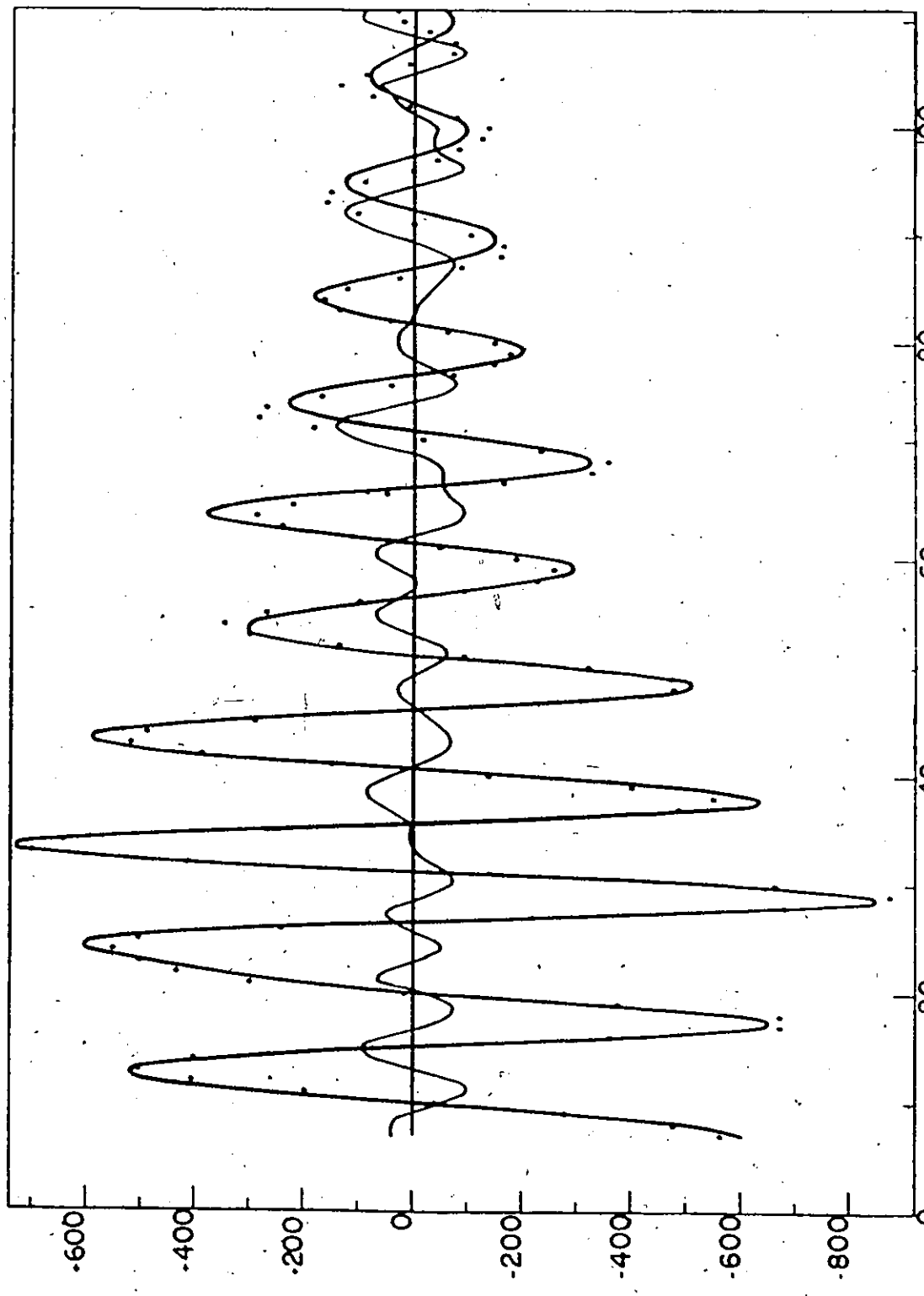

Figure 7. The Theoretical, Experimental (dots) and Difference Molecular Scattering Curve for Tetramethylgermane.

Figure 8

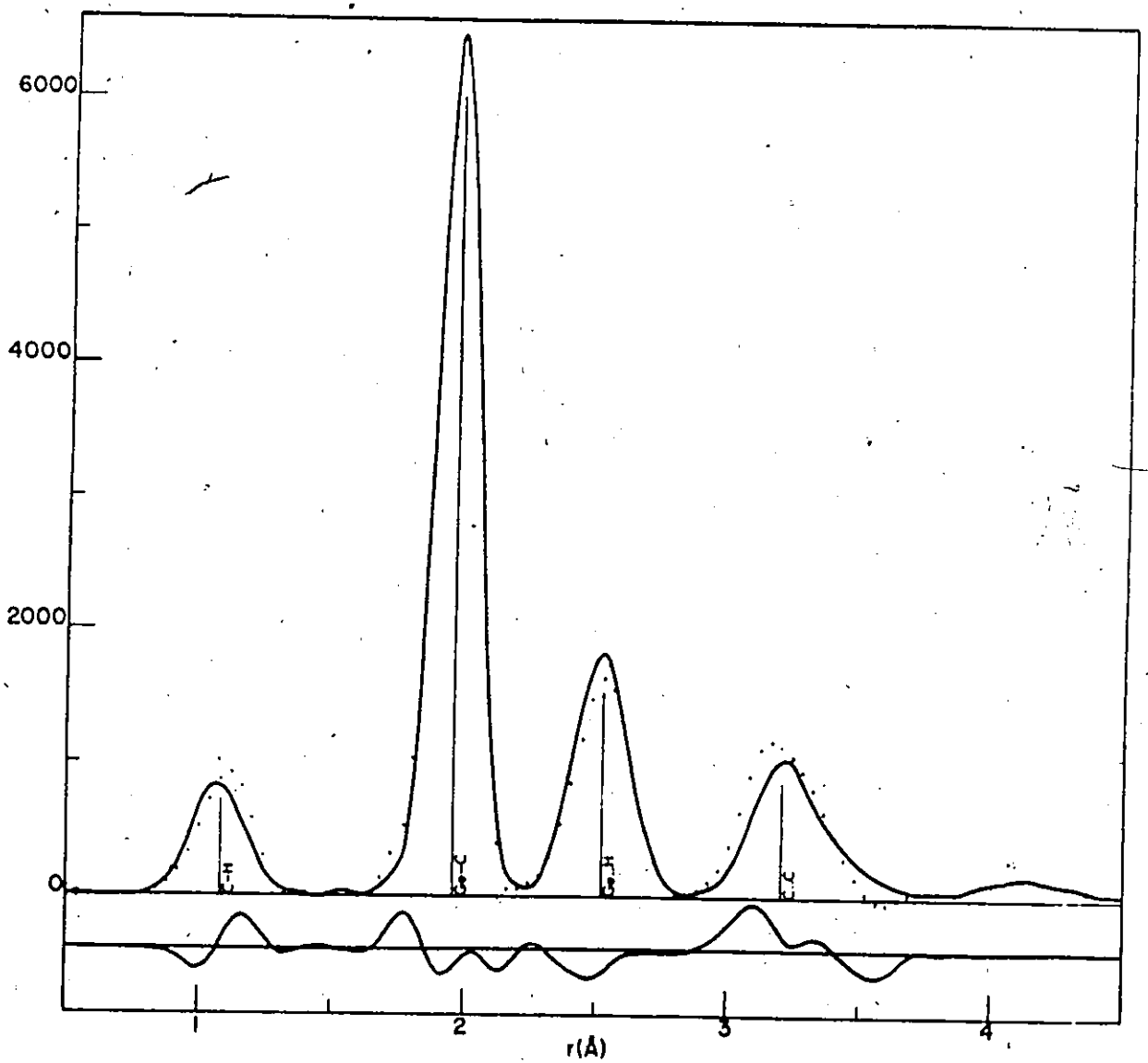

Figure 8. The Theoretical, Experimental (dots) and Difference Radial Distribution Function for Tetramethylgermane.

Figure 9

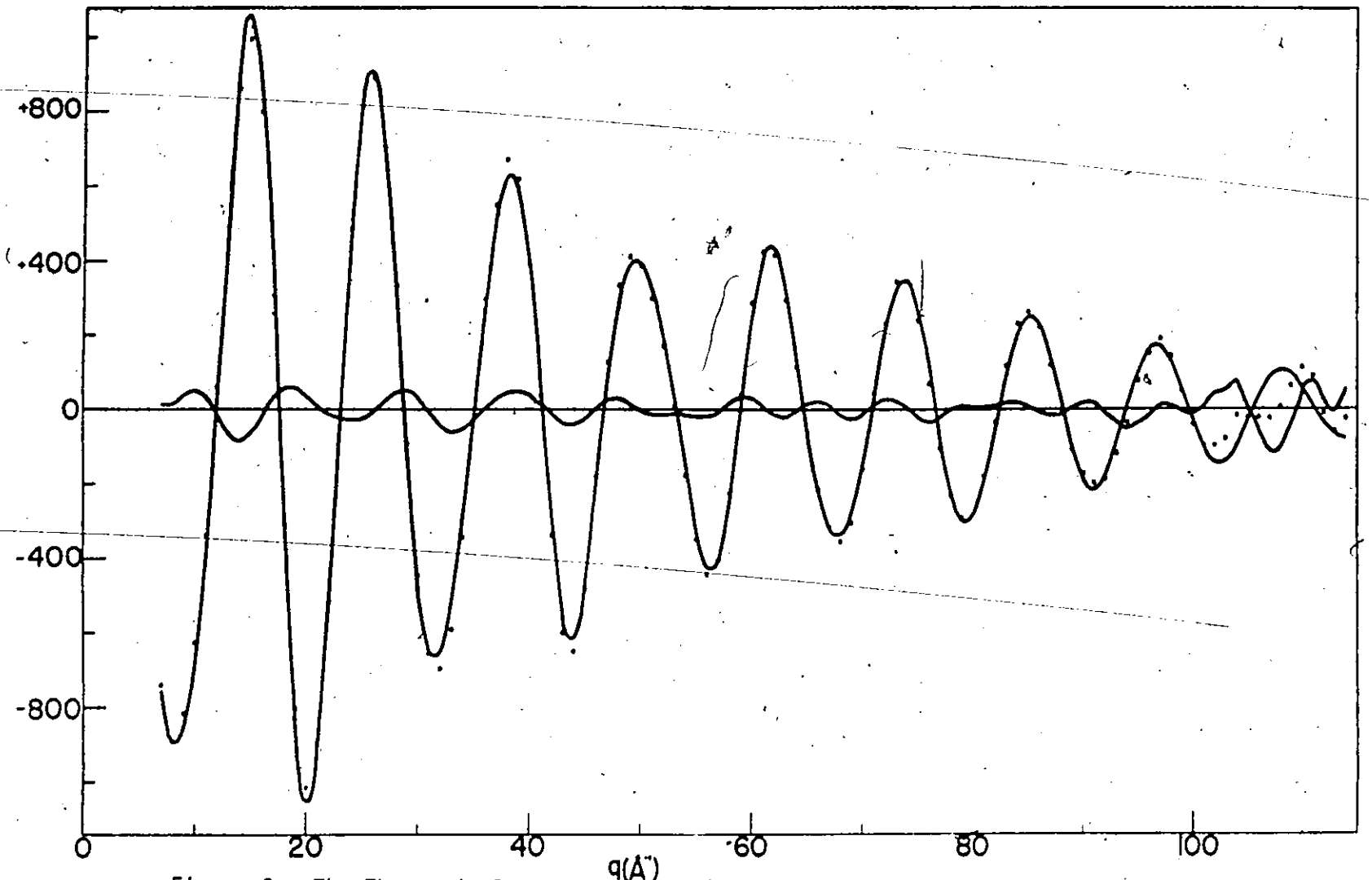

Figure 9. The Theoretical, Experimental (dots) and Difference Molecular Scattering Curve for Trifluoro(methyl)germane

Figure 10

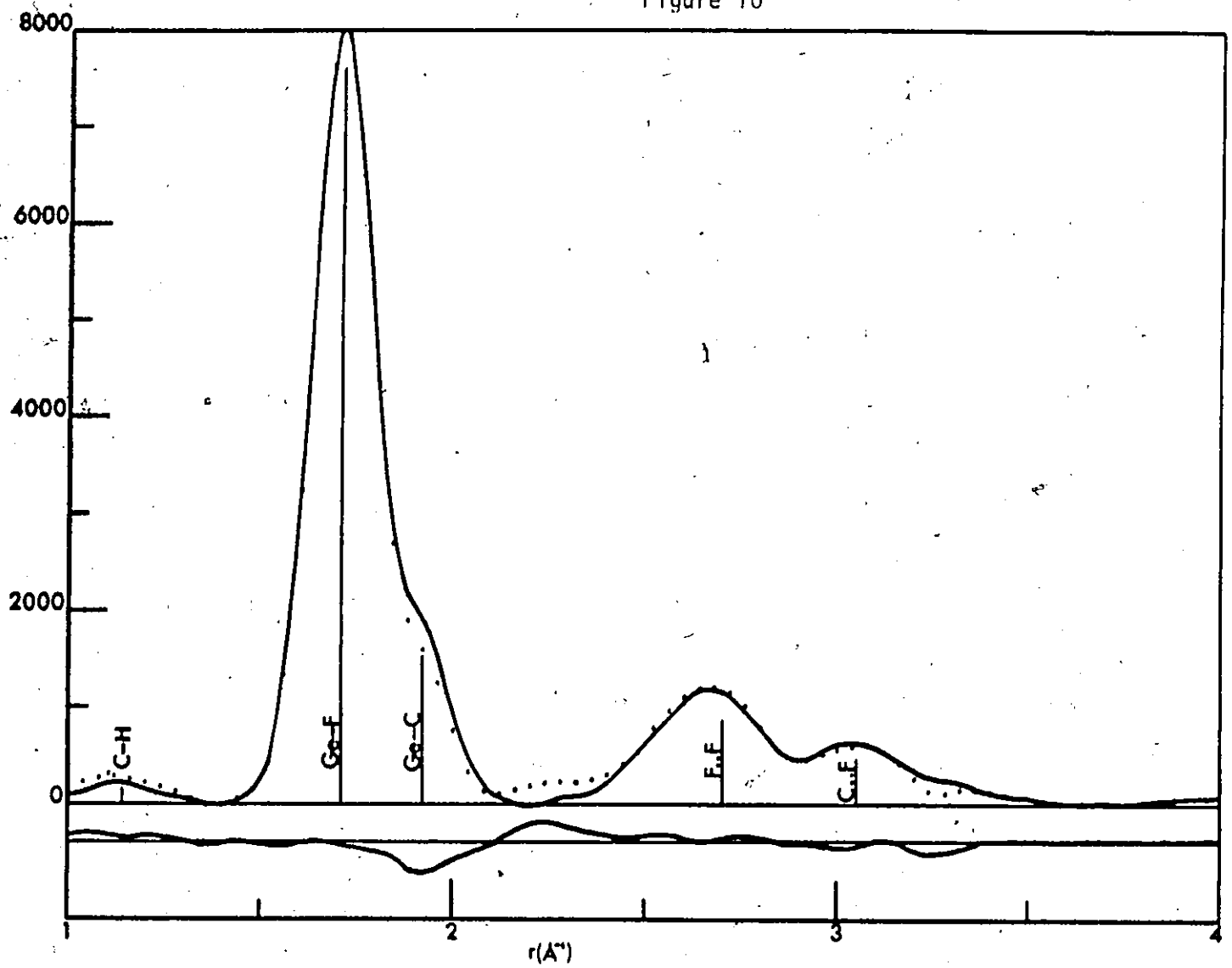

Figure 10. The Theoretical, Experimental (dots) and Difference Radial Distribution Function for Trifluoro(methyl)germane.

Figure 11

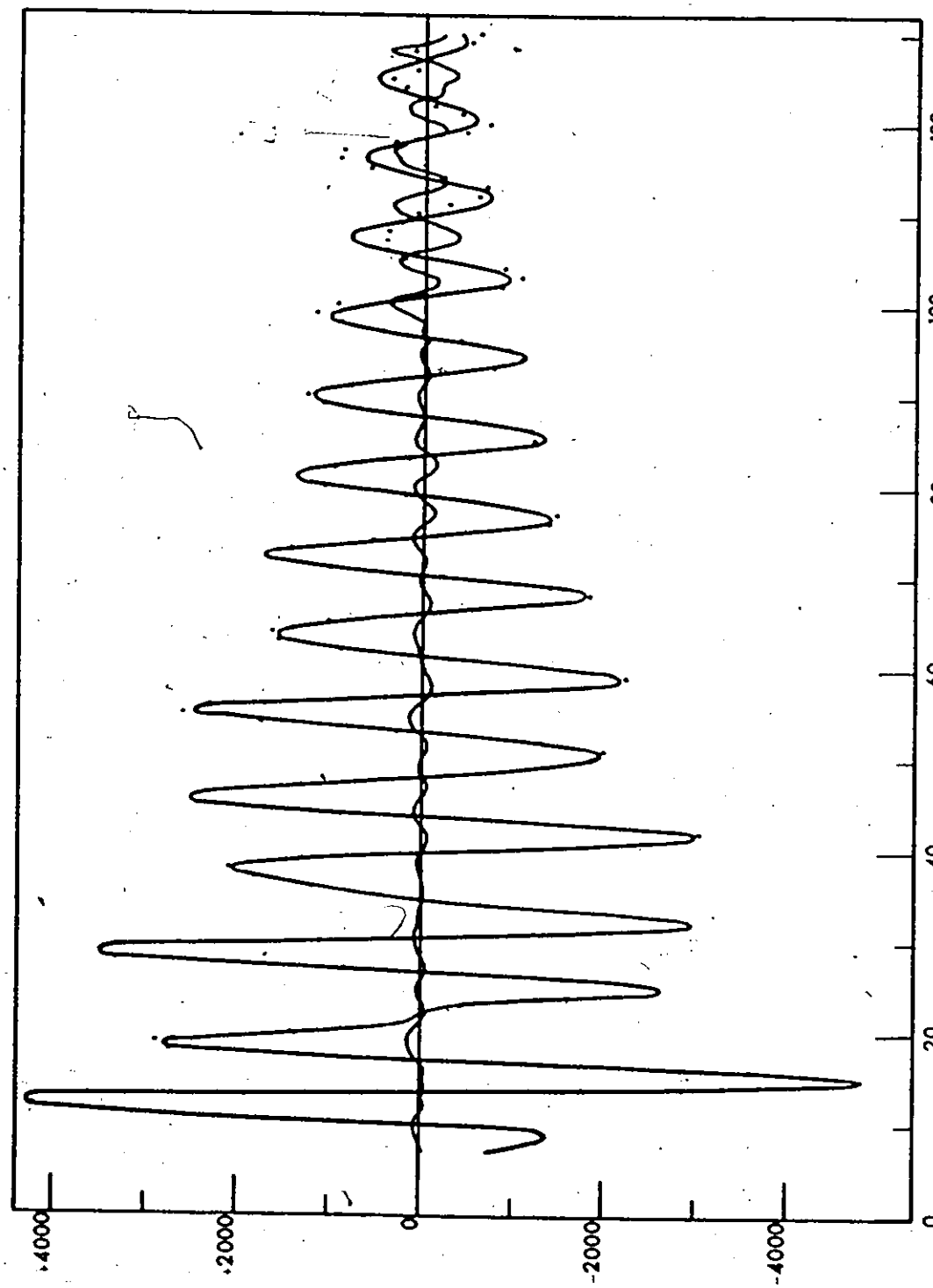

Figure 11. The Theoretical, Experimental (dots) and Difference Molecular Scattering Curve for Tribromo(methyl)germane.

Figure 12

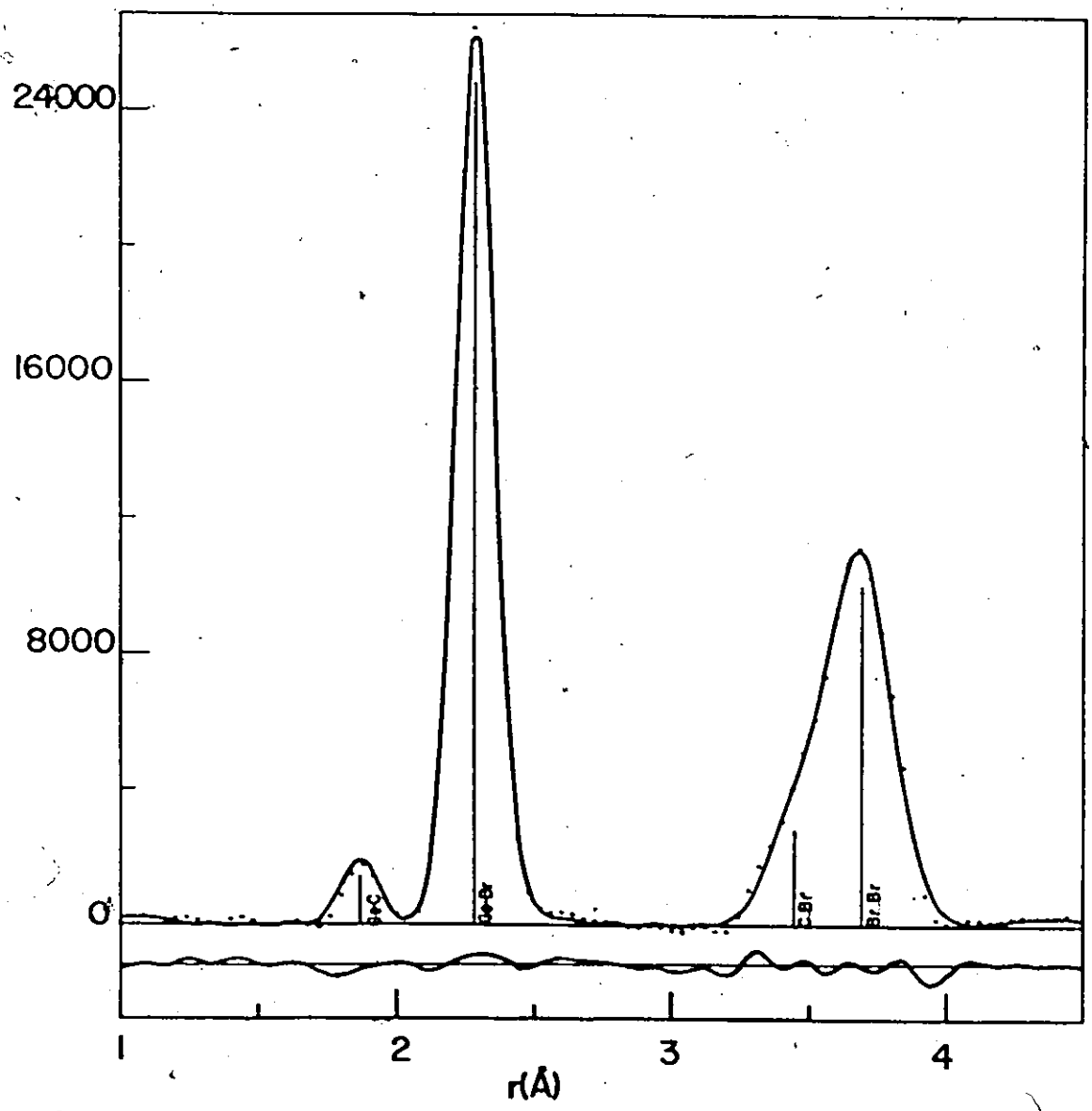

Figure 12: The Theoretical, Experimental (dots) and Difference Radial Distribution Function for Tribromo(methyl)germane

were small, the Ge-C bond cannot be accurately determined. The contribution due to C-H is of the order of the error curve in this molecule, and the parameter was constrained during least squares refinements.

The non-bonded interatomic distances (excluding those involving hydrogen atoms bonded to carbon) are given in Table III, and the correlation matrices derived from the least squares refinement are listed in Appendix G.

Table III

Non-bonded Interatomic Distances of the Heavy Atoms[1] in $(CH_3)_2GeH_2$, $(CH_3)_4Ge$, CH_3GeF_3 and CH_3GeBr_3

	$(CH_3)_2GeH_2$	$(CH_3)_4Ge$	CH_3GeF_3	CH_3GeBr_3
X..X	2.628	-	2.703	3.688
C..X	2.851	-	3.046	3.435
C..C	3.200	3.193	-	-

[1]Hydrogen atoms bonded to carbon are excluded

CHAPTER V

Discussion on the Metal-Carbon Bond for the Group IV Elements

Listed in Table IV are the available M-C bond lengths in the series $M(CH_3)_{4-n}H_n$ where M = Si, Ge, Sn, Pb. Bond lengths (r_s) deduced from microwave studies of isotopically substituted molecules are close to the equilibrium values r_e (40). The thermally averaged distance r_g which can be determined from electron diffraction may be corrected to an approximate r_e value (24), which is comparable to within a few thousands of an angstron to the r_s value:

$$r_e = r_g - \frac{3}{2} a_{ij} \ell_{ij}^2 \qquad (1)$$

The anharmonic constant a_{ij} used for the Ge-C bond was $2A^{-1}$; ℓ_{ij} is the estimated root mean square amplitude of vibration. Table IV shows excellent agreement of the M-C bond in the series $M(CH_3)_{4-n}H_n$ (M = Si, Ge) as determined by electron diffraction and microwave when to an approximate common bond length definition (r_e) is made. The Ge-C bond length in tetramethylgermane as determined from the present study represents a considerable improvement over an earlier value of 1.98 ± 0.03A (41).

An unweighted estimate for the mean equilibrium Si-C bond length in the methyl silanes is 1.868A with an estimated standard deviation of 0.001A. The corresponding values for the Ge-C bond are 1.948 and 0.001A. It is readily apparent that the Ge-C bond in the methyl germanes exhibits a constant value as is the case for the Si-C bond in the methyl silanes.

Table IV

M-C Bond Lengths in $M(CH_3)_{4-n}H_n$. M = Si, Ge, Sn, Pb

	CH_3MH_3		$(CH_3)_2MH_2$		$(CH_3)_3MH$		$(CH_3)_4M$	
Si-C	r_s = 1.867±0.001	(30)	r_s = 1.867±0.002	(31)	r_s = 1.868±0.002	(32)	r_e = 1.869±0.003 r_g = 1.878±0.002	(33)
Ge-C	r_s = 1.945±0.001	(34)	r_s = 1.950±0.003 r_e = 1.947±0.003 r_g = 1.953±0.003	(8) (this work)	r_s = 1.947±0.006	(35)	r_e = 1.949±0.005 r_g = 1.955±0.005	(this work)
Sn-C	r_s = 2.143±0.002	(36)	2.150±0.003	(37)	2.147±0.004	(37)	r_g = 2.134±0.007	(38)
Pb-C	-		-		-		r_e = 2.229±0.009 r_g = 2.238±0.009	(39)

The r_g (Si-Si) bond length in hexamethyldisilane (33) is 2.342 ± 0.009Å (ℓ(Si-Si) = 0.068Å) and in disilane (42) it is 2.331 ± 0.003Å (ℓ(Si-Si) = 0.046Å). The r_e bond distances are thus 2.328 and 2.325Å respectively. An estimate for the bonding radius of silicon can then be made as 1.163 ± 0.003Å. Based on the C-C bond length in ethane (43) the bonding radius of carbon is 0.767 ± 0.001Å. Simple additivity of radii yields a predicted Si-C bond length of 1.930 ± 0.004Å, a value 0.062Å larger than determined in the methyl silanes. This shortening and the possibility of it being due to $p\pi - d\pi$ interaction has been pointed out previously (33).

Similar arguements can be made for the Ge-C bond. The r_g (Ge-Ge) distance in digermane (44) is 2.404 ± 0.003Å. Given the observed mean square amplitude of vibration of 0.047 ± 0.012, the correction to an r_e (Ge-Ge) distance is thus 2.397Å, and the approximate bonding radius for germanium is then 1.199Å. Using this value, the predicted Ge-C bond length is 1.966Å which is 0.018Å larger than experimentally found. This is a much smaller difference than the 0.062Å found for the Si-C bond, and indicates that although the M-C bond length does not vary with the number of methyls substituted in either the germanes or silanes, the nature of the bonding in the two cases may be different.

Despite objections (45) that Pauling's electronegativity values (1) for silicon and germanium are based on bonds which may involve some $(p\text{-}d)\pi$ bonding, the unbiased electronegativities of Si and Ge that have been calculated (45) are still approximately equal. It may therefore be instructive to use Pauling's scheme on a quantitative basis to compare

The Si-C and Ge-C bonds. The electronegativity differences, 0.7, is the same for both pairs and leads to a prediction of 12% ionic character in both bonds (1). The shortening calculated by the Schomaker-Stevenson relationship (46) is 0.042 Å for Si-C and 0.028Å for Ge-C. This leads to a prediction for the Si-C bond length of 1.888 Å, which is larger by 0.020Å than experimentally found. This difference is of the order of the reliability of the Schomkaer-Stevenson equation, and cannot be relied on to suggest bond shortening by (p-d)π interaction in the Si-C bond. It is of note that ab initio LCAO-MO calculations (47) suggest that 10% of the total overlap population for the Si-C bond in methylsilane is due to (p-d)π interaction. The calculated value for the Ge-C bond length is 1.938 Å, which is 0.010 Å shorter than experimentally determined, but well within the reliability of the Schomaker-Stevenson relationship. No evidence for d-orbital involvement can be drawn from the Ge-C bond length.

The electron diffraction technique cannot accurately determine the C-Ge-C angle in $(CH_3)_2GeH_2$. However, the microwave study (8) has determined this angle to be slightly larger than tetrahedral, and a similar result was found for the angle C-Si-C in dimethylsilane (31). It is likely that the small difference in electronegativity of hydrogen as compared to carbon is not enough to affect the bond angles in the manner proposed by Bent (48) and that the major influence is due to non-bonded interactions (49). The Van der Waals radius of the methyl group is about 2.0Å as compared to about 1.2Å for hydrogen.

In the methylstannane series only the structure of CH_3SnH_3 has been published to date (36). The Sn-C bond length was found to be

r_e = 2.143 ± 0.002Å, and it is interesting to note that preliminary values for the Sn-C bond length in $(CH_3)_2SnH_2$ and $(CH_3)_3SnH$ (37) are 2.150 ± 0.003 and 2.147 ± 0.004Å respectively. These preliminary values are probably electron diffraction results and, if so, are in excellent agreement with the Sn-C bond length in CH_3SnH_3 determined by the microwave method. The preliminary Sn-C bond length in tetramethylstannane (38) is r_g = 2.134 ± 0.007Å, which is rather less than expected from the results of other methylstannanes. The preliminary value for the Sn-C bond length in tetramethylstannane therefore is difficult to reconcile in view of the results for the methyl-silanes and germanes. However, discussion on the methylstannane series is without a firm foundation until final publication of their structures.

CHAPTER VI

Discussion on the Molecular Structures of CH_3GeF_3 and CH_3GeBr_3

One of the general features of structural chemistry is a progressive decrease in M-X bond length on increasing the amount of electronegative substitution. In the case of first-row elements, Bent (48) has inferred that the decrease in bond length which is observed with progressive electronegative substitution is due to an increase in s character of the bond. Both Bent's interpretation and the VSEPR theory (50) lead to quantitative predictions for the bond angles in molecules with atoms of different electronegativity. Table V shows a progressive decrease of the Si-F bond in the fluorosilane series and Table VI illustrates that increasing substitution of fluorine in the methylfluorosilane series also causes a shortening of the Si-C bond. This effect has been attributed (3) to resonance structures using the 3d-orbitals of silicon.

There is less structural data available for germanium compounds, and no series as complete as those listed in Tables V and VI. However, the trend is for progressive shortening of the Ge-X and Ge-C bond lengths with increasing amounts of halogen substitution. For instance, the Ge-Cl bond length in $GeCl_4$ (55) is $r_e = 2.106 \pm 0.004$ Å and in $ClGeH_3$ (56) the value is $r_s = 2.148 \pm 0.003$Å, a difference of 0.042 ± 0.007Å. Using a value of 0.99 Å for the single bond radius of the chlorine atom, and making the Schomaker-Stevenson electronegativity correction (46), the predicted Ge-Cl single bond length is 2.141Å, in excellent agreement with the result for $ClGeH_3$. The decrease of the Ge-Cl bond length in the tetra-

Table V

The Si-F bond lengths of fluorinated silanes

Molecule	Si-F	Reference
SiH_3F	$r_s = 1.593 \pm 0.002$	51
SiH_2F_2	$r_s = 1.577 \pm 0.001$	52
$SiHF_3$	$r_s = 1.562 \pm 0.005$	53
SiF_4	$r_e = 1.546 \pm 0.002$	54
	$r_g = 1.552 \pm 0.002$	

Table VI

The Si-F and Si-C bond lengths of methyl fluorosilanes

Molecule	Si-F	Si-C	Reference
CH_3SiH_3	-	$r_s = 1.867 \pm 0.001$	30
CH_3SiH_2F	$r_s = 1.600 \pm 0.005$	$r_s = 1.848 \pm 0.005$	57
CH_3SiHF_2	$r_s = 1.583 \pm 0.002$	$r_s = 1.833 \pm 0.002$	58
CH_3SiF_3	$r_s = 1.574 \pm 0.007$	$r_s = 1.812 \pm 0.014$	59

chloride is 0.032Å and might be due to some (p-d)π interaction. The reported Si-Cl bond lengths in $SiCl_4$ (60) and in $ClSiH_3$ (61) are r_e = 2.013 ± 0.004 and r_s = 2.048 ± 0.001Å respectively. The difference is 0.035Å which, within the estimated errors, is the same as that observed in the germanium molecules. The predicted Si-Cl bond length is 2.079Å, which is 0.03Å longer than found in $ClSiH_3$ and might be due to a small amount of (p-d)π overlap.

The most precise determination of the Ge-C bond length in a molecule with halogen substitution to date is r_s = 1.9400 ± 0.0001 Å in $(CH_3)_3GeCl$ (62). This is a small (0.007Å) but significant decrease of the Ge-C bond length as compared with that found in $(CH_3)_3GeH$ (35). The Ge-Cl bond length was fo nd to be r_s = 2.170 ± 0.001Å which is 0.064Å longer than in $GeCl_4$. For comparison, the Si-C and Si-Cl bond lengths in $(CH_3)_3SiCl$ have been determined (63) as r_s = 1.857 ± 0.005 and 2.022 ± 0.05Å respectively. The large uncertainity in the Si-Cl bond length makes meaningful comparisons difficult, but the value for the Si-C bond length is 0.011Å shorter than in $(CH_3)_3SiH$ (32), a shortening similar to that in the corresponding germanium compounds. However, there is a difference in the angles reported, <CGeCl being 106.2° in $(CH_3)_3GeCl$ and <CSiCl being 110.5° in $(CH_3)_3SiCl$. It should be noted that in $(CH_3)_3SiCl$ the CSiCl angle is reported to be larger than the CSiC angle, a relative difference which would not be predicted by either the VSEPR theory (50) or Bent's rules (48).

The molecular structure of CH_3GeF_3 furter illustrates the power of increasing halogen substitution to shorten the Ge-C and Ge-X bond lengths.

The following values for the Ge-F bond length have been determined: r_s = 1.751 ± 0.005 in CH_3GeH_2F (64), r_s = 1.735 ± 0.01 in GeH_3F (65), r_g = 1.708 ± 0.003Å in CH_3GeF_3, and r_g = 1.67 ± 0.03Å in GeF_4 (28). The predicted value of the Ge-F bond length, making the electronegativity correction (46) is 1.743 Å, which is 0.043Å larger than the equilibrium distance found in this work. Making allowances for the crude approach taken in using the Schomaker-Stevenson equation, there still appears to be some shortening of the Ge-F bond in this molecule that might be due to (p-d)π interaction. Dipole moment studies of the series $(CH_3)_nGeF_{4-n}$ (66) indicates that (p-d)π bonding between germanium and fluorine is very small even in CH_3GeF_3. In contrast, the predicted Si-F bond length is 1.881Å which is 0.131Å longer than that determined in CH_3SiF_3 (59), and can only be accounted for by a significant amount of (p-d)π bonding. A comparison of the bond angles indicates that the Ge-F bond in CH_3GeF_3 might be slightly more polar than the Si-F bond in CH_3SiF_3. The FGeC angle is 114.0 ± 0.1° and the FSiC angle is 112.3 ± 1.1°.

The Ge-C bond distance is r_e = 1.915 ± 0.012Å in CH_3GeF_3 as compared to r_s = 1.925 ± 0.002Å in CH_3GeH_2F (64) and r_s = 1.945 ± 0.001Å in CH_3GeH_3 (36). Some shortening of the Ge-C bond seems to take place with increasing fluorine substitution though the effect is not as large as that found in the corresponding silicon molecules. Further indications of this effect have been observed from force constant studies on the methyl(fluoro)germanes (14). The Ge-C and Ge-F force constants progressively increase with increasing fluorine substitution. The Si-C bond distance in CH_3SiF_3 is r_s = 1.812 ± 0.014Å (57) as compared to 1.848 ± 0.005Å in CH_3SiH_2F (57) and r_s = 1.867 ±

0.001Å in CH_3SiH_3 (30). A more definite indication of greater polarity in the Ge-F bond as comapred to the Si-F bond is given by the CGeF angle of 106° 20' in CH_3GeH_2F (64) and the CSiF angle of 109° 13' in CH_3SiH_2F (57).

The Ge-Br bond distance has been found to be r_s = 2.2970 ± 0.0002Å in GeH_3Br (67), r_s = 2.323 ± 0.001Å in $(CH_3)_3GeBr$(27), r_e = 2.277 ± 0.003Å in this study, and r_g = 2.29 ± 0.02 in $GeBr_4$ (29). A redetermination of the molecular structure of $GeBr_4$ might be expected to place the Ge-Br bond length closer to 2.27Å. It is difficult to make meaningful comparisons of the Si-Br bond length in the corresponding silicon compounds since the distance is known to an accuracy of better than 0.02Å only for $BrSiH_3$ (68) where a value of r_s = 2.209 ± 0.001Å was obtained. Since (p-d)π interaction of the Ge-F bond in CH_3GeF_3 was found to be small the expected interaction leading to a shortening of the Ge-Br bond in CH_3GeBr_3 would be expected to be negligible. After making corrections (46) for the electronegativity differences the predicted Ge-Br and Si-Br distances are 2.299 and 2.261Å respectively. The agreement is excellent for the Ge-Br bond length in GeH_3Br, but significant shortening is indicated for the Si-Br bond distance in SiH_3Br.

The present study has been unable to accurately determine the Ge-C bond distance in CH_3GeBr_3 due to the relatively small contribution to the molecular scattering curve of atom pairs involving carbon. This distance is expected to be less than the values of r_s = 1.9400 ± 0.0001Å in $(CH_3)_3GeCl$ (62) and r_s = 1.936 ± 0.006 in $(CH_3)_3GeBr$ (27), but longer than the value r_e = 1.915 ± 0.012Å found in CH_3GeF_3. The value of 1.87Å

determined for the Ge-C bond distance in CH_3GeBr_3 is very likely too short.

The angle FGeF in CH_3GeF_3 is smaller than the angle BrGeBr in CH_3GeBr_3, and this would have been predicted from both Bent's (48) and the VSEPR (50) theories. However, non-bonded interactions (49) between the halogen atoms is probably of significance since in both molecules the halogen-halogen non-bonded distance is equal to the Van der Waals radius of interaction.

In conclusion, the structural trends in silicon molecules are closely paralleled by those in germanium compounds. The Ge-C bond length has been shown to have an essentially constant value in the methylgermanes, a feature which has been noted in the methylsilanes (33). Increasing halogen substitution has the effect of decreasing both the Ge-X and Ge-C bond lengths, as is the case in silicon compounds. However, this shortening is much less in germanium structures as compared with silicon molecules. Halogen substitution in a silicon molecule can induce a significant amount of (p-d)π bonding, whereas (p-d)π overlap in germanium is of much less significance, even in CH_3GeF_3. It is likely that similar trends will be found in tin and lead structures with (p-d)π bonding being negligible. The only comparable study so far reported for these elements is the series $Sn(CH_3)_{4-n}Cl_n$ (69) where a progressive decrease in the

Sn-Cl bond was observed with increasing chlorine substitution.

CHAPTER VII

Suggestions for Further Studies

Our structural knowledge of germanium and silicon compounds contain many gaps, and early determinations frequently have large error estimates. However, some trends can be inferred from those structures that are accurately known and these trends may be tentatively extrapolated to other molecules where our information is incomplete. The discussion which follows is based on r_s bond lengths from microwave studies, and the r_e values estimated from electron diffraction results by equation 1. These are approximately equivalent bond length definitions and are 0.006 - 0.008Å shorter, depending on the mean square amplitude of vibration, than the usual r_g value derived from electron diffraction.

The contraction of the Si-Cl bond with progressive halogen substitution in the chlorosilane series is, as would be expected, less than that observed for the Si-F bond in the fluorosilanes. The Si-Cl bond length in $ClSiH_3$ is 2.048 ± 0.001Å (59), and in $SiCl_4$ it is 2.013 ± 0.003Å (60), a difference of 0.035 ± 0.004Å. In the corresponding germanium compounds the Ge-Cl bond length is 2.148 ± 0.003Å in $ClGeH_3$ (56) and 2.106 ± 0.001Å in $GeCl_4$, a difference of 0.042 ± 0.004Å. These contractions are fairly similar, and based on the Si-Cl bond length of 2.021 ± 0.002Å in Cl_3SiH (70) one may guess that the Ge-Cl bond length in Cl_3GeH would be about 2.116Å. Presumeably the angle ClGeCl would be the same, or slightly smaller, as the 109° 22′ ± 15′ for ∠ClSiCl in Cl_3SiH (70). Although all the fluorosilanes are known with an accuracy of ± 0.005Å or better (Table V), only monofluorogermane has been studied and the

Ge-F bond length was found to be 1.735 ± 0.01Å (65). A determination of the structures of the remaining fluorogermanes and of GeF_4 would be extremely valuable since the possible (p-d)π interaction between germanium and fluorine would be greatest in these molecules. The tetrafluorogermane molecule has been studied previously (28) and the Ge-F bond length was determined as 1.67 ± 0.03Å. The difference between the Ge-Br bond length in $BrGeH_3$ and $GeBr_4$ should be about the same, or slightly less, than the difference in the Ge-Cl bond length in the corresponding chlorine molecules which is 0.042Å. The only known value for the Ge-Br distance in $GeBr_4$ is 2.29 ± 0.02Å (29) which is longer than this distance in $BrGeH_3$ where a value of 2.2970 ± 0.0002Å was reported (67). Based on this latter determination, the Ge-Br bond length in $GeBr_4$ should be found in the region of 2.265Å.

It has been noted that the substitution of hydrogen by a methyl group has the effect of lengthening the M-X bond, where M = Si or Ge and X = halogen. There is some indication that a similar substitution could lengthen the M-M bond since the Si-Si distance in hexamethyldisilane is 2.342 (33) and in disilane it is 2.325Å (42), although the error involved in $(CH_3)_3Si.Si(CH_3)_3$ is about 0.01Å. The Ge-Ge bond length in digermane is 2.397 ± 0.004Å (44) and it would be interesting to determine this bond length in hexamethyldigermane.

REFERENCES

(1) L. Pauling. The Nature of the Chemical Bond. Cornell University Press, Ithaca, N.Y. 3rd edition, 1960.

(2) D. R. Lide, Jr. J. Chem. Phys. 33, 1519 (1960).

(3) F. G. A. Stone and D. Seyferth, J. Inorg. Nuclear Chem. 1, 112 (1955).

(4) S. Cradock and R. A. Whiteford. J. Chem. Soc. Faraday Trans. II. 68, 281 (1972).

(5) S. Cradock and E. A. V. Ebsworth. Chem. Comm. 571 (1971).

(6) A. Breeze, G. A. D. Collins, and D. W. J. Cruickshank. Chem. Comm. 445 (1971).

(7) J. M. Bellama, S. O. Wandiga, and A. A. Maryott. Inorg. Nucl. Chem. Lett. 7, 71 (1971).

(8) E. C. Thomas and V. W. Laurie. J. Chem. Phys. 50, 3512 (1956).

(9) J. E. Griffiths. Inorg. Chem. 2, 375 (1963).

(10) D. F. Van de Vondel and G. P. Van der Kelen. Bull. Soc. Chim. Belges. 74, 467 (1965).

(11) H. Schmidbaur. Chem. Ber. 97, 1639 (1964).

(12) Handbook of Chemistry and Physics. R.C. West, ed., The Chemical Rubber Co., Cleveland, Ohio (1969).

(13) E. R. Lippincott and M. C. Tobin. J. Amer. Chem. Soc. 75, 4141 (1953).

(14) J. W. Anderson, A. J. F. Clark, G. K. Barker, J. E. Drake and R. T. Hemmings. Spectrochim. Acta, in press (1973).

(15) V. A. Ponomarenko and G. Ya. Vzenkova. Izv. Akad. Nauk SSSR 1020 (1957).

(16) R.T. Hemmings. Ph.D. Thesis. University of Windsor, Windsor, Ontario. 1973.

(17) K. Moedritzer and J.R. Van Wazer. Rev. Chim. Mineral 6, 293 (1969).

(18) D.F. Van de Vondel, G.P. Van der Kelen and G. Van Hooydonk. J. Organometal. Chem., 23, 431 (1970).

(19) W. Harshbarger, G. Lee, R.F. Porter, and S.H. Bauer. Inorg. Chem. 8, 1683 (1969).

(20) J.L. Hencher and S. H. Bauer. J. Amer. Chem. Soc. 89, 5527 (1967).

(21) T.G. Strand, D.A. Kohl, and R.A. Bonham. J. Chem. Phys. 39, 1307 (1963).

(22) Y. Murata and Y. Morino. Acta Cryst. 20, 605 (1966).

(23) R.A. Bonham, L Schäfer and A.C. Yates. J. Chem. Phys. 55, 3055 (1971).

(24) L.S. Bartell. ibid. 23, 1219 (1955).

(25) K. Kuchitsu and L.S. Bartell. ibid, 35, 1945 (1961).

(26) R.L. Hilderbrandt. J. Chem. Phys. 51, 1654 (1969).

(27) Y.S.Li and J.R. Durig. Inorg. Chem. 12, 306 (1973).

(28) A.D.Caunt, M. Mackle and L.E. Sutton. Trans. Faraday Soc. 47, 943 (1951).

(29) M.W. Lister and L.E. Sutton. ibid. 37, 393 (1941).

(30) R.W.Kilb and L. Pierce. J. Chem. Phys. 27, 108 (1957).

(31) L. Pierce. ibid. 34, 498 (1961).

(32) L. Pierce and D.H. Petersen. ibid. 33, 907 (1960).

(33) B. Beagley, J.J. Monaghan and T.G. Mewitt. J. Mol. Struct. 8, 401 (1971).

(34) V.W. Laurie. J. Chem. Phys. 50, 1210 (1969).

(35) J.R. Durig, M.M. Chen, Y.S. Li, and J.B. Turner. J. Phys. Chem. 77, 227 (1973).

(36) D.R. Lide. J. Chem. Phys. 19, 1605 (1951).

(37) K. McAloon. Preliminary result quoted in reference 70.

(38) H. Fujii and M. Kimura. Preliminary result quoted in reference 70.

(39) T. Oyamada, T. Iijuma and M. Kimura. Bull.Chem. Soc. Japan. 44, 2638 (1971).

(40) L.E. Sutton. Chem. Soc. Special Publ. 18, 4 (1965).

(41) L.O. Brockway and H.O. Jenkins. J. Amer. Chem. Soc. 58, 2036 (1936).

(42) B. Beagley, A.R. Conrad, J.M. Freeman, J.J. Monaghan, B.G.Norton and G.C. Holywell. J. Mol. Struct. 11, 371 (1972).

(43) L.S.Bartell and H.K. Higginbotham. J. Chem. Phys. 42, 851 (1965).

(44) B. Beagley and J.J. Monaghan. Trans. Faraday Soc. 66, 575 (1970).

(45) D. Quane. J. Inorg. Nucl. Chem. 33, 2722 (1971).

(46) V. Schomaker and D.P. Stevenson. J. Amer. Chem. Soc. 63, 37 (1941).

(47) A. Breeze, G.A.D. Collins and D.W.J. Cruickshank. Private communication quoted in reference 36.

(48) H. A. Bent. Chem. Rev. 61, 275 (1961).

(49) L. S. Bartell. J. Chem. Educ. 45, 754 (1968).

(50) R. J. Gillespie and R. S. Nyholm. Quart. Rev. (London) 11, 339 (1957); R. J. Gillespie. Can. J. Chem. 38, 818 (1960); R.J. Gillespie. J. Chem. Educ. 40, 295 (1963); R.J. Gillespie. ibid. 47, 18 (1970).

(51) A. H. Sharbaugh, V. G. Thomas and B. S. Pritchard. Phys. Rev. 78, 64 (1950).

(52) V. W. Laurie, J. Chem. Phys. 26, 1359 (1957).

(53) A. R. Moy, M. Bertram and I. M. Mills. J. Mol. Spectrosc. 46, 429 (1973).

(54) K. Hagen and K. Hedberg. ibid. 59, 1549 (1973).

(55) Y. Morino, Y. Nakamura and T. Iijima. ibid. 32, 643 (1960).

(56) J. M. Mays and B. P. Dailey, ibid. 20, 1695 (1952).

(57) L. Pierce. ibid. 29, 383 (1958).

(58) D. R. Swalen and B. P. Stoicheff. ibid. 28, 671 (1958).

(59) J. R. Durig, Y. S. Li and C. C. Tong. J. Mol. Strucut. 14, 255 (1972).

(60) Y. Morino and Y. Murata. Bull. Chem. Soc. Japan. 38, 104 (1965); R. R. Ryan and K. Hedberg. J. Chem. Phys. 50, 4986 (1969).

(61) B. Bak. J. Bruhn, and J. Rastrup-Andersen. Acta Chem. Scand. 8, 367 (1954).

(62) J. R. Durig and K. L. Hellams. Results quoted in reference 30.

(63) J. R. Durig, R. O. Carter and Y. S. Li. J. Mol. Spect. 44, 18 (1972).

(64) R. F. Roberts. Diss. Abstr. Int. B. 33, 2549 (1972).

(65) K. H. Rhee and M. K. Wilson. J. Chem. Phys. 43, 333 (1965); J. E. Griffiths, T. N. Srivastava and M. Onyszchuk Can. J. Chem. 40, 579 (1962); L. C. Krishner, J. A. Morrison, and W. A. Watson. J. Chem. Phys. 57, 1357 (1972).

(66) D. F. Van de Vondel and G. P. Van der Kelen. J. Organometal Chem. 55, 85 (1973).

(67) A. H. Sharbaugh, B. S. Pritchard, V. A. Thomas, J. M. Mays and B. P. Dailey. Phys. Rev. 79, 189 (1950); S. R. Wolf and L. C. Krishner. J. Chem. Phys. 56, 1040 (1972).

(68) A. H. Sharbaugh, J. K. Bragg, T. C. Madison, and V. G. Thomas. Phys. Rev. 76, 1419 (1949).

(69) H. Fujii and M. Kimura. Bull. Chem. Soc. Japan. 44, 2643 (1971).

(70) R. C. Mockler, J. H. Bailey and W. Gordy. J. Chem. Phys. 21, 1710 (1953).

PART III

THE CONFORMATION OF RACEMIC 4,6-DIMETHYLTRIMETHYLENE SULFITE

CHAPTER 1

INTRODUCTION

The considerable controversy in recent literature prompted this study of a dimethyl substituted six membered cyclic sulfite in which steric interactions might be expected to play an important role in determining the conformation. The early literature of trimethylene sulfite and its derivatives is mainly concerned with the orientation of the exocyclic oxygen atom (1 - 6), although equilibrium mixtures of conformers are suggested (7,8). The positioning of exocyclic oxygen has since been shown to be axial in solution studies (9 - 13), in X-ray diffraction of solid crystals (14,15) and in the gas phase by electron diffraction (16). The same conclusion has been drawn from infrared studies on trimethylene sulfite in the liquid, solution and gas phases (17).

The first isomers of trimethylene sulfite substituted in the 4 and 6 positions were isolated by Lauterbur (3) who, on the basis of i.r. and n.m.r. spectra assigned the racemic isomer a chair form with equatorial S=O. Overberger (8) concluded from temperature dependance of the n.m.r. and i.r. spectra that a conformational mixture of chair forms (S=O axial and S=O equatorial) was present with S=O axial predominating. However, the proton n.m.r. spectra of the racemic molecule

has been reinterpreted as evidence for non-chair forms and this view is now generally accepted (18). From spectral studies and dipole moments, Wucherpfennig (19) proposed a mixture of twist and perhaps chair forms. A previous spectral study (20) of the analagous racemic 4,6-diisopropyl trimethylene sulfite was in favour of the twist form. Wyn-Jones (21-24) has used ultrasonic techniques to study various sulfites and has concluded that anacomeric equilibria of inverting chair conformations are present. More recently, a study (25) by high resolution n.m.r. spectroscopy of 4,6,6-trimethyl- and 4-phenyl-trimethylene sulfite has indicated that these molecules exist in either a chair-nonchair equilibrium or a twist conformation.

The work of Wood, and co-workers' (26,27,28) has indicated that racemic 4,6-dimethyltrimethylene sulfite is at least partially in a non-chair form in solution, a view that has found some support in the results cited above (19,25).

CHAPTER II

EXPERIMENTAL

A gas chromatographically pure sample of the racemic compound was provided by Dr. M. H. Miskow (27), for which the author is very grateful. Sectored electron diffraction photographs were recorded on the Cornell aparatus (29). A suitable vapor pressure was obtained with the sample at a temperature about 10°C lower than that of the nozzle which was at 130°C as measured by an attached thermocouple. Optical densities as a function of radial position were obtained with a digitized microphotometer (30). The data reduction procedure was that of Bauer and his coworkers (30,31), using the Hartley modification to the least square procedure (32) and a weight matrix that includes the first off-diagonal terms (33). Anharmonicity corrections were made for bonded atom pairs (34,35).

CHAPTER III

RESULTS

Experimental relative intensities of four plates were obtained, covering the ranges $q = 14 - 96\text{Å}^{-1}$ (data set I) and $q = 6 - 93\text{Å}^{-1}$ (data set II), where $q = (40/\lambda)\sin(\Theta/2)$, λ is the electron wavelength and Θ the scattering angle. Both sets of data are listed in Appendix H, and the intensities for data set I are plotted with the refined backgrounds in Figure 1.

Six conformations, described using Hilderbrandt's algorithm (36), were tested against the experimental reduced intensity $\frac{\pi}{10} q M_{expt}(q)$ by the method of least squares. The conformations were labelled A through F and are presented in Figure 2. A larger drawing of model A with numbered atoms is shown in Figure 3. The endocyclic carbon atoms and their attached hydrogen atoms were positioned routinely by means of C-C, C-H and <CCH = <CCC = <HCH. The endocyclic oxygens were positioned by means of C-C, C-O, <CCC, <CCO and the angle τOCC (e.g. the non-valence angle between C4-C5 and C6-O1. A value of zero for τOCC would correspond to these oxygens lying in the plane formed by C5C5C6). The position of the sulfur atom was obtained using the distance C5...S2 (parameter C....S) and angle H1C5S2 (parameter <SCH). This ensures that both S-O lengths are equivalent and conveniently allows the boat or chair conformations to be determined primarily by the value of <SCH.

Figure 1 The experimental intensity and background curves for racemic 4,6-dimethyltrimethylene sulfite data set I.

Figure 1

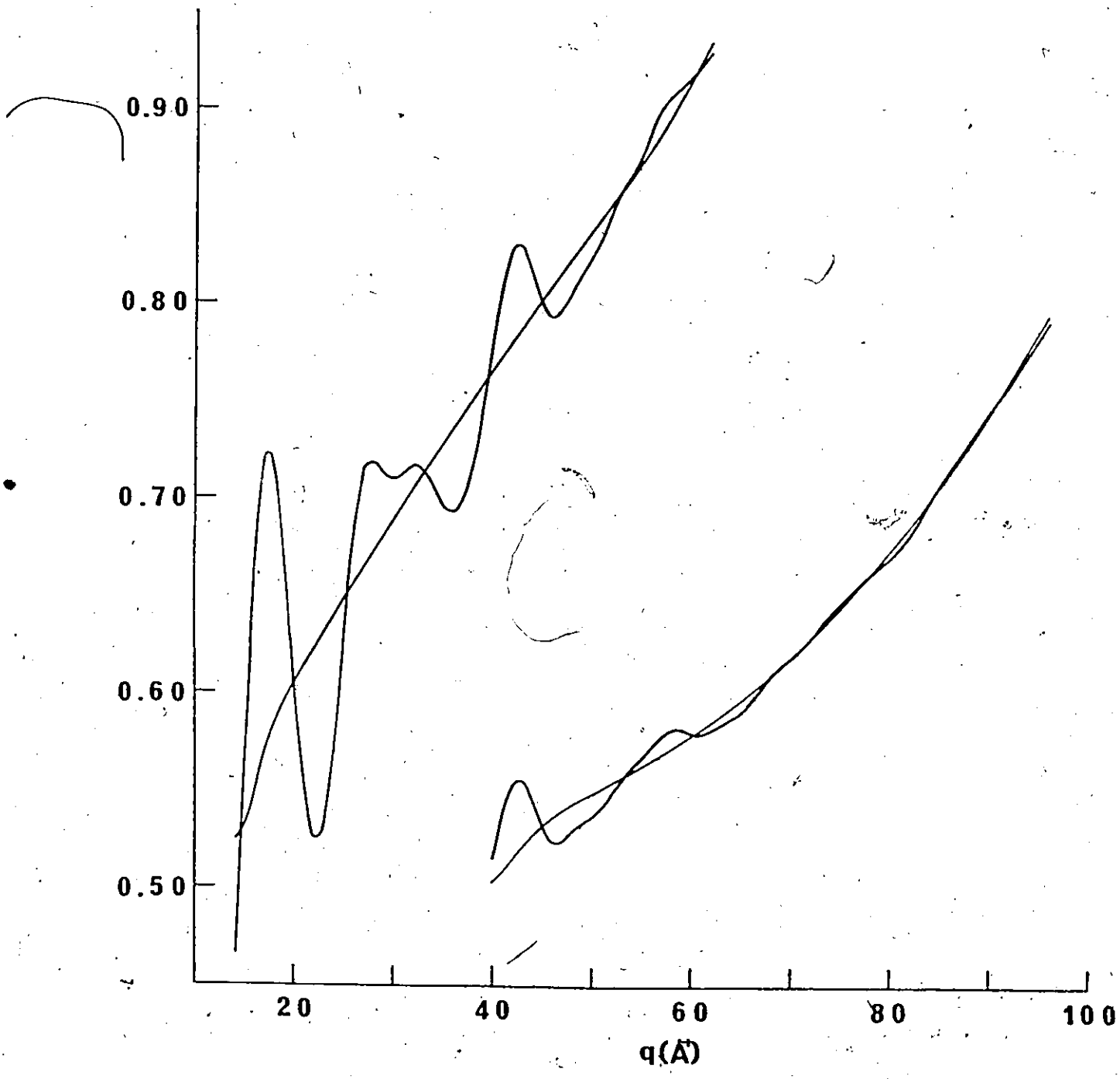

Figure 2 The six different conformations analysed by least squares fitting of the reduced experimental molecular scattering curve.

Figure 2

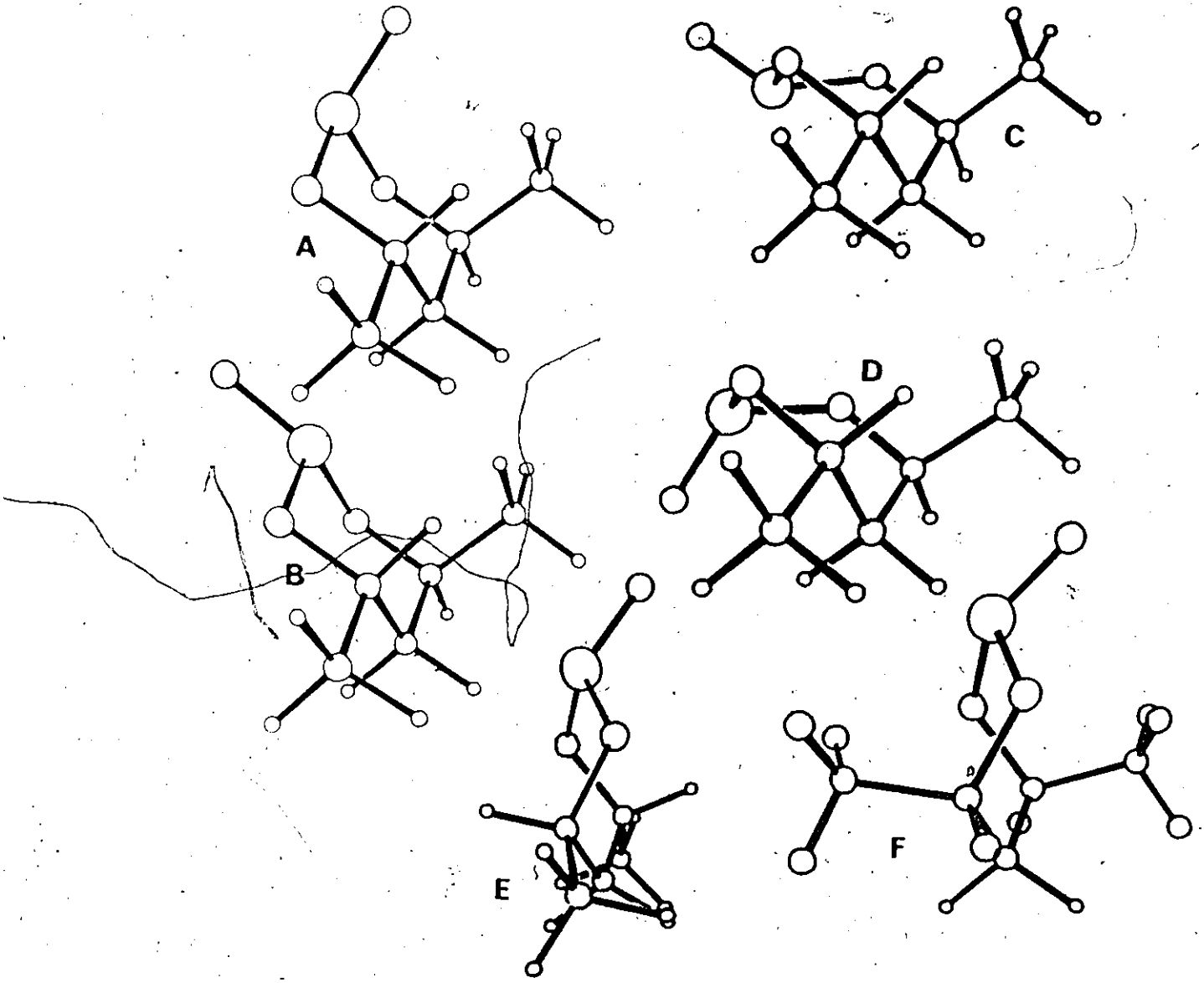

Figure 3. The conformation, with numbered atoms, for model A.

Figure 3

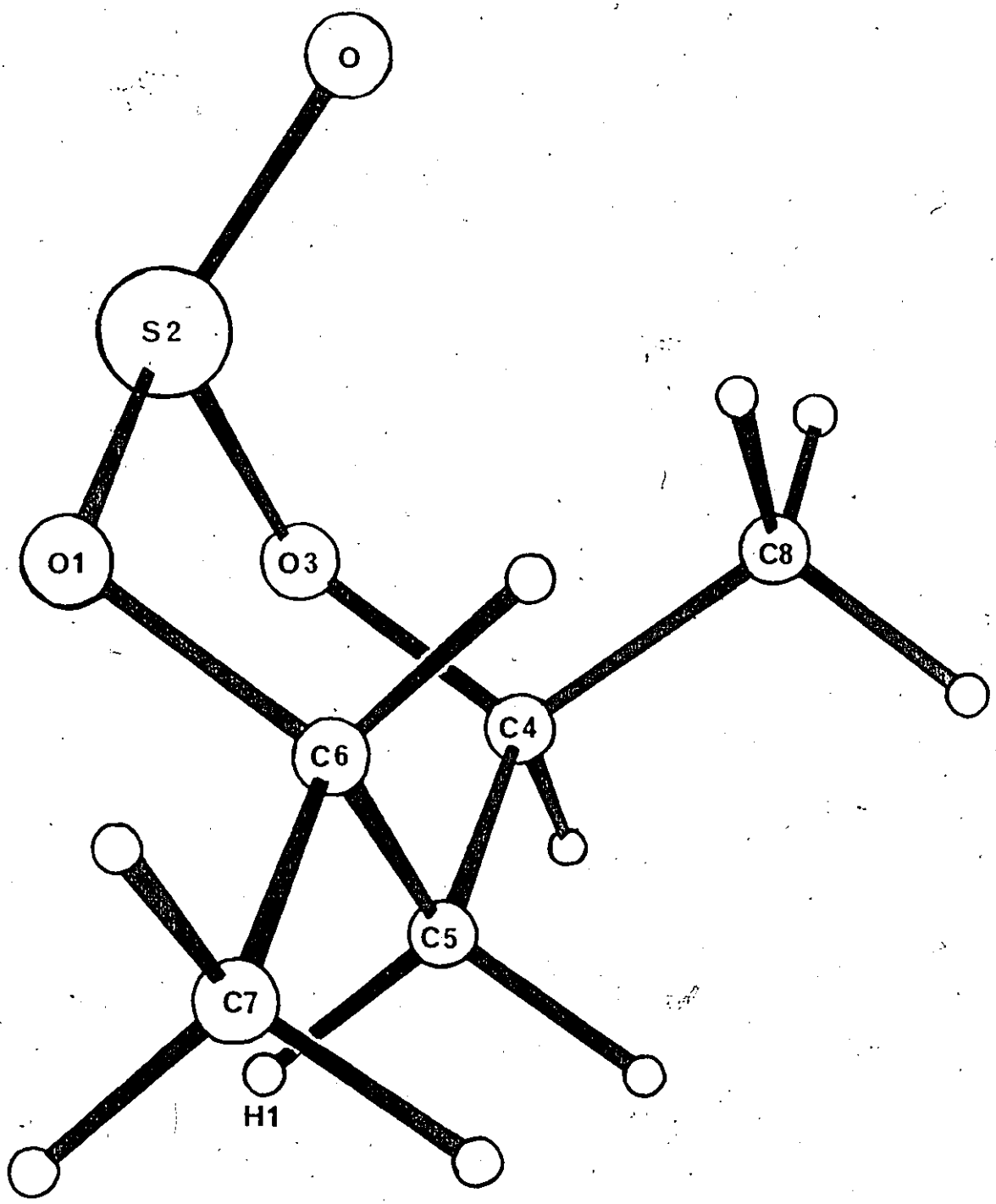

The twist forms were obtained by rotating the C-O bonds against each other by means of τOCC (See Figure 2). Due to the complexity of the molecule it was assumed that all CCH, HCH and CCC angles were tetrahedral, and that the endo- and exocyclic CCO angles were equivalent.

The selection of initial parameter values for least squares refinement was straight forward for the bond lengths and valence angles. However, initial values of <SCH, C....S and τOCC had to be found by trial and error in order that the redundant parameters <COS, <OSO and S-O would have reasonable starting values, as calculated from the interatomic distance matrix. In order to test each conformation it was necessary to attempt a refinement of as many parameters as possible, although under these conditions large correlation coefficients were found between the parameters and convergence was difficult to obtain.

Radial distribution curves were calculated using a value of 0.0025 for the Degard damping constant. Only the contributions due to C-H and S-O were clearly resolved. By fitting the intensity curves we find two solutions for each of the chair models, placing the S-O distance at 1.62Å. The parameter values obtained when both sets of data were treated independently for the preferred chair form of model A are given in Table I. The corresponding interatomic distances and mean square amplitudes of vibration for the heavy atoms are given in Table II and the correlation coefficients between the parameters in this solution are listed in Table III. Some of the parameters are highly correlated,

Table I

The Structural Parameters[1] and Standard Deviations Obtained from Independent Least Squares Fits to Data SetI ($q = 14 - 96\ \text{Å}^{-1}$) and Data Set II ($q = 6 - 93\ \text{Å}^{-1}$) for Model A

Parameter	Data Set I		Data Set II		Weighted
	Value	σ	Value	σ	Value[2]
C-H	1.125	0.0058	1.106	0.0090	1.119
C-C	1.505	0.0044	1.505	0.0049	1.505
C-O	1.411	0.0035	1.417	0.0058	1.413
S=O	1.479	0.0068	1.481	0.0081	1.480
<CCO	111.2	0.3956	110.9	0.5199	111.1
<OS=O	116.8	0.3942	116.4	0.6247	116.7
C...S	3.002	0.0185	3.011	0.0106	3.009
<SCH	101.8	0.7508	101.2	0.2356	100.3
<OCC	58.8	0.9246	59.8	0.2847	59.7
Redundant Parameters					
S-O	1.621	0.0032	1.623	0.0026	1.622
<COS	114.0	0.2481	114.9	0.5894	114.1
<OSO	100.7	0.5815	100.8	0.8304	100.7
R^3	0.0646		0.1010		

[1] Bond lengths are r_g values in Å, angles are in degrees. The following angles were constrained to be tetrahedral: <CCC, <CCH, <HCH.

Table 1 Continued

[2] The values are weighted by the standard deviations:

$$X = \frac{\sum_i (x_i/\sigma_i^2)}{\sum_i (1/\sigma_i^2)}$$

[3]

$$R = \left[\frac{\sum_q \left(\frac{\pi}{10} q\, M(q)_{expt} - \frac{\pi}{10} q\, M(q)_{theor} \right)^2 \cdot W_q}{\sum_q \left(\frac{\pi}{10} q\, M(q)_{expt} \right)^2 \cdot W_q} \right]^{1/2}$$

Table II

	O	O1	S2	O3	C4	C5	C6	C7	C8
O	0.0	2.642 (0.060)	1.479 (0.047)	2.642 (0.060)	3.247 (0.121)	3.875 (0.121)	3.247 (0.121)	4.587 (0.121)	2.965 (0.121)
O1		0.0	1.621 (0.049)	2.497 (0.070)	2.850 (0.121)	2.406 (0.075)	1.411 (0.050)	2.406 (0.075)	3.493 (0.121)
S2			0.0	1.621 (0.049)	2.546 (0.083)	3.002 (0.121)	2.546 (0.083)	3.892 (0.121)	2.996 (0.121)
O3				0.0	1.411 (0.050)	2.406 (0.075)	2.850 (0.121)	4.250 (0.121)	2.406 (0.075)
C4					0.0	1.505 (0.050)	2.455 (0.082)	3.786 (0.121)	1.505 (0.050)
C5						0.0	1.505 (0.050)	2.458 (0.082)	2.458 (0.082)
C6							0.0	1.505 (0.050)	2.928 (0.121)
C7								0.0	4.273 (0.121)
C8									0.0

[1] These are r_g values, in A.

[2] The lij values presented in this table were determined during previous least squares analysis and were constrained during the later stages of refinement. Mean square amplitudes involving hydrogen were as follows: C-H = 0.080; H..H = 0.120; with geminal C or O atom = 0.100; with all other heavy atoms = 0.150; all long H...H distances = 0.200. All values are in A.

[3] The conformation and designation of the atoms corresponds to Figure 3. The distances presented above were calculated for this conformation using the parameter values listed for data set I in Table I.

Table III

Diagonal Elements and Correlation Coefficients for Model A[1]

	C-H	C-C	C-O	<CCO	τOCC	C...S	<SCH	S=O	<OS=O
σ	0.0058	0.0044	0.0035	0.3956	0.9246	0.0185	0.7508	0.0068	0.3942
C-H	1	-0.01	0.05	0.10	-0.02	0.00	-0.01	0.04	-0.02
C-C		1	0.36	-0.86	-0.70	0.77	-0.69	-0.89	0.53
C-O			1	-0.51	-0.25	0.41	-0.26	-0.44	0.30
<CCO				1	0.60	-0.78	0.58	0.84	-0.37
τOCC					1	-0.94	0.98	0.69	-0.20
C...S						1	-0.90	-0.74	0.17
<SCH							1	0.68	-0.24
S=O								1	-0.64
<OS=O									1

[1]The individual standard deviations are given by

$$\sigma = \left[\frac{B_{ii}^{-1} V'WV}{n-m} \right]^{1/2}$$

and the correlation coefficients by

$$\rho_{ij} = \frac{B_{ij}^{-1}}{(B_{ii}^{-1} \; B_{jj}^{-1})^{1/2}}$$

and although convergence was not obtained, the parameter values were oscillating with amplitudes less than the given uncertainties.

The alternate form of model A, again refined independently from the two sets of data, gave valence parameter values in close agreement with each other, and within the errors given for the preferred model, with the exceptions of <OS=O, <COS and <OSO. For these respective parameters were determined the values 107.9°, 117.9°, and 106.9° from data set I (R = 0.0846) and 108.6°, 118.3° and 106.1° from data set II (R = 0.0986). Although the fit to data set II for this form is better than that given in Table I, it is not significantly so at the 99.5% confidence level (37,38), and the values for <OS=O are smaller than expected.

A similar result was obtained for model B, the chair form with equatorial S=O bond, although the best fits to both data sets were obtained with parameter values similar to those discussed above for the alternate form of model A. These results are presented in Table IV. On comparing Tables I and IV it is evident that the differences in the chair forms are due largely to the parameters <SCH and τOCC. Transfering the parameters given in Table I as an initial structure for model B, we find that allowing the valence and conformational determining parameters to vary results in solutions with valence parameters as given in Table I, within the given errors, with the exception of <OSO. Data sets I and II yield values of 92.4° and 91.0° respectively for <OSO, values which are approximately 10° less than the similar angle determined in trimethylene

Table IV

The Structural Parameters and Standard Deviations Obtained from Independent Least Square Fits to Data Set I and Data Set II for Model B.

Parameter	Data Set I		Data Set II		Weighted
	Value	σ	Value	σ	Value
C-H	1.117	0.0075	1.101	0.0083	1.110
C-C	1.512	0.0036	1.514	0.0039	1.513
C-O	1.427	0.0060	1.428	0.0062	1.427
S=O	1.469	0.0070	1.473	0.0078	1.471
<CCO	108.8	0.4288	109.1	0.4726	108.9
<OS=O	108.3	0.4747	109.3	0.5645	108.7
C...S	2.983	0.0120	2.992	0.0139	2.987
<SCH	89.9	0.7228	88.9	0.8770	89.5
τOCC	66.1	0.7332	65.9	0.8805	66.0
Redundant Parameters					
S-O	1.621	0.0024	1.626	0.0028	1.623
<COS	119.3	0.5833	120.3	0.6766	119.7
<OSO	105.8	0.8430	106.0	0.9095	105.9
R	0.0746		0.0863		

sulfite (14,16) and 2,2 -dichloro trimethylene sulfite (15).

The boat forms C and D were analysed using data set I only. The best fits obtained for these conformations had R values of 0.1878 and 0.2186 respectively, and are not significant at the 99.5% confidence level (37,38). Partially twisted boat conformations did not successfully refine, hence the completely twisted forms E and F were assumed by constraining the sulfur atom to the position shown in Figure 2 by means of ∠SCH = 125.25°. Model E was analysed using data set I only and refined to a set of valence parameter values consistent with those of Table I, but again the fit (R = 0.1701) is not statistically significant. Model F was analysed using both data sets, but the fits obtained (R = 0.1101 for Set I and R = 0.1469 for set II) are still not significant at the 99.5% confidence level (37,38).

The experimental reduced intensity $\frac{\pi}{10} q\, M_{expt}(q)$ is compared with $\frac{\pi}{10} q\, M_{theor.}(q)$ for A in Figure 4 along with the difference curves for A through F. The corresponding radial distribution curves calculated from the reduced intensity curves are presented in Figure 5 for the region of structural interest. The full experimental radial distribution curve is compared with that calculated for model A in Figure 6.

Figure 4 The reduced experimental molecular scattering curve, the corresponding theoretical curve calculated for model A, and the difference curves (experimental - theoretical) for models A through F data set I.

Figure 4

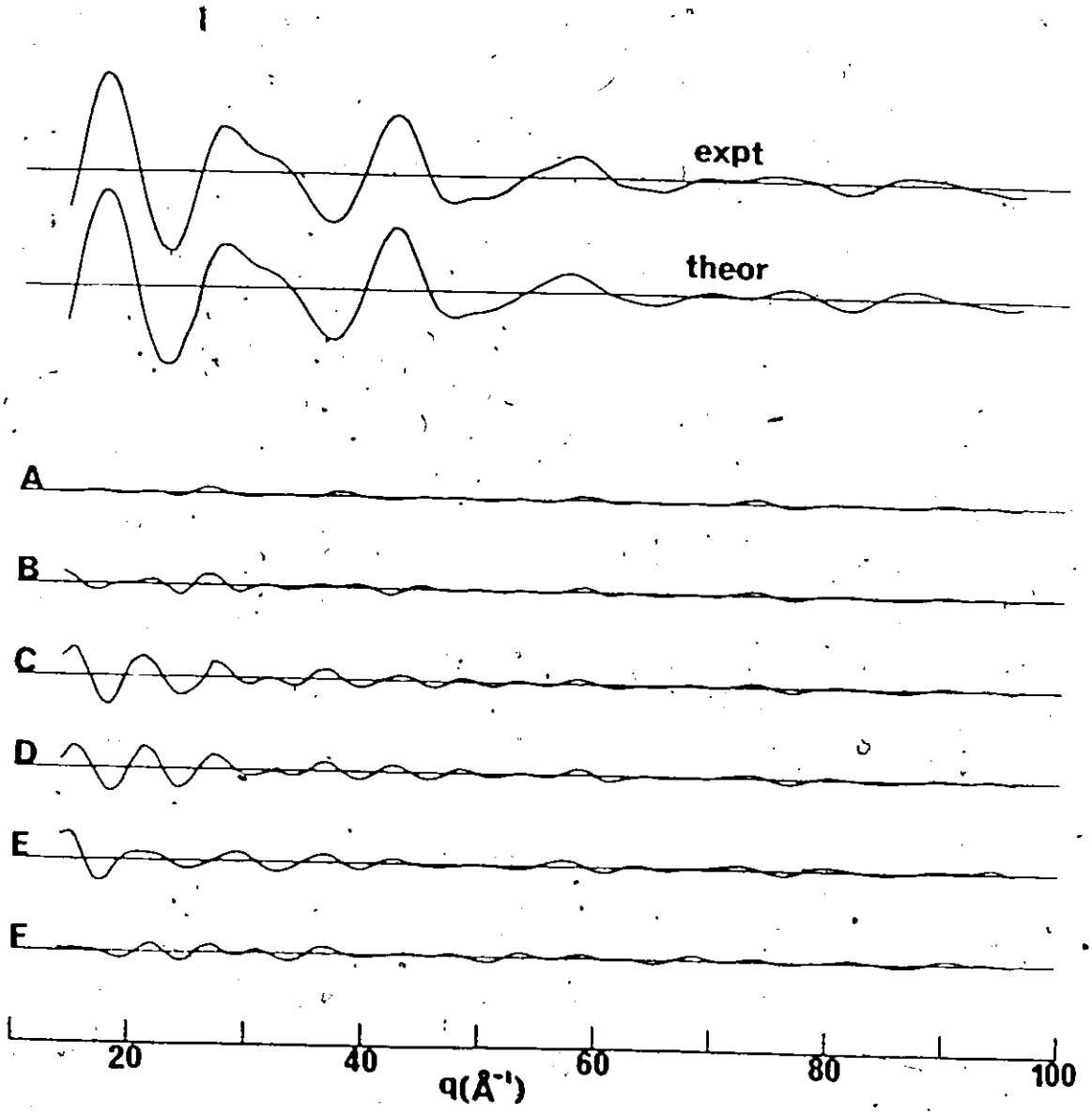

Figure 5 The experimental radial distribution function in the region of structural interest, together with the corresponding theoretical function for model A and the difference curves (experimental - theoretical) for models A through F.

Figure 5

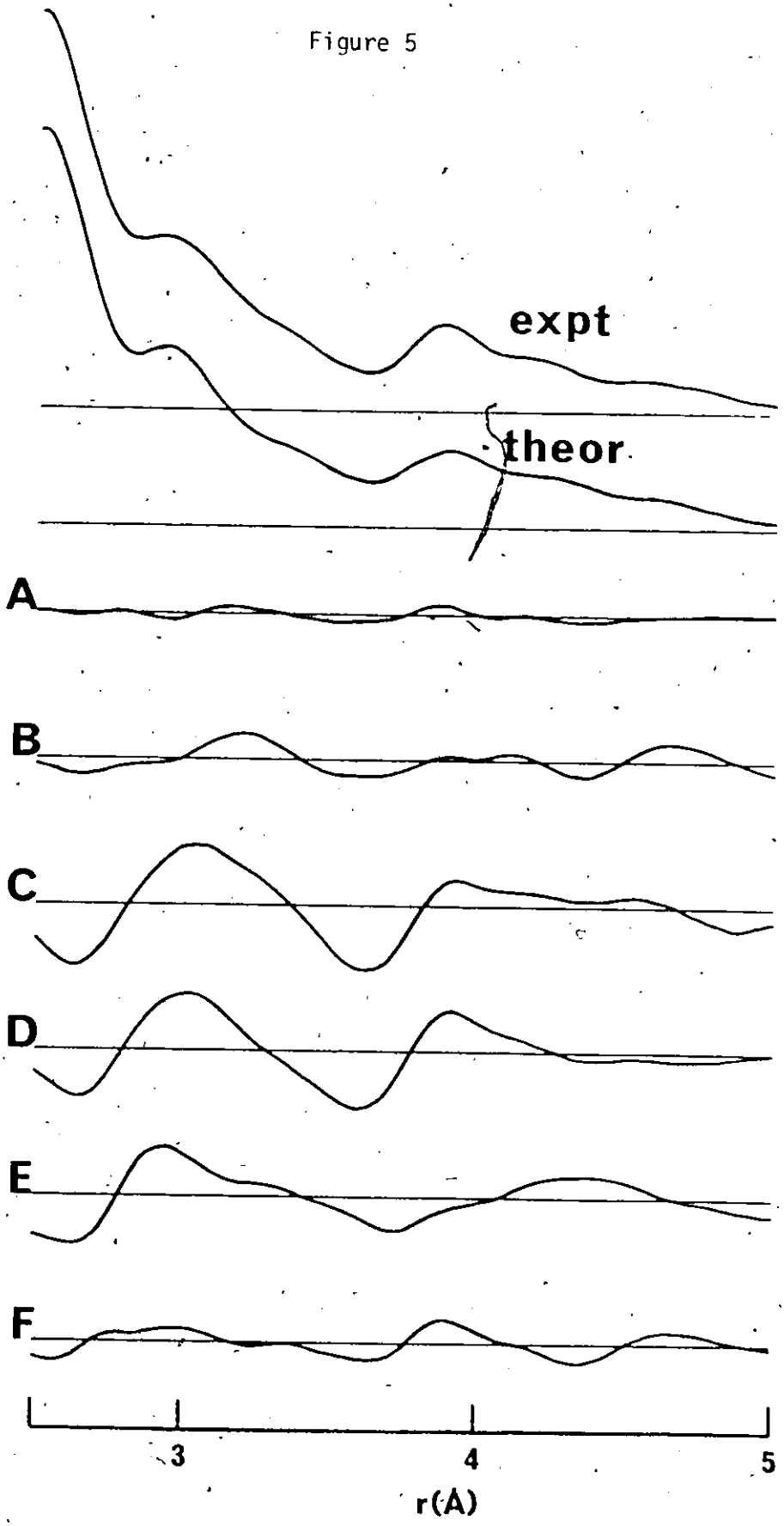

Figure 6 The refined experimental radial distribution curve.

$$\Delta f(r) = [f(r)_{expt} - f(r)_{theor}]$$

Figure 6

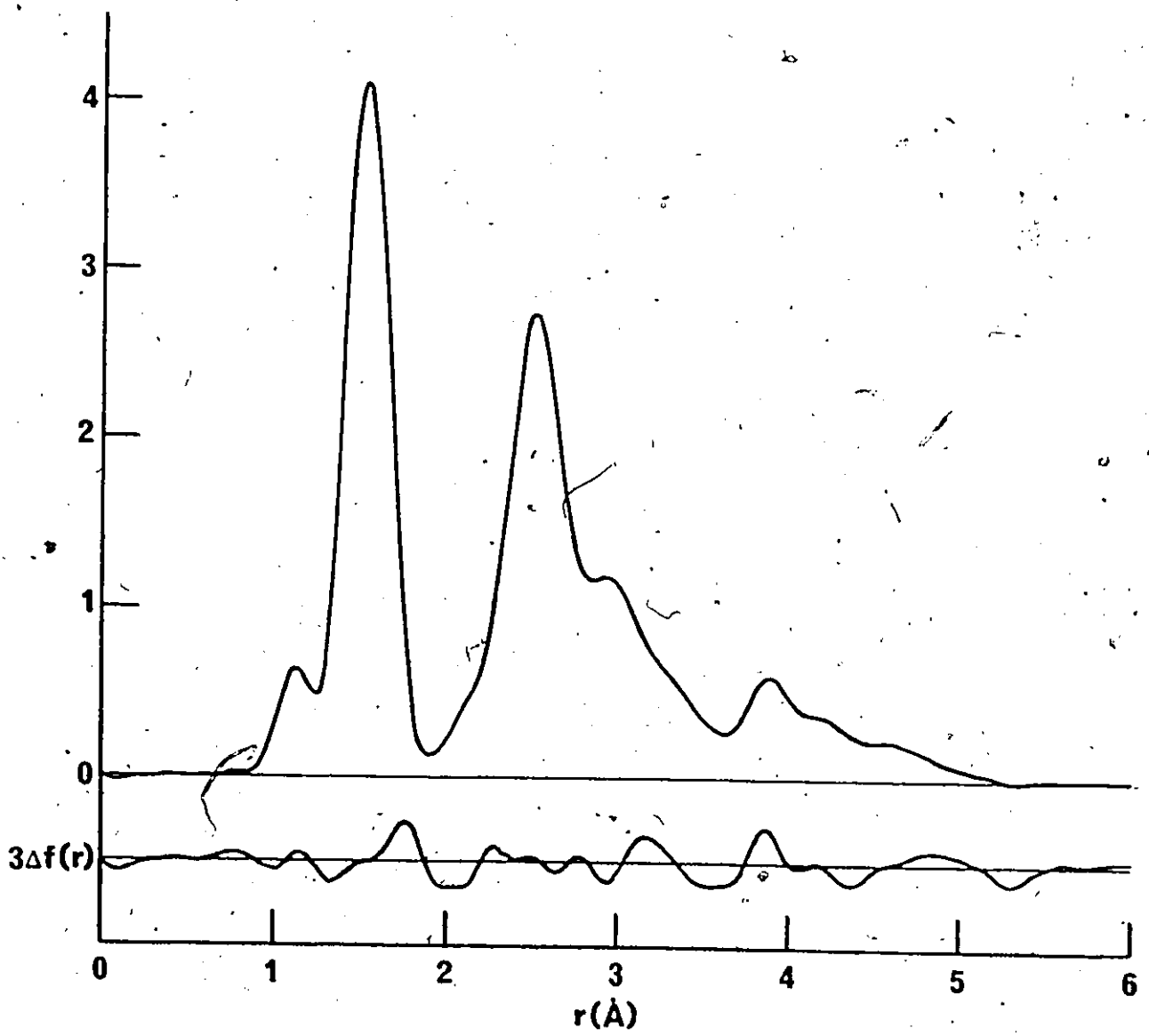

CHAPTER IV

DISCUSSION

While the analyses of the two sets of data are consistent in that the parameter values obtained for models A, B and F are the same, within calculated errors, the normalized standard deviations for models A and B are not consistent: for data set I the lowest value for R is given by model A, the chair form with axial S=O bond, while for data set II the lowest value for R is given by model B, a chair form having different ring valence angles than those of model A, with an equatorial bond. However, the R factor ratio 0.0746/0.0646 = 1.155 for the two fits to data set I does not allow us to statistically reject the hypothesis that model B is an acceptable solution at the 1% level of significance for this data (37,38).

We tested the tetrahedral constraint on <CCC for model A and data set I. Using the parameters of Table I as an initial model, we found a minimum (R = 0.0585) with the exocyclic <CCC = 111.1° and the endocyclic angle = 106.6°. As a second test we constrained <CCC at 110.5° and obtained a fit with R = 0.0704. In both cases the other parameters were unchanged, within the estimated errors, and the addition of <CCC to the varied parameters, or the change in the value of the constraint, do not make a significant difference to the fit obtained. We therefore conclude that <CCC might well be a degree or so larger than tetrahedral.

A more serious constraint of our analysis was the use of the same mean square amplitudes of vibration for all the models. The mean square amplitudes given in Table II are certainly not unique, and we would expect different results depending on the values used. However, it is beyond the capabilities of our experiment to determine the non-bonded amplitudes for this molecule, so we have assumed a resonable set of values and admit that an alternate set might give an improved fit to any of the models tested, although it is highly unlikely that the rejected models would become statistically significant.

The parameter values for models A and B are again listed and compared with the values in trimethylene sulfite (14,16) and 2,2 -dichlorotrimethylene sulfite (15) in Table V. The errors given for the two models in the present work are three times the calculated uncertainties and are estimated to be at the 95% confidence level and to include systematic errors. It can be seen that model A agrees reasonably well with the electron diffraction results for the unsubstituted molecule, while model B compares more favourably with the X-ray results, particularly in that <COS is much larger than <OS=O. This is an unexpected trend, and we note that in model A the peak in the radial distribution curve just less than 4 Å is due to the exocyclic oxygen to carbon distances. When this oxygen is placed in the equatorial position, as in model B, it is precisely these distances which change the most. It is therefor reasonable to assume, as Naumov

Table V

Comparison of the molecular parameters[1] for racemic 4,6-dimethyltrimethylene sulfite with trimethylene sulfite (TMS) and 2,2-dichlorotrimethylene sulfite (DTS)

Parameters	Model A	Model B	E.D. TMS (16)	X-Ray TMS (14)	X-ray DTS (15)
C-H	1.119 ± 0.020(0.08)	1.110 ± 0.023	1.12(assumed)(0.08)	-	-
C-C	1.505 ± 0.014(0.05)	1.513 ± 0.011	1.52 ± 0.02(0.049)	1.52 ± 0.018	1.523 ± 0.008
C-O	1.413 ± 0.013(0.05)	1.427 ± 0.018	1.42 ± 0.02(0.049)	1.46 ± 0.015	1.462 ± 0.007
S=O	1.480 ± 0.022(0.05)	1.471 ± 0.022	1.45 ± 0.02(0.049)	1.45 ± 0.011	1.442 ± 0.006
S-O	1.622 ± 0.009(0.05)	1.623 ± 0.007	1.62 ± 0.01(0.055)	1.60 ± 0.008	1.622 ± 0.004
<CCC	109.5 (assumed)	109.5 (assumed)	110 ± 3	110 ± 1.3	110.6 ± 0.6
<CCO	111.1 ± 1.3	108.9 ± 1.3	112 ± 3	109 ± 1.2	108.8 ± 0.4
<OSO	100.7 ± 2.0	105.9 ± 2.6	99 ± 2	100 ± 0.6	97.8 ± 0.3
<COS	114.1 ± 1.0	119.7 ± 1.9	113 ± 2	116 ± 0.7	116.2 ± 0.3
<OS=O	116.7 ± 1.4	108.7 ± 1.5	113.5 ± 3	107 ± 0.4	107.2 ± 0.2

[1] Bond lengths in Å, angles in degrees. The mean square amplitudes of vibration are given in parenthesis.

and his co-workers have pointed out (15), that the <OS=O would tend to become much smaller than that determined for an axial S=O model in an effort to make these distances the same as before.

In summary, the electron diffraction data is not consistent with a static boat, or fully twisted conformation for racemic 4,6-dimethyl trimethylene sulfite. It has been pointed out (25) that the axial position for the S=O group experiences a minimum of gauche interactions with the geminal electron pairs at the adjacent ring atoms, as compared to an equatorial S=O bond. The available evidence favors a chair form with an axial S=O bond, although the equatorial form, or mixture of conformers could not be definitely eliminated.

REFERENCES

(1) P.B.D. de la Mare, W. Klyne, D.J. Millen, J. G. Pritchard, and D. Watson. J. Chem. Soc. 1813 (1956).

(2) J.G. Pritchard and R.L. Vollmer. J. Org. Chem. 28, 1545 (1963).

(3) P.C. Lauterbur, J.G.Pritchard, and R.L. Vollmer, J. Chem. Soc. 5307 (1963).

(4) D.G. Hellier, J.G. Tillett, H.F. van Woerden, and R.F.M. White. Chem. Ind. (London). 1956 (1963).

(5) R.S. Edmundson. Tetrahedron Lett. 1649 (1965).

(6) H.F. van Woerden. ibid. 2407 (1966).

(7) B.A. Arbuzov. Bull. Soc. Chim. Fr. 1311 (1960).

(8) C.G. Overberger, T. Kurtz, and S. Yaroslavsky. J. Org. Chem. 30, 4363 (1965).

(9) H.F. van Woerden. Ph.D. Thesis, Leiden, 1964.

(10) H.F. van Woerden and E. Havinga. Rec. Trav. Chim. 86, 341 (1967).

(11) H.F. van Woerden and E. Havinga. ibid. 86, 353 (1967).

(12) D.G. Hellier. Ph.D. Thesis. University of London, London, England, 1966.

(13) P. Albriktsen. Acta Chem. Scand. 25, 478 (1971).

(14) C. Altona, H.J. Geise, and C. Romers. Rec. Trav. Chim. 85, 1197 (1966).

(15) J.W.L. van Oyen, R.C.D.E. Hasekamp, G.C. Verschoor, and C. Romers. Acta Cryst. B24, 1471 (1968).

(16) V.A. Naumov, N.M.Zaripov, and LF. Shatrukov. Zh. Strukt. Khim. 8, 291 (1967).

(17) A.B. Remizov. Zh. Prikl. Spektroskopii 14, 425 (1971).

(18) A.B. Remizov. Zh. Strukt. Khim. 12, 1101 (1971).

(19) W. Wucherpfennig. Justus Liebigs Ann. Chem. 737, 144 (1970).

(20) L. Cazaux and P. Maroni. Tetrahedron Lett. 3667 (1969).

(21) R. Pethrick, E. Wyn-Jones, P. Hamblin, and R. White. J. Mol. Struct. 1, 333 (1967-68).

(22) (a) R.A.Pethrick, E. Wyn-Jones, P. Hamblin, and R. White. Trans. Faraday Soc. 66, 310 (1970); (b) E. Wyn-Jones and R.A. Pethrick. In topics in Stereochemistry. Vol. 5. Edited by E. L. Eliel and W. L. Allinger, Interscience, New York, N.Y. 1970. p. 205.

(23) R.A. Pethrick, E. Wyn-Jones, P.C. Hamblin, and R.F.M. White. J. Chem. Soc. A, 2252 (1969).

(24) R.A. Pethrick and E. Wyn-Jones. Quart. Rev. (London), 23, 304 (1969).

(25) P. Albriksten. Acta Chem. Scand. 26, 1783 and 3678 (1972).

(26) G. Wood and M. H. Miskow. Tetrahedron Lett. 14, 1109 (1969).

(27) M. H. Miskow Ph.D. Thesis. University of Windsor, Windsor, Ontario, 1971.

(28) G.W.Wood, J.M. McIntosh and M.H. Miskow. Can. J. Chem. 49, 1202 (1971).

(29) S.H. Bauer and K. Kimura. J. Phys. Soc. Jap. 17, 300 (1962).

(30) W. Harshbarger, G. Lee, R. F. Porter, and S. H. Bauer. Inorg. Chem. 8, 1683 (1969).

(31) J.L. Hencher and S.H. Bauer. J. Amer. Chem. Soc. 89, 5527 (1967).

(32) T.G. Strand, D.A. Kohl, and R.A. Bonham. J. Chem. Phys. 39, 1307 (1963).

(33) Y. Murata and Y. Morino. Acta Cryst. 20, 605 (1966).

(34) L.S. Bartell. J. Chem. Phys. 23, 1219 (1955).

(35) K. Kuchitsu and L.S. Bartell. ibid. 35, 1945 (1961).

(36) R.L. Hilderbrandt. ibid. 51, 1654 (1969).

(37) W.C. Hamilton. Statistics in physical science. The Ronald Press Company, New York. 1964.

(38) W.C. Hamilton. Acta Cryst. 18, 502 (1965).

APPENDIX A

SECTOR FUNCTION FROM CARBON DISULFIDE SCATTERING

LONG DISTANCE 296.16MM

7	0.00426	8	0.00500	9	0.00573	10	0.00660	11	0.00796
12	0.01057	13	0.01505	14	0.02181	15	0.03108	16	0.04207
17	0.05427	18	0.06648	19	0.07887	20	0.09241	21	0.10739
22	0.12455	23	0.14437	24	0.16662	25	0.19316	26	0.22374
27	0.25967	28	0.30061	29	0.34443	30	0.39286	31	0.44302
32	0.49718	33	0.55756	34	0.62525	35	0.69739	36	0.77498
37	0.85780	38	0.94668	39	1.04446	40	1.15603	41	1.27700
42	1.40752	43	1.55184	44	1.69151	45	1.82883		

SHORT DISTANCE 95.45MM

35	0.01044	36	0.01126	37	0.01228	38	0.01350	39	0.01498
40	0.01682	41	0.01892	42	0.02132	43	0.02411	44	0.02732
45	0.03092	46	0.03478	47	0.03896	48	0.04347	49	0.04832
50	0.05346	51	0.05873	52	0.06416	53	0.06983	54	0.07550
55	0.08125	56	0.08700	57	0.09278	58	0.09859	59	0.10438
60	0.11025	61	0.11620	62	0.12244	63	0.12871	64	0.13512
65	0.14163	66	0.14819	67	0.15494	68	0.16197	69	0.16872
70	0.17587	71	0.18336	72	0.19120	73	0.19926	74	0.20773
75	0.21676	76	0.22601	77	0.23565	78	0.24539	79	0.25582
80	0.26688	81	0.27804	82	0.28978	83	0.30166	84	0.31406
85	0.32713	86	0.34083	87	0.35521	88	0.37017	89	0.38527
90	0.40077	91	0.41667	92	0.43288	93	0.44958	94	0.46668
95	0.48398	96	0.50204	97	0.51961	98	0.53792	99	0.55735
100	0.57739	101	0.59738	102	0.61836	103	0.63990	104	0.66134
105	0.68493	106	0.70916	107	0.73361	108	0.75710	109	0.78056
110	0.80475	111	0.82991	112	0.85585	113	0.88288	114	0.90975
115	0.93671	116	0.96529	117	0.99493	118	1.02673	119	1.05966
120	1.09213	121	1.12398	122	1.15652	123	1.19048	124	1.22477
125	1.26006	126	1.29668	127	1.33362	128	1.36902	129	1.40768
130	1.44795	131	1.48912	132	1.53396	133	1.57875	134	1.62359
135	1.67082								

Appendix B

Calculation of Scale Parameters from Magnesium Oxide

Approximate MgO-photographic Plate Distance = 307.05 mm

Miller Indecis	Diameter Measurements mm				Average Radius mm	Standard Deviation	s(experimental)[1]	s(theoretical)[2]
111	12.605	12.625	12.600	12.615	6.306	0.005	0.204066	0.204985
200	14.594	14.619	14.611	14.610	7.304	0.005	0.236372	0.236697
220	20.667	20.655	20.715	20.686	10.340	0.011	0.334552	0.334740
222	25.351	25.315	25.347	25.353	12.671	0.008	0.409862	0.409971
400	29.276	29.266	29.290	29.304	14.642	0.007	0.473525	0.473394
420	32.703	32.723	32.765	32.754	16.368	0.012	0.529236	0.529270
422	35.862	35.819	35.852	35.885	17.927	0.012	0.579525	0.579786
440	41.396	41.442	41.442	41.417	20.712	0.010	0.669265	0.669480
600	43.941	43.945	43.969	44.011	21.983	0.014	0.710186	0.710090
620	46.362	46.336	46.436	46.448	23.198	0.024	0.749258	0.748501

Final scale parameters were L = 307.24 mm

λ = 0.050279 Å

[1] $s(\text{experimental}) = |(4\pi/\lambda)\sin(0.5 \tan^{-1}(r/L))$

[2] $s(\text{theoretical}) = 4\pi (h^2+k^2+\ell^2)^{1/2}/a_o$

APPENDIX C

EXPERIMENTAL INTENSITIES FOR (CH3)2CFH2

CURVE I. WAVELENGTH=0.050664A SAMPLE DISTANCE=296.16mm

7	0.4673	8	0.5126	9	0.4064	10	0.3397	11	0.3089	12	0.3199	13	0.3488	14	0.3939	15	0.4361	16	0.4608
17	0.4763	18	0.4840	19	0.4912	20	0.5011	21	0.5090	22	0.5156	23	0.5199	24	0.5185	25	0.5126	26	0.5050
27	0.4930	28	0.4874	29	0.4878	30	0.4926	31	0.5011	32	0.5086	33	0.5092	34	0.5043	35	0.4947	36	0.4860
37	0.4765	38	0.4720	39	0.4708	40	0.4721	41	0.4739	42	0.4768	43	0.4733						

CURVE II. WAVELENGTH=0.050664A SAMPLE DISTANCE=296.16mm

7	0.4526	8	0.5137	9	0.4042	10	0.3368	11	0.3070	12	0.3147	13	0.3490	14	0.3953	15	0.4362	16	0.4623
17	0.4774	18	0.4851	19	0.4916	20	0.5012	21	0.5093	22	0.5147	23	0.5184	24	0.5179	25	0.5109	26	0.5015
27	0.4926	28	0.4872	29	0.4883	30	0.4936	31	0.5023	32	0.5090	33	0.5093	34	0.5034	35	0.4955	36	0.4836
37	0.4761	38	0.4716	39	0.4704	40	0.4718	41	0.4729	42	0.4743	43	0.4727						

CURVE III. WAVELENGTH=0.050664A SAMPLE DISTANCE=296.16mm

7	0.4743	8	0.5196	9	0.4141	10	0.3460	11	0.3152	12	0.3214	13	0.3538	14	0.3971	15	0.4404	16	0.4673
17	0.4816	18	0.4906	19	0.4957	20	0.5055	21	0.5146	22	0.5214	23	0.5255	24	0.5251	25	0.5207	26	0.5087
27	0.4988	28	0.4927	29	0.4930	30	0.4988	31	0.5059	32	0.5147	33	0.5161	34	0.5121	35	0.5027	36	0.4926
37	0.4822	38	0.4792	39	0.4783	40	0.4790	41	0.4795	42	0.4809	43	0.4798						

CURVE IV. WAVELENGTH=0.050664A SAMPLE DISTANCE=296.16mm

7	0.4898	8	0.5199	9	0.4096	10	0.3418	11	0.3115	12	0.3190	13	0.3530	14	0.3995	15	0.4399	16	0.4673
17	0.4826	18	0.4902	19	0.4963	20	0.5047	21	0.5154	22	0.5199	23	0.5233	24	0.5227	25	0.5165	26	0.5072
27	0.4973	28	0.4916	29	0.4923	30	0.4983	31	0.5046	32	0.5116	33	0.5127	34	0.5081	35	0.4983	36	0.4886
37	0.4831	38	0.4795	39	0.4784	40	0.4748	41	0.4795	42	0.4778	43	0.4756						

CURVE V. WAVELENGTH=0.050661A SAMPLE DISTANCE=95.45mm

35	0.2181	36	0.2076	37	0.2012	38	0.1993	39	0.2004	40	0.2045	41	0.2106	42	0.2170	43	0.2231	44	0.2275
45	0.2355	46	0.2404	47	0.2453	48	0.2500	49	0.2541	50	0.2604	51	0.2649	52	0.2687	53	0.2706	54	0.2722
55	0.2718	56	0.2705	57	0.2683	58	0.2659	59	0.2649	60	0.2617	61	0.2594	62	0.2577	63	0.2546	64	0.2513
65	0.2479	66	0.2438	67	0.2406	68	0.2372	69	0.2339	70	0.2317	71	0.2295	72	0.2282	73	0.2261	74	0.2241
75	0.2221	76	0.2203	77	0.2186	78	0.2166	79	0.2160	80	0.2151	81	0.2142	82	0.2130	83	0.2121	84	0.2114
85	0.2111	86	0.2099	87	0.2094	88	0.2087	89	0.2086	90	0.2079	91	0.2073	92	0.2068	93	0.2063	94	0.2057
95	0.2052	96	0.2046	97	0.2039	98	0.2034	99	0.2027	100	0.2020	101	0.2014	102	0.2009	103	0.2005	104	0.2001
105	0.1994																		

CURVE VI. WAVELENGTH=0.050661A SAMPLE DISTANCE=95.45mm

35	0.2122	36	0.2030	37	0.1973	38	0.1951	39	0.1970	40	0.2015	41	0.2072	42	0.2134	43	0.2199	44	0.2247
45	0.2324	46	0.2379	47	0.2430	48	0.2478	49	0.2526	50	0.2578	51	0.2626	52	0.2668	53	0.2693	54	0.2701
55	0.2696	56	0.2677	57	0.2653	58	0.2655	59	0.2642	60	0.2612	61	0.2591	62	0.2553	63	0.2527	64	0.2494
65	0.2459	66	0.2423	67	0.2387	68	0.2351	69	0.2321	70	0.2301	71	0.2282	72	0.2263	73	0.2242	74	0.2225
75	0.2205	76	0.2186	77	0.2167	78	0.2152	79	0.2138	80	0.2128	81	0.2119	82	0.2115	83	0.2108	84	0.2100
85	0.2093	86	0.2088	87	0.2082	88	0.2077	89	0.2072	90	0.2071	91	0.2066	92	0.2062	93	0.2061	94	0.2057
95	0.2048	96	0.2042	97	0.2034	98	0.2028	99	0.2020	100	0.2015	101	0.2011	102	0.2005	103	0.1998	104	0.1992
105	0.1986																		

CURVE VII. WAVELENGTH=0.050661A SAMPLE DISTANCE=95.45mm

35	0.3643	36	0.3467	37	0.3358	38	0.3324	39	0.3347	40	0.3420	41	0.3525	42	0.3629	43	0.3735	44	0.3835
45	0.3940	46	0.4028	47	0.4110	48	0.4203	49	0.4296	50	0.4381	51	0.4470	52	0.4539	53	0.4581	54	0.4598
55	0.4591	56	0.4562	57	0.4516	58	0.4474	59	0.4431	60	0.4391	61	0.4348	62	0.4313	63	0.4268	64	0.4215
65	0.4157	66	0.4090	67	0.4017	68	0.3954	69	0.3902	70	0.3855	71	0.3815	72	0.3785	73	0.3755	74	0.3729
75	0.3685	76	0.3645	77	0.3607	78	0.3577	79	0.3552	80	0.3529	81	0.3515	82	0.3504	83	0.3490	84	0.3477
85	0.3464	86	0.3450	87	0.3438	88	0.3427	89	0.3417	90	0.3408	91	0.3402	92	0.3395	93	0.3383	94	0.3375
95	0.3360	96	0.3344	97	0.3335	98	0.3322	99	0.3307	100	0.3293	101	0.3285	102	0.3280	103	0.3266	104	0.3254
105	0.3244																		

CURVE VIII. WAVELENGTH=0.050661A SAMPLE DISTANCE=95.45mm

35	0.3566	36	0.3415	37	0.3303	38	0.3253	39	0.3285	40	0.3366	41	0.3467	42	0.3573	43	0.3690	44	0.3799
45	0.3902	46	0.3992	47	0.4076	48	0.4162	49	0.4254	50	0.4338	51	0.4421	52	0.4493	53	0.4538	54	0.4556
55	0.4548	56	0.4512	57	0.4471	58	0.4424	59	0.4383	60	0.4340	61	0.4300	62	0.4264	63	0.4218	64	0.4161
65	0.4100	66	0.4036	67	0.3966	68	0.3902	69	0.3850	70	0.3808	71	0.3770	72	0.3735	73	0.3708	74	0.3681
75	0.3645	76	0.3609	77	0.3570	78	0.3544	79	0.3520	80	0.3498	81	0.3484	82	0.3473	83	0.3457	84	0.3443
85	0.3434	86	0.3425	87	0.3411	88	0.3402	89	0.3395	90	0.3385	91	0.3379	92	0.3370	93	0.3363	94	0.3351
95	0.3336	96	0.3323	97	0.3312	98	0.3297	99	0.3285	100	0.3274	101	0.3264	102	0.3260	103	0.3245	104	0.3235
105	0.3224																		

CURVE IX. WAVELENGTH=0.050661A SAMPLE DISTANCE=95.45mm

35	0.5106	36	0.4861	37	0.4685	38	0.4633	39	0.4665	40	0.4765	41	0.4918	42	0.5065	43	0.5216	44	0.5370
45	0.5521	46	0.5649	47	0.5763	48	0.5884	49	0.6015	50	0.6149	51	0.6271	52	0.6370	53	0.6434	54	0.6460
55	0.6451	56	0.6410	57	0.6351	58	0.6283	59	0.6224	60	0.6172	61	0.6115	62	0.6052	63	0.5994	64	0.5921
65	0.5820	66	0.5719	67	0.5631	68	0.5539	69	0.5448	70	0.5403	71	0.5352	72	0.5302	73	0.5260	74	0.5209
75	0.5161	76	0.5109	77	0.5059	78	0.5011	79	0.4972	80	0.4947	81	0.4920	82	0.4903	83	0.4887	84	0.4872
85	0.4852	86	0.4826	87	0.4811	88	0.4791	89	0.4781	90	0.4763	91	0.4751	92	0.4737	93	0.4728	94	0.4719
95	0.4697	96	0.4681	97	0.4655	98	0.4638	99	0.4620	100	0.4601	101	0.4588	102	0.4568	103	0.4555	104	0.4539
105	0.4525																		

CURVE X. WAVELENGTH=0.050661A SAMPLE DISTANCE=95.45mm

35	0.4990	36	0.4754	37	0.4612	38	0.4554	39	0.4583	40	0.4691	41	0.4813	42	0.4973	43	0.5158	44	0.5304
45	0.5436	46	0.5562	47	0.5702	48	0.5819	49	0.5913	50	0.6038	51	0.6162	52	0.6265	53	0.6325	54	0.6344
55	0.6333	56	0.6286	57	0.6232	58	0.6161	59	0.6091	60	0.6037	61	0.5976	62	0.5935	63	0.5894	64	0.5820
65	0.5740	66	0.5636	67	0.5529	68	0.5439	69	0.5360	70	0.5284	71	0.5231	72	0.5181	73	0.5137	74	0.5099
75	0.5060	76	0.4990	77	0.4958	78	0.4918	79	0.4877	80	0.4855	81	0.4842	82	0.4820	83	0.4800	84	0.4785
85	0.4767	86	0.4751	87	0.4737	88	0.4727	89	0.4708	90	0.4688	91	0.4680	92	0.4673	93	0.4663	94	0.4650
95	0.4634	96	0.4614	97	0.4596	98	0.4554	99	0.4532	100	0.4513	101	0.4503	102	0.4490	103	0.4470	104	0.4456
105	0.4446																		

APPENDIX D

EXPERIMENTAL INTENSITIES FOR (CH3)4GE

CURVE I. WAVELENGTH=0.05060A SAMPLE DISTANCE=296.16MM

7	0.7459	8	0.5775	9	0.4548	10	0.3796	11	0.3531	12	0.3712	13	0.4135	14	0.4576	15	0.4831	16	0.4855
17	0.4865	18	0.5012	19	0.5294	20	0.5557	21	0.5668	22	0.5691	23	0.5696	24	0.5671	25	0.5586	26	0.5386
27	0.5127	28	0.4925	29	0.4882	30	0.4977	31	0.5173	32	0.5332	33	0.5384	34	0.5338	35	0.5161	36	0.4971
37	0.4859	38	0.4796	39	0.4811	40	0.4846	41	0.4881	42	0.4898	43	0.4890						

CURVE II. WAVELENGTH=0.05060A SAMPLE DISTANCE=296.16MM

7	0.7581	8	0.5784	9	0.4482	10	0.3743	11	0.3493	12	0.3676	13	0.4121	14	0.4562	15	0.4812	16	0.4829
17	0.4847	18	0.5007	19	0.5281	20	0.5529	21	0.5646	22	0.5660	23	0.5655	24	0.5627	25	0.5537	26	0.5330
27	0.5082	28	0.4891	29	0.4853	30	0.4959	31	0.5135	32	0.5302	33	0.5350	34	0.5272	35	0.5092	36	0.4925
37	0.4805	38	0.4756	39	0.4768	40	0.4796	41	0.4830	42	0.4844	43	0.4836						

CURVE III. WAVELENGTH=0.05054A SAMPLE DISTANCE=95.45MM

35	0.3355	36	0.3137	37	0.3011	38	0.2982	39	0.3024	40	0.3123	41	0.3228	42	0.3335	43	0.3451	44	0.3554
45	0.3630	46	0.3685	47	0.3745	48	0.3830	49	0.3926	50	0.4021	51	0.4109	52	0.4191	53	0.4237	54	0.4243
55	0.4215	56	0.4159	57	0.4102	58	0.4049	59	0.4002	60	0.3967	61	0.3933	62	0.3901	63	0.3856	64	0.3795
65	0.3719	66	0.3637	67	0.3563	68	0.3505	69	0.3431	70	0.3415	71	0.3410	72	0.3371	73	0.3329	74	0.3287
75	0.3228	76	0.3185	77	0.3144	78	0.3110	79	0.3079	80	0.3060	81	0.3047	82	0.3034	83	0.3021	84	0.3005
85	0.2991	86	0.2972	87	0.2955	88	0.2941	89	0.2927	90	0.2917	91	0.2909	92	0.2901	93	0.2895	94	0.2879
95	0.2861	96	0.2843	97	0.2828	98	0.2810	99	0.2797	100	0.2784	101	0.2774	102	0.2763	103	0.2747	104	0.2737
105	0.2726	106	0.2711	107	0.2694	108	0.2680	109	0.2666	110	0.2652	111	0.2643						

CURVE IV. WAVELENGTH=0.05054A SAMPLE DISTANCE=95.45MM

35	0.4868	36	0.4554	37	0.4389	38	0.4350	39	0.4440	40	0.4593	41	0.4760	42	0.4937	43	0.5118	44	0.5281
45	0.5393	46	0.5485	47	0.5571	48	0.5677	49	0.5833	50	0.6004	51	0.6136	52	0.6237	53	0.6305	54	0.6309
55	0.6257	56	0.6183	57	0.6097	58	0.6014	59	0.5953	60	0.5899	61	0.5858	62	0.5816	63	0.5750	64	0.5669
65	0.5576	66	0.5456	67	0.5343	68	0.5247	69	0.5179	70	0.5128	71	0.5091	72	0.5053	73	0.5011	74	0.4954
75	0.4890	76	0.4828	77	0.4771	78	0.4722	79	0.4682	80	0.4657	81	0.4638	82	0.4622	83	0.4610	84	0.4592
85	0.4567	86	0.4544	87	0.4518	88	0.4498	89	0.4486	90	0.4479	91	0.4468	92	0.4458	93	0.4445	94	0.4430
95	0.4404	96	0.4379	97	0.4357	98	0.4333	99	0.4312	100	0.4291	101	0.4272	102	0.4261	103	0.4245	104	0.4225
105	0.4208	106	0.4189	107	0.4166	108	0.4143	109	0.4123	110	0.4106	111	0.4083						

CURVE V. WAVELENGTH=0.05054A SAMPLE DISTANCE=95.45MM

35	0.4889	36	0.4562	37	0.4376	38	0.4336	39	0.4418	40	0.4568	41	0.4741	42	0.4909	43	0.5083	44	0.5244
45	0.5364	46	0.5451	47	0.5534	48	0.5645	49	0.5805	50	0.5977	51	0.6139	52	0.6267	53	0.6336	54	0.6331
55	0.6285	56	0.6220	57	0.6161	58	0.6086	59	0.6021	60	0.5970	61	0.5928	62	0.5883	63	0.5812	64	0.5712
65	0.5591	66	0.5462	67	0.5349	68	0.5255	69	0.5166	70	0.5107	71	0.5068	72	0.5028	73	0.4979	74	0.4921
75	0.4863	76	0.4804	77	0.4741	78	0.4690	79	0.4653	80	0.4629	81	0.4607	82	0.4590	83	0.4575	84	0.4550
85	0.4526	86	0.4497	87	0.4472	88	0.4456	89	0.4437	90	0.4422	91	0.4414	92	0.4404	93	0.4387	94	0.4369
95	0.4348	96	0.4325	97	0.4300	98	0.4275	99	0.4252	100	0.4234	101	0.4219	102	0.4203	103	0.4187	104	0.4169
105	0.4146	106	0.4129	107	0.4106	108	0.4082	109	0.4063	110	0.4045	111	0.4027						

APPENDIX E

EXPERIMENTAL INTENSITIES FOR CH3CEF3

CURVE I. WAVELENGTH=0.05007 SAMPLE DISTANCE=296.16MM

7	0.4707	8	0.3556	9	0.2821	10	0.2373	11	0.2233	12	0.2430	13	0.2911	14	0.3566	15	0.4137	16	0.4438
17	0.4399	18	0.4169	19	0.3935	20	0.3847	21	0.3925	22	0.4113	23	0.4320	24	0.4471	25	0.4559	26	0.4580
27	0.4490	28	0.4381	29	0.4269	30	0.4124	31	0.4037	32	0.4000	33	0.4011	34	0.4037	35	0.4079	36	0.4119
37	0.4139	38	0.4129	39	0.4078	40	0.3997	41	0.3897	42	0.3804	43	0.3738	44	0.3704	45	0.3707		

CURVE II. WAVELENGTH=0.05007 SAMPLE DISTANCE=296.16MM

7	0.4772	8	0.3545	9	0.2779	10	0.2339	11	0.2210	12	0.2420	13	0.2934	14	0.3596	15	0.4165	16	0.4450
17	0.4402	18	0.4168	19	0.3931	20	0.3852	21	0.3942	22	0.4132	23	0.4332	24	0.4482	25	0.4567	26	0.4571
27	0.4510	28	0.4389	29	0.4238	30	0.4111	31	0.4031	32	0.4007	33	0.4004	34	0.4033	35	0.4070	36	0.4108
37	0.4134	38	0.4121	39	0.4070	40	0.3986	41	0.3884	42	0.3794	43	0.3727	44	0.3694	45	0.3694		

CURVE III. WAVELENGTH=0.05007 SAMPLE DISTANCE=296.16MM

7	0.5726	8	0.4235	9	0.3226	10	0.2727	11	0.2621	12	0.2904	13	0.3521	14	0.4279	15	0.4919	16	0.5214
17	0.5137	18	0.4840	19	0.4578	20	0.4494	21	0.4601	22	0.4835	23	0.5065	24	0.5242	25	0.5330	26	0.5331
27	0.5258	28	0.5121	29	0.4966	30	0.4819	31	0.4716	32	0.4668	33	0.4674	34	0.4713	35	0.4761	36	0.4813
37	0.4847	38	0.4834	39	0.4779	40	0.4672	41	0.4561	42	0.4450	43	0.4364	44	0.4316	45	0.4314		

CURVE IV. WAVELENGTH=0.05007 SAMPLE DISTANCE=296.16MM

7	0.5655	8	0.4249	9	0.3356	10	0.2816	11	0.2611	12	0.2817	13	0.3353	14	0.4078	15	0.4785	16	0.5168
17	0.5165	18	0.4908	19	0.4622	20	0.4489	21	0.4563	22	0.4772	23	0.5018	24	0.5205	25	0.5313	26	0.5333
27	0.5275	28	0.5161	29	0.5003	30	0.4851	31	0.4737	32	0.4675	33	0.4663	34	0.4692	35	0.4745	36	0.4795
37	0.4834	38	0.4834	39	0.4788	40	0.4694	41	0.4582	42	0.4462	43	0.4372	44	0.4315	45	0.4298		

CURVE V. WAVELENGTH=0.05015A SAMPLE DISTANCE=95.45MM

35	0.3148	36	0.3071	37	0.3031	38	0.3001	39	0.2992	40	0.2990	41	0.2987	42	0.3002	43	0.3038	44	0.3114
45	0.3237	46	0.3380	47	0.3506	48	0.3613	49	0.3699	50	0.3759	51	0.3796	52	0.3820	53	0.3819	54	0.3803
55	0.3779	56	0.3755	57	0.3741	58	0.3735	59	0.3734	60	0.3727	61	0.3697	62	0.3650	63	0.3595	64	0.3539
65	0.3462	66	0.3397	67	0.3346	68	0.3302	69	0.3260	70	0.3232	71	0.3211	72	0.3193	73	0.3168	74	0.3139
75	0.3102	76	0.3066	77	0.3028	78	0.2992	79	0.2969	80	0.2951	81	0.2944	82	0.2939	83	0.2934	84	0.2927
85	0.2915	86	0.2904	87	0.2890	88	0.2876	89	0.2861	90	0.2846	91	0.2835	92	0.2829	93	0.2827	94	0.2828
95	0.2823	96	0.2815	97	0.2804	98	0.2791	99	0.2774	100	0.2760	101	0.2745	102	0.2734	103	0.2724	104	0.2719
105	0.2712	106	0.2707	107	0.2701	108	0.2690	109	0.2680	110	0.2668	111	0.2656	112	0.2645	113	0.2631	114	0.2621

CURVE VI. WAVELENGTH=0.05015A SAMPLE DISTANCE=95.45MM

35	0.3192	36	0.3121	37	0.3077	38	0.3048	39	0.3040	40	0.3034	41	0.3034	42	0.3046	43	0.3087	44	0.3157
45	0.3291	46	0.3428	47	0.3550	48	0.3659	49	0.3745	50	0.3807	51	0.3841	52	0.3864	53	0.3868	54	0.3851
55	0.3825	56	0.3798	57	0.3786	58	0.3776	59	0.3775	60	0.3770	61	0.3745	62	0.3696	63	0.3637	64	0.3576
65	0.3506	66	0.3441	67	0.3387	68	0.3337	69	0.3295	70	0.3273	71	0.3253	72	0.3229	73	0.3207	74	0.3175
75	0.3137	76	0.3098	77	0.3062	78	0.3029	79	0.3005	80	0.2986	81	0.2980	82	0.2977	83	0.2968	84	0.2962
85	0.2951	86	0.2936	87	0.2923	88	0.2908	89	0.2891	90	0.2880	91	0.2879	92	0.2869	93	0.2869	94	0.2857
95	0.2858	96	0.2855	97	0.2845	98	0.2829	99	0.2814	100	0.2795	101	0.2781	102	0.2776	103	0.2765	104	0.2757
105	0.2750	106	0.2745	107	0.2738	108	0.2728	109	0.2722	110	0.2709	111	0.2704	112	0.2680	113	0.2675	114	0.2670

CURVE VII. WAVELENGTH=0.05015A SAMPLE DISTANCE=95.45MM

35	0.3112	36	0.3037	37	0.3006	38	0.2978	39	0.2965	40	0.2960	41	0.2969	42	0.2978	43	0.3026	44	0.3107
45	0.3222	46	0.3365	47	0.3496	48	0.3603	49	0.3695	50	0.3747	51	0.3787	52	0.3805	53	0.3814	54	0.3791
55	0.3772	56	0.3757	57	0.3739	58	0.3724	59	0.3726	60	0.3717	61	0.3688	62	0.3644	63	0.3579	64	0.3514
65	0.3436	66	0.3394	67	0.3333	68	0.3293	69	0.3256	70	0.3222	71	0.3200	72	0.3180	73	0.3158	74	0.3132
75	0.3101	76	0.3047	77	0.3008	78	0.2985	79	0.2958	80	0.2940	81	0.2935	82	0.2934	83	0.2927	84	0.2920
85	0.2911	86	0.2905	87	0.2891	88	0.2874	89	0.2861	90	0.2851	91	0.2860	92	0.2835	93	0.2833	94	0.2833
95	0.2824	96	0.2823	97	0.2813	98	0.2796	99	0.2782	100	0.2771	101	0.2754	102	0.2741	103	0.2731	104	0.2727
105	0.2723	106	0.2719	107	0.2711	108	0.2701	109	0.2688	110	0.2688	111	0.2669	112	0.2657	113	0.2646	114	0.2640

APPENDIX F

EXPERIMENTAL INTENSITIES FOR CH3CEBr3

CURVE I. WAVELENGTH=0.05025A SAMPLE DISTANCE=296.16MM

7	0.2353	8	0.1621	9	0.1184	10	0.0974	11	0.0962	12	0.0999	13	0.1004	14	0.0974	15	0.0991	16	0.1152
17	0.1392	18	0.1556	19	0.1574	20	0.1506	21	0.1467	22	0.1439	23	0.1423	24	0.1377	25	0.1351	26	0.1392
27	0.1492	28	0.1577	29	0.1582	30	0.1525	31	0.1448	32	0.1446	33	0.1440	34	0.1479	35	0.1510	36	0.1527
37	0.1540	38	0.1538	39	0.1516	40	0.1480	41	0.1441	42	0.1429	43	0.1459	44	0.1504	45	0.1548		

CURVE II. WAVELENGTH=0.05025A SAMPLE DISTANCE=296.16MM

7	0.2320	8	0.1570	9	0.1105	10	0.0935	11	0.0910	12	0.0948	13	0.0935	14	0.0967	15	0.0986	16	0.1155
17	0.1396	18	0.1552	19	0.1565	20	0.1498	21	0.1444	22	0.1432	23	0.1412	24	0.1367	25	0.1340	26	0.1381
27	0.1483	28	0.1558	29	0.1581	30	0.1514	31	0.1439	32	0.1413	33	0.1438	34	0.1474	35	0.1493	36	0.1509
37	0.1520	38	0.1524	39	0.1500	40	0.1454	41	0.1418	42	0.1406	43	0.1431	44	0.1466	45	0.1490		

CURVE III. WAVELENGTH=0.05025A SAMPLE DISTANCE=296.16MM

7	0.3922	8	0.2785	9	0.2045	10	0.1747	11	0.1707	12	0.1767	13	0.1772	14	0.1731	15	0.1766	16	0.2076
17	0.2393	18	0.2648	19	0.2689	20	0.2597	21	0.2510	22	0.2482	23	0.2454	24	0.2384	25	0.2339	26	0.2395
27	0.2547	28	0.2684	29	0.2698	30	0.2608	31	0.2486	32	0.2448	33	0.2480	34	0.2538	35	0.2583	36	0.2602
37	0.2618	38	0.2625	39	0.2590	40	0.2521	41	0.2461	42	0.2442	43	0.2480	44	0.2541	45	0.2577		

CURVE IV. WAVELENGTH=0.05025A SAMPLE DISTANCE=296.16MM

7	0.3894	8	0.2761	9	0.1995	10	0.1708	11	0.1681	12	0.1740	13	0.1748	14	0.1711	15	0.1761	16	0.2018
17	0.2401	18	0.2656	19	0.2691	20	0.2595	21	0.2504	22	0.2477	23	0.2450	24	0.2384	25	0.2344	26	0.2398
27	0.2550	28	0.2682	29	0.2698	30	0.2604	31	0.2490	32	0.2444	33	0.2477	34	0.2536	35	0.2575	36	0.2594
37	0.2610	38	0.2612	39	0.2576	40	0.2504	41	0.2438	42	0.2420	43	0.2461	44	0.2524	45	0.2558		

CURVE V. WAVELENGTH=0.05006A SAMPLE DISTANCE=95.45MM

35	0.2249	36	0.2190	37	0.2153	38	0.2134	39	0.2114	40	0.2094	41	0.2097	42	0.2145	43	0.2241	44	0.2378
45	0.2498	46	0.2576	47	0.2626	48	0.2653	49	0.2683	50	0.2724	51	0.2765	52	0.2823	53	0.2887	54	0.2942
55	0.2958	56	0.2936	57	0.2879	58	0.2819	59	0.2789	60	0.2782	61	0.2782	62	0.2780	63	0.2760	64	0.2730
65	0.2677	66	0.2621	67	0.2566	68	0.2532	69	0.2507	70	0.2497	71	0.2501	72	0.2491	73	0.2462	74	0.2429
75	0.2395	76	0.2368	77	0.2354	78	0.2345	79	0.2331	80	0.2333	81	0.2329	82	0.2319	83	0.2298	84	0.2287
85	0.2272	86	0.2267	87	0.2286	88	0.2301	89	0.2309	90	0.2308	91	0.2298	92	0.2284	93	0.2266	94	0.2257
95	0.2255	96	0.2282	97	0.2295	98	0.2264	99	0.2265	100	0.2255	101	0.2237	102	0.2235	103	0.2229	104	0.2229
105	0.2237	106	0.2233	107	0.2235	108	0.2236	109	0.2217	110	0.2209	111	0.2214	112	0.2214	113	0.2214	114	0.2219
115	0.2224	116	0.2225	117	0.2229	118	0.2235	119	0.2226	120	0.2224	121	0.2231	122	0.2236	123	0.2236	124	0.2245
125	0.2248	126	0.2249	127	0.2250	128	0.2252	129	0.2253	130	0.2260								

CURVE VI. WAVELENGTH=0.05006A SAMPLE DISTANCE=95.45MM

35	0.2214	36	0.2155	37	0.2127	38	0.2105	39	0.2090	40	0.2073	41	0.2075	42	0.2122	43	0.2235	44	0.2379
45	0.2504	46	0.2593	47	0.2645	48	0.2673	49	0.2708	50	0.2742	51	0.2791	52	0.2855	53	0.2922	54	0.2975
55	0.2999	56	0.2967	57	0.2906	58	0.2853	59	0.2813	60	0.2801	61	0.2805	62	0.2802	63	0.2786	64	0.2752
65	0.2702	66	0.2641	67	0.2587	68	0.2546	69	0.2523	70	0.2516	71	0.2511	72	0.2498	73	0.2474	74	0.2442
75	0.2401	76	0.2366	77	0.2347	78	0.2340	79	0.2341	80	0.2344	81	0.2340	82	0.2327	83	0.2308	84	0.2292
85	0.2283	86	0.2280	87	0.2285	88	0.2304	89	0.2313	90	0.2314	91	0.2311	92	0.2298	93	0.2286	94	0.2282
95	0.2279	96	0.2286	97	0.2292	98	0.2295	99	0.2293	100	0.2284	101	0.2275	102	0.2267	103	0.2259	104	0.2270
105	0.2275	106	0.2279	107	0.2282	108	0.2284	109	0.2281	110	0.2275	111	0.2270	112	0.2270	113	0.2272	114	0.2279
115	0.2288	116	0.2291	117	0.2295	118	0.2293	119	0.2293	120	0.2302	121	0.2305	122	0.2309	123	0.2317	124	0.2328
125	0.2334	126	0.2339	127	0.2347	128	0.2353	129	0.2359	130	0.2367								

CURVE VII. WAVELENGTH=0.05006A SAMPLE DISTANCE=95.45MM

35	0.2286	36	0.2224	37	0.2186	38	0.2161	39	0.2139	40	0.2123	41	0.2122	42	0.2166	43	0.2270	44	0.2406
45	0.2542	46	0.2632	47	0.2679	48	0.2709	49	0.2744	50	0.2786	51	0.2803	52	0.2855	53	0.2930	54	0.2990
55	0.3011	56	0.2987	57	0.2926	58	0.2870	59	0.2838	60	0.2829	61	0.2833	62	0.2831	63	0.2814	64	0.2780
65	0.2734	66	0.2679	67	0.2622	68	0.2582	69	0.2558	70	0.2547	71	0.2544	72	0.2533	73	0.2506	74	0.2467
75	0.2428	76	0.2402	77	0.2380	78	0.2370	79	0.2374	80	0.2377	81	0.2370	82	0.2354	83	0.2337	84	0.2322
85	0.2318	86	0.2306	87	0.2314	88	0.2323	89	0.2322	90	0.2324	91	0.2322	92	0.2311	93	0.2300	94	0.2295
95	0.2296	96	0.2304	97	0.2304	98	0.2309	99	0.2307	100	0.2340	101	0.2315	102	0.2277	103	0.2275	104	0.2286
105	0.2286	106	0.2292	107	0.2294	108	0.2295	109	0.2296	110	0.2288	111	0.2285	112	0.2288	113	0.2288	114	0.2296
115	0.2305	116	0.2311	117	0.2315	118	0.2310	119	0.2315	120	0.2313	121	0.2320	122	0.2327	123	0.2337	124	0.2349
125	0.2356	126	0.2363	127	0.2368	128	0.2374	129	0.2379	130	0.2388								

CURVE VIII. WAVELENGTH=0.05006A SAMPLE DISTANCE=95.45MM

35	0.2193	36	0.2144	37	0.2108	38	0.2095	39	0.2078	40	0.2060	41	0.2062	42	0.2111	43	0.2224	44	0.2360
45	0.2485	46	0.2568	47	0.2614	48	0.2639	49	0.2676	50	0.2709	51	0.2757	52	0.2816	53	0.2882	54	0.2921
55	0.2933	56	0.2916	57	0.2854	58	0.2801	59	0.2770	60	0.2761	61	0.2757	62	0.2756	63	0.2741	64	0.2706
65	0.2654	66	0.2598	67	0.2545	68	0.2512	69	0.2490	70	0.2481	71	0.2484	72	0.2453	73	0.2437	74	0.2398
75	0.2362	76	0.2335	77	0.2325	78	0.2316	79	0.2295	80	0.2305	81	0.2302	82	0.2291	83	0.2276	84	0.2257
85	0.2246	86	0.2244	87	0.2250	88	0.2261	89	0.2265	90	0.2284	91	0.2256	92	0.2245	93	0.2240	94	0.2232
95	0.2226	96	0.2239	97	0.2233	98	0.2231	99	0.2238	100	0.2229	101	0.2220	102	0.2213	103	0.2206	104	0.2207
105	0.2209	106	0.2214	107	0.2211	108	0.2202	109	0.2201	110	0.2205	111	0.2197	112	0.2193	113	0.2197	114	0.2203
115	0.2206	116	0.2210	117	0.2210	118	0.2210	119	0.2208	120	0.2207	121	0.2212	122	0.2217	123	0.2220	124	0.2223
125	0.2229	126	0.2227	127	0.2227	128	0.2239	129	0.2234	130	0.2246								

Appendix G

Correlation matrices[1] for $(CH_3)_2GeH_2$, $(CH_3)_4Ge$, CH_3GeF_3 and CH_3GeBr_3

$(CH_3)_2GeH_2$

	r(Ge-C)	r(C-H)	r(Ge-H)	ℓ(Ge-C)	ℓ(Ge-H)
σ	0.001	0.0054	0.0115	0.0013	0.0049
r(Ge-C)	1				
r(C-H)	-0.22	1			
r(Ge-H)	0.42	0.02	1		
ℓ(Ge-C)	0.04	0.02	-0.08	1	
ℓ(Ge-H)	-0.10	0.05	-0.07	-0.21	1

$(CH_3)_4Ge$

	r(Ge-C)	r(C-H)	ℓ(Ge-C)	ℓ(Ge-H)	ℓ(C..C)
σ	0.0016	0.0094	0.0023	0.0097	0.0098
r(Ge-C)	1				
r(C-H)	-0.20	1			
ℓ(Ge-C	0.06	0.15	1		
ℓ(Ge-H)	-0.21	0.09	-0.18	1	
ℓ(C..C)	0.01	-0.08	0.00	-0.13	1

Appendix G (continued)

CH_3GeF_3

	r(Ge-C)	r(C-H)	r(Ge-F)	<FGeC	ℓ(Ge-F)	ℓ(C..F)	ℓ(F..F)
σ	0.0041	0.0258	0.0009	0.2660	0.0009	0.0069	0.0053
r (Ge-C)	1						
r (C-H)	-0.07	1					
r (Ge-F)	0.29	-0.01	1				
<FGeC	-0.18	-0.06	0.06	1			
ℓ(Ge-F)	0.25	-0.03	0.14	-0.05	1		
ℓ(C..F)	-0.06	-0.05	-0.03	0.23	-0.01	1	
ℓ(F..F)	0.13	0.41	0.08	0.01	0.03	-0.12	1

CH_3GeBr_3

	r(Ge-C)	r(Ge-Br)	<BrCGe	ℓ(Ge-C)	ℓ(Ge-Br)	ℓ(C..Br)	ℓ(Br..Br)
σ	0.0113	0.0006	0.1002	0.0189	0.0006	0.0121	0.0020
r (Ge-C)	1						
r (Ge-Br)	-0.04	1					
<BrCGe	-0.04	0.35	1				
ℓ(Ge-C)	0.09	-0.03	0.01	1			
ℓ(Ge-Br)	0.01	0.08	0.04	-0.02	1		

Appendix G (continued)

ℓ(C..Br)	-0.06	0.00	-0.02	0.02	-0.01	1	
ℓ(Br..Br)	0.07	0.02	-0.03	0.04	0.01	0.37	1

The calculated least squares standard deviation σ is given by

$$\sigma = \left[\frac{B_{11}^{-1} V' W V}{n - m} \right]^{1/2}$$

, and the correlation coefficients by

$$\rho_{ij} = \frac{B_{ij}^{-1}}{\left(B_{11}^{-1} \; B_{jj}^{-1} \right)^{1/2}}$$

APPENDIX H

EXPERIMENTAL INTENSITIES FOR RACEMIC 4,6-DIMETHYL TRIMETHYLENE SULFITE

DATA SET I.

WAVELENGTH=0.04871A SAMPLE DISTANCE=262.97MM

14	0.4659	15	0.5687	16	0.6668	17	0.7210	18	0.7129	19	0.6665	20	0.6036	21	0.5542
22	0.5258	23	0.5314	24	0.5703	25	0.6299	26	0.6856	27	0.7151	28	0.7180	29	0.7119
30	0.7091	31	0.7124	32	0.7155	33	0.7128	34	0.7046	35	0.6945	36	0.6922	37	0.6994
38	0.7170	39	0.7465	40	0.7798	41	0.8088	42	0.8271	43	0.8275	44	0.8139	45	0.7988
46	0.7922	47	0.7969	48	0.8053	49	0.8147	50	0.8229	51	0.8328	52	0.8456	53	0.8574
54	0.8651	55	0.8754	56	0.8883	57	0.8998	58	0.9060	59	0.9107	60	0.9155	61	0.9215
62	0.9290														

WAVELENGTH=0.04871A SAMPLE DISTANCE=262.97MM

40	0.5145	41	0.5373	42	0.5520	43	0.5543	44	0.5444	45	0.5318	46	0.5231	47	0.5240
48	0.5294	49	0.5331	50	0.5366	51	0.5414	52	0.5487	53	0.5558	54	0.5620	55	0.5671
56	0.5729	57	0.5783	58	0.5816	59	0.5819	60	0.5796	61	0.5793	62	0.5814	63	0.5845
64	0.5874	65	0.5909	66	0.5963	67	0.6028	68	0.6095	69	0.6144	70	0.6186	71	0.6233
72	0.6288	73	0.6352	74	0.6412	75	0.6468	76	0.6520	77	0.6568	78	0.6619	79	0.6659
80	0.6699	81	0.6754	82	0.6823	83	0.6904	84	0.6996	85	0.7078	86	0.7157	87	0.7229
88	0.7300	89	0.7380	90	0.7452	91	0.7523	92	0.7588	93	0.7670	94	0.7748	95	0.7830
96	0.7916														

DATA SET II.

WAVELENGTH=0.04871A SAMPLE DISTANCE=167.42MM

6	0.1629	7	0.1417	8	0.1322	9	0.1254	10	0.1220	11	0.1133	12	0.1086	13	0.1136
14	0.1315	15	0.1557	16	0.1793	17	0.1915	18	0.1879	19	0.1771	20	0.1609	21	0.1501
22	0.1444	23	0.1467	24	0.1571	25	0.1729	26	0.1866	27	0.1927	28	0.1932	29	0.1915
30	0.1913	31	0.1921	32	0.1926	33	0.1918	34	0.1895	35	0.1870	36	0.1871	37	0.1906
38	0.1961	39	0.2050	40	0.2144	41	0.2223	42	0.2266	43	0.2271	44	0.2237	45	0.2206
46	0.2206	47	0.2230	48	0.2261	49	0.2288	50	0.2314	51	0.2352	52	0.2392	53	0.2428
54	0.2459	55	0.2493	56	0.2532	57	0.2570	58	0.2593	59	0.2603	60	0.2613	61	0.2633
62	0.2656	63	0.2674												

WAVELENGTH=0.04871A SAMPLE DISTANCE=167.42MM

40	0.2064	41	0.2165	42	0.2224	43	0.2243	44	0.2209	45	0.2152	46	0.2127	47	0.2136
48	0.2161	49	0.2177	50	0.2190	51	0.2216	52	0.2250	53	0.2287	54	0.2326	55	0.2352
56	0.2380	57	0.2412	58	0.2431	59	0.2437	60	0.2440	61	0.2442	62	0.2453	63	0.2466
64	0.2481	65	0.2495	66	0.2518	67	0.2545	68	0.2578	69	0.2599	70	0.2619	71	0.2640
72	0.2670	73	0.2696	74	0.2720	75	0.2743	76	0.2769	77	0.2788	78	0.2814	79	0.2835
80	0.2855	81	0.2879	82	0.2914	83	0.2949	84	0.2987	85	0.3025	86	0.3060	87	0.3101
88	0.3133	89	0.3169	90	0.3208	91	0.3250	92	0.3276	93	0.3310				

VITA AUCTORIS

Born: May 6, 1947; Hitchin, Hertfordshire, England

Son of Mr. Frederick and Mrs. Nancy Mustoe

Primary School:

Wilbury Primary School, Letchworth, Hertfordshire, England.

Secondary School:

Letchworth Grammar School, Letchworth, Hertfordshire, England.

University:

University of Aston in Birmingham, Gosta Green, Birmingham, England. 1965-1968. Degree: Combined Honours Bachelor of Science in Chemistry and Physics.

University of Windsor, Windsor, Ontario, Canada, 1969 - 1973. Graduate Research.

Publication:

The Conformation of Racemic 4,6-Dimethyl Trimethylene Sulfite by Gas Phase Electron Diffraction, Canadian Journal of Chemistry, 50, 3892 (1972).

Paper Presented at Conference:

The Vapor Phase Molecular Structures of Some Germanium Methyl Halides by Electron Diffraction, Canadian Chemical Conference, Montreal, Canada, 1973.

Professional Societies:

Member, Chemical Institute of Canada

Associate Member, Institute of Physics (London).

Marital Status:

Married July 28, 1973 to Judith Carol Lemmon.